2010-06-30

Corrosion-related Gas Measurements and Analysis for a Suite of Coals in Staged Pulverized Coal Combustion

Todd A. Reeder
Brigham Young University - Provo

Corrosion-related Gas Measurements and Analysis for a Suite of Coals in Staged Pulverized Coal Combustion

Todd A. Reeder

A thesis submitted to the faculty of
Brigham Young University
in partial fulfillment of the requirements for the degree of

Master of Science

Dale R. Tree, Chair
Thomas H. Fletcher
Matthew R. Jones

Department of Mechanical Engineering

Brigham Young University

August 2010

ABSTRACT

Corrosion-related Gas Measurements and Analysis for a Suite of Coals in Staged Pulverized Coal Combustion

Todd A. Reeder

Department of Mechanical Engineering

Master of Science

Eleven gas species, including CO, CO_2, H_2, H_2O, H_2S, HCl, NO_X, O_2, SO_2, COS and SO_3, were measured in a 150 kW_{th}, staged, pulverized coal, down-fired combustor using a Fourier transform infrared (FTIR) spectrometer, gas chromatograph (GC), and a Horiba PG-250 5-gas analyzer. Additional gases such as HCN, NH_3, CH_4, and other hydrocarbons were also measured. Seven coals of varying rank and composition were investigated. Measurements were obtained in reducing (S.R. = 0.85) and oxidizing (S.R. = 1.15) conditions. In particular, sulfur- and chlorine-containing species including H_2S, SO_2, COS, SO_3, and HCl are discussed.

In the reducing zone, all four measured sulfur species were present although SO_3 was only 1-3% of the total coal sulfur. A trade-off between SO_2, H_2S, and COS was clearly identifiable according to S.R. H_2S and COS increased and SO_2 decreased in highly reducing or high-CO regions. The total amount of sulfur in the measured species in the reducing zone was estimated to be about 65-80% of the total coal sulfur. The total amount of sulfur measured in the four gases increased linearly with coal sulfur in both the oxidizing and reducing zones for the seven coals considered. In the oxidizing zone, SO_3 remained low (1-3% of total sulfur) with the only other measurable sulfur bearing species being SO_2.

Chlorine was found to be released in the reducing zone and form primarily HCl. As the HCl was transported into the oxidizing region, the chlorine remained as HCl. Measurement of HCl was difficult, making some of the data incomplete. The HCl concentration was found to be affected by the flow rate of gases into the sampling line and gas analyzers suggesting HCl is highly reactive and needs to be quenched rapidly or it will react during sampling.

Several trends in the data were matched by equilibrium calculations including trends for H_2S, COS and SO_2 in both reducing and oxidizing conditions. SO_3 did not match equilibrium although the amount of SO_3 was proportional to the amount of sulfur in the coal. HCl, though consistent with cited literature for several coals, did not agree with equilibrium trends or values.

Keywords: coal, swirl, reducing, oxidizing, corrosion, sulfur, chlorine, BFR, equilibrium

ACKNOWLEDGEMENTS

I would first like to express my gratitude to my wife, Haley, for her loving and endless support in pursuing a graduate degree. Dr. Dale Tree deserves tremendous thanks also for even considering me as his graduate student. His knowledge, experience, and guidance have transformed the way I think.

Funding for this work was provided by Babcock & Wilcox for which I am very grateful, for without it we could not have even begun a project of this magnitude. A big thank you goes to Dr. Steven Kung of B&W for overseeing this project and freely giving of his time, energy, and knowledge to continually further our progress.

Next, I would like to express thanks to Bill Murphy, Emily Pearson, Sylvie Bosch-Charpenay, Andy Nguyen, Troy Curtis, and others at MKS Online Products who helped me understand the fundamentals of infrared spectroscopy and helped me keep the spectrometer running long enough to finish my research. I would recommend them and their expertise to anyone considering infrared spectroscopy.

I would like to express thanks to my coworkers, all of whom I now consider to be good friends. They are, in no particular order, Kendall Hill, Curtis Stimpson, David Brunner, Brad Roper, Darrel Zeltner, Teri Snow, and Ezekiel Merriam. Their willingness to get dirty and think of solutions for various problems was critical to the success of this research.

Finally, I would like to thank the rest of my graduate committee, Dr. Thomas Fletcher and Dr. Matthew Jones for their support and input. Dr. Larry Baxter, though not on my graduate committee, offered several hours of his time and expertise which is greatly appreciated.

TABLE OF CONTENTS

LIST OF TABLES

LIST OF FIGURES

NOMENCLATURE

Acronyms

B&W	The Babcock & Wilcox Company
BFR	Burner Flow Reactor
BYU	Brigham Young University
CFD	Computational Fluid Dynamics
DOE	Department of Energy
EIA	Energy Information Administration
FTIR	Fourier Transform Infrared Gas Spectrometer
GC	Gas Chromatograph
IR	Infrared
NBE	National Bulk Equipment
S.R.	Stoichiometric Ratio
SEM	Scanning Electron Microscope
USC	Ultra-supercritical

Arabic Letters

A/F	air-fuel ratio
B	vane thickness
C	number of carbon atoms per molecule
m	mass
MW	molecular weight
N	number of moles
R	inner diameter of secondary air exit into BFR
R_h	outer diameter of secondary air exit into BFR
S	swirl
X	mole fraction
y	mass fraction

Greek Letters

α	vane angle
ξ	angle of adjustment
ξ_m	maximum angle of adjustment
σ	angular momentum flux

Subscripts

act	actual
air	air used as oxidizer to burn the fuel
c	carbon
f	fuel
$stoich$	stoichiometric
th	thermal
tot	total

1 INTRODUCTION

1.1 Background

In recent years, energy has been an increasingly important topic in political debates and even daily conversation. As the global population steadily increases and nations continue to become more industrialized, the worldwide demand for energy will continue to rise. According to the Energy Information Administration (EIA) (2009), electricity demand in the United States alone will increase by 26% between 2007 and 2030. Of the many sources of electricity, coal is unquestionably the most abundant; according to EIA projections, coal will continue to provide the largest share of energy for U.S. electricity generation, decreasing slightly from 49 percent in 2007 to 47 percent in 2030.

The largest concern with using coal as an energy source is the exorbitant amount of pollutants emitted into the atmosphere. As stated by the EIA, in 2007 the world produced over 12 billion metric tons (26.5 trillion pounds) of carbon dioxide (CO_2) from coal alone. It is suspected that this pollution is contributing to global climate change; for this and other reasons, research is being done to create boiler systems that are more efficient and produce less CO_2 or are capable of capturing CO_2.

The amount of CO_2 produced by a coal-fired boiler is directly proportional to the amount of coal burned and, for a given amount of energy, the amount of coal burned is inversely

proportional to the boiler thermodynamic efficiency. It is well understood that cycle efficiency is a function of steam pressure and temperature.

Recently, emissions and fuel cost incentives have increased the desire to develop ultra-supercritical (USC) boilers that have a steam outlet temperature and pressure of up to 760°C (1400°F) and 35 MPa (5000 psi), respectively. These extreme conditions lead to higher efficiency and reduced emissions (Kung, 2006).

Though the increased efficiency is a tremendous benefit, the increased temperatures cause accelerated fireside corrosion (Kung, 2006). Accelerated corrosion increases maintenance time, decreasing boiler availability and reliability. Reliability is of critical importance in the energy industry and is often considered more important than efficiency. To minimize corrosion, the Department of Energy (DOE) has contracted The Babcock & Wilcox Company (B&W) to produce corrosion tests and a corrosion model relating coal properties to corrosion in ultra-supercritical boilers. In order to produce long term corrosion tests needed to develop corrosion models, B&W needs to know the gas species and deposit composition that fire side steam tubes will be subjected to. The measured gas species from these pulverized coal tests will be used to produce synthetic gases to be used in 1000 hr corrosion tests on numerous test coupons. The corrosion tests and model require a database of coal chemistry, operating conditions, and corresponding gas species data. The coals tested for this work are listed in Table 1, along with their respective ranks. With many differences among the selected coals, the model will contain a large range of chemical data. Using these data, B&W will produce a mathematical model to estimate the amount of expected corrosion for a given combination of coal, boiler tube material, and operating conditions.

Table 1: List of Coals Selected for This Work.

Coal	Rank
Illinois No. 6, Galatia	Bituminous
Powder River Basin (PRB), Black Thunder	Sub-bituminous
Beulah Zap	Lignite
Mahoning	Bituminous
Indiana No. 6	Bituminous
Gatling	Bituminous

Independent of the modeling work being done at B&W, the gas species data being collected will produce the most comprehensive set of gas species data over the largest variety of coals available in the literature. The gas species data will provide new information on the evolution of sulfur, chlorine, and nitrogen in pulverized coal flames. In addition to the 10 gas species required by B&W, NH_3 and HCN will be measured, two species critical to understanding the formation and destruction of NO_X. A map of H_2S and SO_2 measurements within a coal flame has not been reported in the literature and will help explain the intermediate behavior of sulfur between pyrolysis and effluent gas measurements obtained previously.

1.2 Research Objectives

The objective of this research was to obtain the combustion product gas composition for a suite of coals under staged combustion conditions. The gas species measurements will be adjacent to deposition measurements that are being analyzed by Brunner (2011). The gas data were collected in the Burner Flow Reactor (BFR) located on the Brigham Young University (BYU) campus. Combustion in the BFR was staged, creating two combustion regions, a reducing (S.R. = 0.85) zone and an oxidizing (S.R. = 1.15) zone, to simulate conditions normally present in commercial pulverized-coal fired boilers. The tube temperatures used to collect deposits were selected to simulate temperatures in an ultra-supercritical boiler.

1.2.1 Gas Species Data

Eleven combustion product gases were selected for measurement because of their relevance to corrosion. Each gas was measured in multiple axial and radial locations to obtain a comprehensive understanding of corrosion in both the near burner region and the superheater region of a boiler. The gases were measured directly above or below the location where deposits were collected but were also measured in additional locations when time permitted. These gases included: carbon monoxide (CO), carbon dioxide (CO_2), water (H_2O), hydrogen disulfide (H_2S), hydrogen chloride (HCl), nitrogen oxide (NO), sulfur dioxide (SO_2), sulfur trioxide (SO_3), carbonyl sulfide (COS), oxygen (O_2), and hydrogen gas (H_2).

1.2.2 Deposit Data

Deposits were collected in both combustion zones on stainless steel sleeves placed at 1/3, 1/2, and 2/3 of the way across the 75-cm inner diameter of the BFR. The deposits were then prepared for insertion into a scanning electron microscope (SEM) where they were analyzed for elemental composition. Some elements indicate a high potential for corrosion and are therefore of particular interest. These elements include, but are not limited to, chlorine, calcium, iron, sodium, and sulfur.

1.3 Scope

As stated earlier, although deposits were collected at the same time as most of the gas species data, the deposit method, results, and discussion will not be presented here and are not the focus of this work. There will also be no attempt to produce a corrosion model or corrosion

measurements. Although B&W performed some CFD analysis of the tertiary air injection, there has also been no attempt to model the BFR combustion process.

The gas species data will be compared to equilibrium results based on the fuel composition and local measured stoichiometry. Sulfur evolution in the combustion process is of particular interest because of its role in corrosion and will be the primary focus. Chlorine evolution is also of interest and will also be discussed in some detail.

2 LITERATURE REVIEW

The extent and severity of corrosion varies widely between boilers depending on the type of fuel burned and the design being used. Boilers are typically classified in terms of the steam pressure and temperature as measured at the superheater or reheater exit. Typical boilers and their approximate operating conditions are outlined in Table 2 [See Babcock & Wilcox (2010), and Kitto and Stultz, (2001)].

Table 2: Typical Boilers with Respective Steam Properties.

Boiler Type	Steam Exit Temperature, °C (°F)	Steam Exit Pressure, MPa (psi)
Sub-critical	538 – 566 (1000 – 1050)	12.4 – 16.5 (1800 – 2400)
Supercritical	550 – 590 (1022 – 1094)	20.7 – 26.2 (3000 – 3800)
Ultra-supercritical	760 (1400)	35 (5000)

Numerous investigators have measured flue gas products produced by pulverized coal-fired boilers while a relatively small number have obtained spatially resolved in-boiler or in-flame measurements. A thorough review of the literature is presented in this chapter.

Gas concentrations existing in a boiler are a strong function of the fuel burned and the local stoichiometric ratio (S.R.). Several studies deal with pyrolysis experiments, considering the evolution of certain elements in the combustion process. Some of the results from these studies are then extrapolated to predict gas concentrations actually occurring in a boiler. Few studies were found where gases were measured in different combustion regions within a boiler.

This remainder of this section discusses the evolution of sulfur and chlorine, their significance in coal-fired boilers, and methods used to measure sulfur- and chlorine-containing gas species.

2.1 H_2S, SO_2, and SO_3

Sulfur-containing species such as H_2S, SO_2, SO_3, and COS are known to cause fireside corrosion, as referenced by Kung (2006), Kihara et al. (1985), Devito & Smith (1991), and Ivanova & Svistanova (1971). To properly understand corrosion mechanisms, the original form of sulfur in the parent coal and its evolution in combustion must be investigated. There are many papers reporting the forms of sulfur in coal (see Huffman et al, 1991; Calkins, 1987; Kelemen et al, 1990; Gorbaty et al, 1990; LaCount et al, 1993; and Boudou et al, 1987). As summarized by Bassilakis et al (1993), sulfur comes in three different forms: organic, pyritic, and sulfatic (small fraction).

Chou et al (1986) predicted that coal-derived sulfur is released mostly as H_2S. This is in good agreement with Bassilakis et al (1993) who determined the evolution of sulfur in all eight Argonne Premium coals. In the study, samples of each coal underwent pyrolysis, where it was found that approximately 50 percent of parent coal sulfur was released, mostly in the form of H_2S. The rest of the evolved sulfur was in the tar, char and other sulfur-containing gases. As the H_2S was transported through an oxidizing region, H_2S was converted to SO_2 and H_2O. Duan, Zhao et al (2009) also performed some coal pyrolysis studies with an FTIR. In Duan's case, however, it was stated that pyritic sulfur initially becomes pyrrhotite ($Fe_{1-X}S$, $0 \leq x \geq 0.2$) in inert atmospheres, rapidly combining with hydrogen radicals to form H_2S in pyrolysis. No such

distinction was made by Bassilakis but this clarification helps to understand more precisely the process by which H_2S is formed.

It is important to note that Bassilakis et al. measured gases with a Fourier transform infrared (FTIR) gas spectrometer but H_2S was not measured directly because of its weak infrared (IR) absorbance. Bassilakis resorted to a post-oxidation technique where heat and oxygen were added to the gas sampling stream after the furnace and before the spectrometer to convert the H_2S to SO_2. By monitoring the SO_2 evolution rate, a measurement for H_2S was recorded. In Duan's case, however, H_2S was measured directly, despite the low absorbance of H_2S. The uncertainty of Duan's measurements is unknown. No literature was found where H_2S was measured directly from a coal boiler. The most relevant pieces of literature found are Bassilakis et al. and Duan et al. but in both studies, H_2S was measured from small amounts of coal under pyrolysis studies only.

Models have been created to predict the amount of H_2S in a localized region. Kaminskii (1996) performed research based on pulverized anthracite in various boilers and went so far as to develop equations predicting the amount of H_2S (as well as other gases) as a function of CO, SO_2, and an excess air coefficient. The reported range of H_2S, dependent on local stoichiometry, was up to 1400 ppm. The relevance of the model to coals other than the anthracite reported in the study is questionable and would need to be determined.

Since SO_3 is a small fraction (~1%) of SO_2 (Srivastava et al, 2004), it is not expected to have a large impact on the total sulfur in the gas phase. As will be discussed in the results section of this work, equilibrium calculations also specify that SO_3 will be a very small fraction of the total sulfur at high combustion temperatures.

SO_2 and SO_3 can be measured in a variety of ways. SO_2 measurements are common and are typically measured using infrared absorption. Fukuchi and Ninomiya (2006) measured SO_3 by ultraviolet absorption and also developed a method to measure SO_3 by thermal conversion of SO_3 to SO_2. Jaworowski and Mack (1979) reviewed a few methods for measuring SO_3 including an isopropyl alcohol method, controlled condensation, and dew point measurement. It was concluded that no one method was clearly superior but that the controlled condensation method produced the most reliable results. Finally, Himes (2006) reported measuring SO_3 by way of FTIR spectroscopy. This latter approach of FTIR is of particular interest as it was the method used in the current work to measure SO_3. Steps taken in recording accurate SO_3 data will be discussed in subsequent chapters.

Models have been created to predict both the amount of H_2S in a localized region and the amount of corrosion on furnace walls. Kaminskii (1996) performed research based on pulverized anthracite in various boilers and went so far as to develop equations predicting the amount of H_2S (as well as other gases) as a function of CO, SO_2, and an excess air coefficient.

In summary, H_2S, SO_2, SO_3, and COS are known to cause fireside corrosion, H_2S being the most corrosive of the four gases. Sulfur is reported to be initially released as H_2S in a reducing zone, with some of it converting to SO_2 and small fractions as SO_3 and COS. Models have been created to try and predict the amount of H_2S based on the amounts of other gases; these models, however, prove to be case-limited and their efficacy with conditions different from those with which they were created would need to be determined. No literature was found where direct measurements of H_2S and SO_3 were obtained from a coal-fired boiler, making this work of significant value.

2.2 Hydrogen Chloride

It is well known that hydrogen chloride (HCl) is a common product gas found in coal furnaces (Boll and Patel, 1961; Clarke and Morris, 1983). According to Manolescu and Mayer (1979), HCl has an effect on fireside corrosion. In their study, conditions for superheater tubes of a pulverized coal boiler were simulated by exposing tubes to a synthetic flue gas, often termed syngas, which contained HCl. It was reported that the corrosion rate, composition, and morphology of the samples were similar to those found on actual superheater tubes. Because of these and other studies, it is critical that the fate of chlorine be considered when investigating corrosion in coal-fired boilers.

There have been numerous studies on the nature of chlorine in coal. Gibb (1983) reported on several of these studies and, in addition, performed his own experiments regarding this topic. Edgecombe (1956) reported that most, if not all the chlorine in coal was organically bound while Daybell and Pringle (1958) postulated that much of the chlorine is in the form of NaCl. The form of chlorine is important because the molecular structure and bonding determines the availability and evolution from the coal during combustion. Gibb, in performing his own independent studies, saw chlorine decompose and measured 42-71% of original coal chlorine in dry, oxygen-free nitrogen at 258 °C. His studies concluded that the majority of chlorine is weakly bonded to coal as ions, and not in the form of NaCl.

Another result from Gibb's study showed that 90-100% of evolved chlorine came out in the form of HCl. Additionally, chlorine was found to evolve out of the coal very rapidly, leaving little chlorine left in coal particles that impact furnace walls. Gibb concluded that chlorine impacts the water tubes primarily as HCl, forming ferrous chloride ($FeCl_2$).

Another study, performed by Ershov et al (1992), showed similar results. In their study, Ershov et al measured HCl with a mercurimetric method from a 1-m long x 44-mm inner diameter test rig. A Russian (Lake-region, Targai field) coal with a chlorine content of 0.21 wt% was combusted in multiple stoichiometries with four variables, including an excess air factor, flame temperature, coal chlorine content, and residence time of the coal/air in the reaction chamber. It was concluded that conversion of chlorine in the coal to HCl in the gas phase was a strong function of residence time, increasing from 30 to 68% with a residence time increase from 0.2 to 0.3 seconds. As residence time was increased to 0.8 seconds, HCl conversion increased to 94%. Additionally, the rate of HCl conversion was found to be a function of flame temperature, albeit somewhat weak. In all cases, completion of HCl formation occurred at a rate faster than the rate of carbon burnout. The results from Ershov's study are consistent with those found by Gibb, indicating that maximum HCl concentrations in a boiler are directly proportional to the amount of Chlorine in the coal and chlorine is not found to be abundant in any other gas species.

There are multiple ways to measure HCl, including FTIR spectroscopy (Oppenheimer et al, 2006), ion chromatography (Giuriati et al, 2003), and diode laser spectroscopy (Linnerud et al, 1998), among others. HCl does not appear to be a difficult gas to detect. However, chlorine is very reactive and can condense or react in a sample line. For example, chlorine is known to react with iron to form $FeCl_2$. It is therefore important to prevent HCl from reacting in the sampling line before reaching the instrumentation.

Though some research has been done in the area of chlorine evolution, the objective of this work is to characterize the fate of chlorine in staged combustion representative of modern full-scale boilers, an area that lacks comprehensive study. One study, Hack et al (2008), discusses USC oxy-fuel boilers where gases such as H_2S, SO_2, and HCl are mentioned as having

higher concentrations compared to standard sub-critical boilers but no reference is made to air-fired cases.

2.3 Conclusions

Summarizing the literature of in situ gas measurements, a few studies have been performed that help in understanding the evolution of certain species, namely sulfur and chlorine. There have been several studies in the literature regarding flue gas measurements of SO_2 and SO_3 but measurements of HCl, H_2S, SO_2, and SO_3 from within a boiler or experimental coal flame were not found.

Subsequent chapters discuss measurements of the eleven gas species listed earlier. Since such a comprehensive set of data has not yet been obtained from coal-fired boilers, it is anticipated that these measurements will be of tremendous value to the coal power industry in understanding the behavior of corrosive gas species in both reducing and oxidizing regions of full-scale coal-fired boilers.

3 METHOD

This work required the simultaneous operation of several systems to produce and acquire the desired data. This section discusses these systems and how they were integrated. Although these systems may have evolved during the course of testing, improvements made to each system will not be discussed unless (1) data were acquired with multiple configurations of a system and (2) the change in configurations produced differences in the results.

3.1 Combustion Facility

The Burner Flow Reactor (BFR) facility at BYU was used to produce the combustion environment required for this work. The BFR is a down-fired, pulverized-coal, swirl-stabilized combustor with a nominal coal feed rate of 22.5 kg/hr (50 lb/hr) as shown in Figure 1. The BFR has access ports allowing gas and deposit sampling probes to be inserted at any axial position 23 – 257 cm (9.0 – 101.2 inches) below the primary fuel injection tube of the burner. Probes can span across the 75 cm inner diameter of the BFR to reach any radial location.

The BFR is supplied with compressed, cleaned air for the primary, secondary, and tertiary (NO_X port) air. The compressor used in this work was manufactured by Ingersoll-Rand, model SSR 75. The secondary air is heated to 138°C (280°F) by an electric heater and temperature controller. Fuel is supplied by a twin screw auger, loss-in-weight feeder. Flue gas is cooled by a wet spray scrubber and moved through the stack using an induction draft fan. The pressure in the BFR can be changed with a bypass valve which allows the exhaust fan to draw a

variable mixture of room air and BFR flue gas. Opening the bypass valve produces a positive gauge pressure in the BFR and, similarly, closing the bypass valve creates a negative gauge pressure. While collecting data, the BFR was run at a slightly positive pressure (0.1 – 0.5 in. H_2O) to eliminate air leakage into the BFR. This practice created a potentially hazardous situation by allowing product gases into the room housing the BFR. Gas monitors were located in three positions in the building that were continuously monitoring CO and SO_2. For some coals, respirators were worn when coal concentrations high in sulfur were burned.

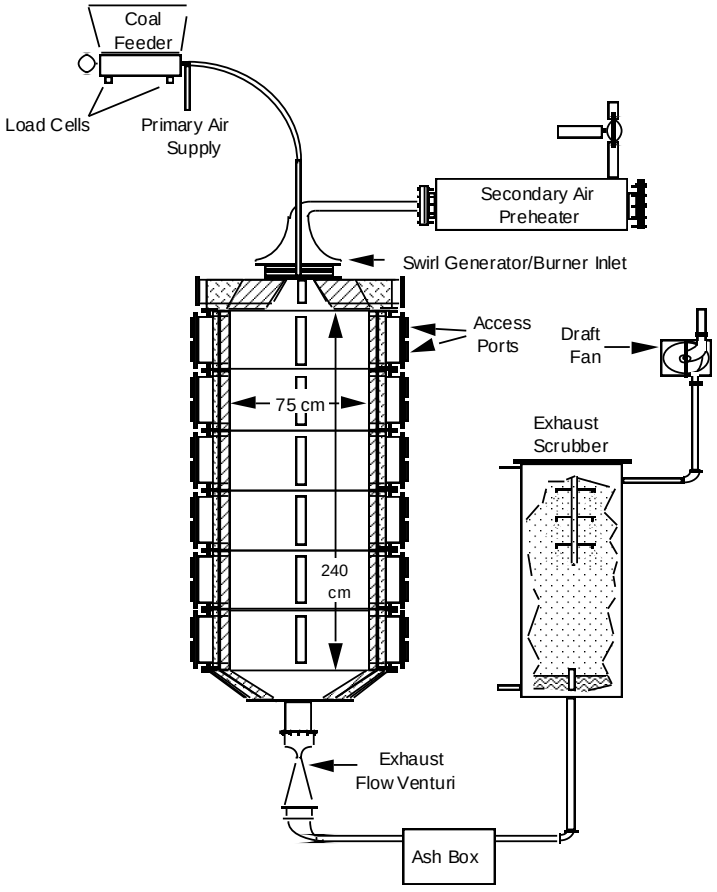

Figure 1: Diagram of the BFR Including Feed and Exhaust System.

The flow of primary air, secondary air, and tertiary air (sometimes termed overfire or burnout air) to the reactor were measured using calibrated orifice plates. Natural gas was

measured using a rotometer. Natural gas was used only to preheat the BFR and was turned off when the coal feed is turned on. All of the orifice plates were calibrated and compared to the choked flow equation. An example of the primary air (the smallest orifice) calibration results are shown in Figure 2. The resulting discharge coefficient, C_D, for the primary air is 0.967. Similar results were obtained for each controlled flow.

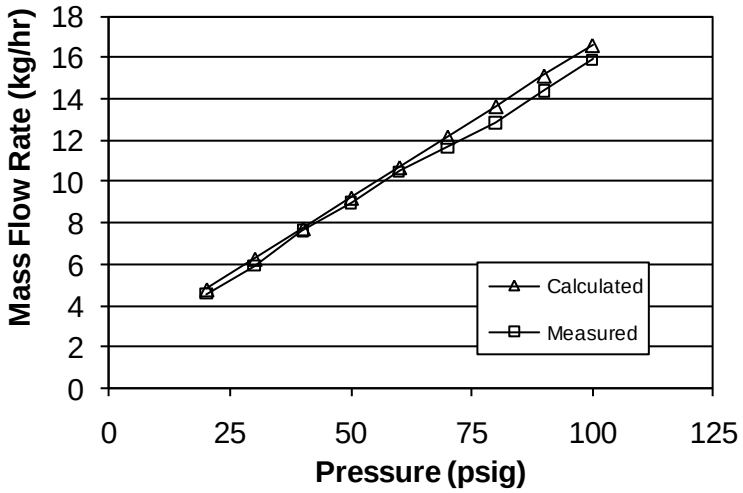

Figure 2: Measured and Calculated Mass Flow Rate as a Function of Upstream Pressure for 1.8 mm, Primary Air Orifice.

3.1.1 Air Staging

Product gas measurements were required from both a fuel rich and fuel lean combustion zone. The two zones were created in the BFR by running the primary and secondary air of the burner at sub-stoichiometric flow rates and then adding tertiary or burnout air downstream of the burner. Staged combustion is a common technology used for NO_X control in commercial boilers. The BFR was used previously in reburning and advanced reburning experiments that required staging of natural gas and air and as a result, water-cooled air injection probes were already available at the start of this project. A schematic diagram of the original water cooled injection probes is shown in Figure 3.

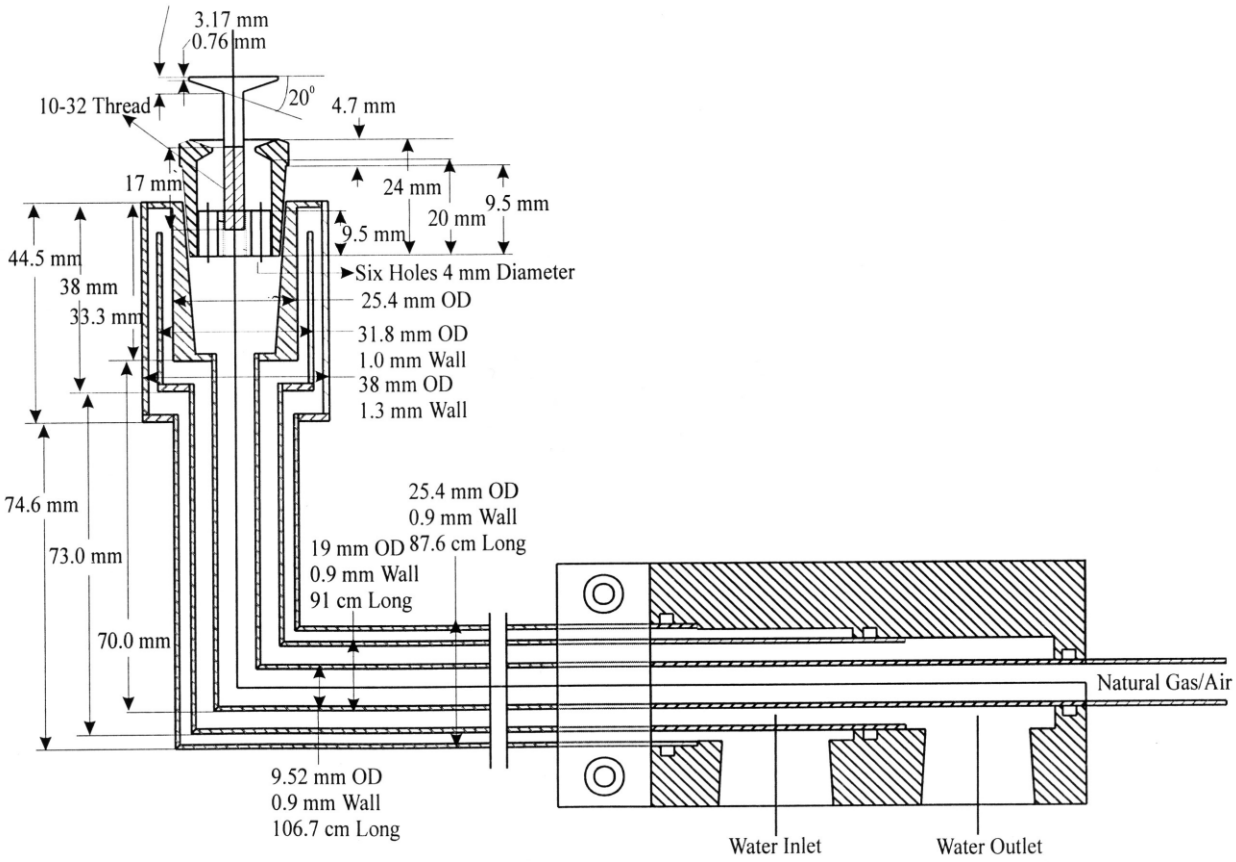

Figure 3: Drawing of the Tertiary Air Device for Staged Combustion used by Nazeer (1997).

The flow rates used previously for natural gas reburning were much lower than those required for the air flow of this project. Consequently, the six, 4mm diameter holes through which the gas had to flow were too small for the desired flow rate. CFD calculations completed by B&W also suggested that the spindle was too small and the higher flow rates of air would produce a jet that penetrated upward into the fuel rich region near the burner. They suggested an outlet diameter of 50 mm and a spindle diameter of 59.4 mm be used in order to direct flow away from the fuel rich zone. The larger exit diameter would have required a completely new water cooled probe. As a result, the largest exit area possible was selected for the existing probe and the six holes were increased from 4 mm to 4.09 mm which was the largest hole size possible.

The spindle diameter was increased from 17.4 to 44 mm as shown in Figure 4. The selection of the spindle diameter was somewhat arbitrary. It was feared that if the spindle diameter were too large, the outer edges of the spindle would not be cooled sufficiently by the exiting air and would melt when placed inside the hot combustion product gases.

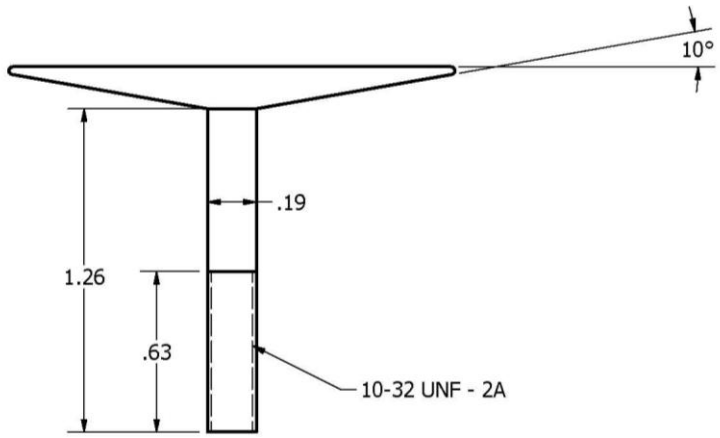

Figure 4: of Spindle Used to Modify the Original Air Injection Probe.

3.1.2 Burner

Commercial low-NO_X burners create a swirled flame to reduce emissions. The burner used in this work was a movable block swirl type, simulating a commercial low-NO_X burner by producing a longer, richer flame—thereby reducing the flame temperature and NO_X concentration. Having been used in previous experiments, the burner was originally built to accommodate two fuels. The burner consists of the components shown in Figure 5. Coal is conveyed by primary air into the injection tubes at the center of the burner. Secondary air enters the upper plenum and is directed downward into the swirl plenum. The air is then directed inward toward the fuel injection tubes through a set of triangular blocks as shown by a top view in Figure 6. One path through the blocks directs the air radially inward, producing no swirl while the second path through the blocks directs air tangentially around the center of the burner. The blocks are adjustable, producing different amounts of swirl according to their position.

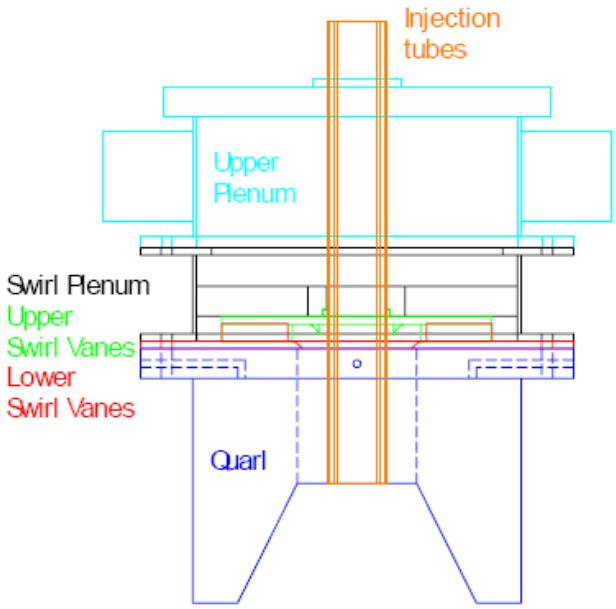

Figure 5: Components of the Variable Swirl Burner.

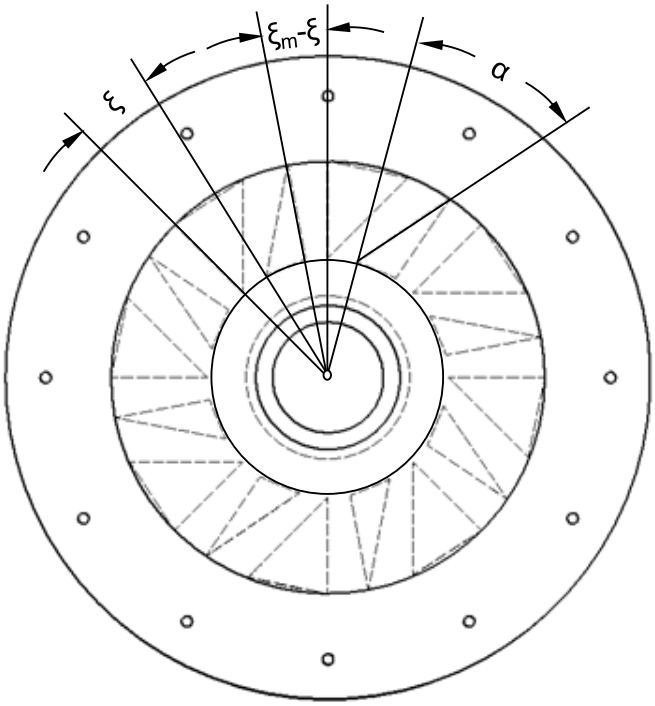

Figure 6: Top View of Swirl Plate.

The swirl is calculated by equations listed by Beér and Chigier (1972). Since this work did not include an in depth study of the burner, the reader is referred to the text for a complete

discussion of the burner geometry, though some detail is given here. Swirl, *S*, is defined by Equation (1), where σ is the angular momentum flux, defined by Equation (2).

$$S = \sigma \frac{R}{2B}\left[1-\left(\frac{R_h}{R}\right)^2\right] \tag{1}$$

$$\sigma = \frac{2\pi}{z\xi_m}\sin\alpha\,\frac{\cos\alpha\left[1+\tan\alpha\tan\left(\xi/2\right)\right]\left(\xi/\xi_m\right)}{\left\{1-\left[1-\cos\alpha\left(1+\tan\alpha\tan\left(\xi/2\right)\right)\right]\xi/\xi_m\right\}} \tag{2}$$

Most of the variables in these equations are defined in Figure 6: R_h and R are the inner and outer radii of the secondary air duct, respectively; B is the vane thickness; α is the angle of the vane; and ξ and ξ_m are the rotation and maximum rotation of the swirl plate, respectively. Values for the fixed variables associated with this swirl plate are listed in Table 3.

Table 3: Constant Values Used on Swirl of Dual Fuel Burner.

Variable	Value
R_h	0.5 in.
R	1.5 in.
B	0.591 in.
α	45.00°
ξ_m	21.56°

To change the swirl on the BFR, a threaded rod has been attached to the swirl plate. When the rod is turned counterclockwise the plates move toward a maximum swirl of 1.70 and all incoming secondary air travels between vanes with a tangential component into the burner. Conversely, if the threaded rod is turned all the way clockwise, zero swirl is achieved. The linear translation of the threaded rod was used to produce a measured vane angle. Equations 1 and 2 were used to calculate a theoretical swirl versus the number of turns on the threaded rod. The results are shown in Figure 7 as indicated by the solid symbols. A second order equation was fit to the data as shown in Figure 7 and was used to create Table 4, where the swirl can be seen for

any number of rod rotations. It should be recognized that this swirl is a theoretical value based on the geometry of the burner and the assumption of uniform velocity in the channels and pipes therein.

Some key geometric dimensions of the burner are given in Table 5. Because only one fuel was used in this work, either fuel tube in the burner could have been used to convey the coal from the feeder to the BFR. The annular tube, having a 14% larger cross sectional area than the center tube, was selected. This larger area causes lower momentum at the tube exit, thereby creating a shorter flame than if the center tube were to be used. In addition, the annular tube, being on the outside, produces more mixing between the fuel and air.

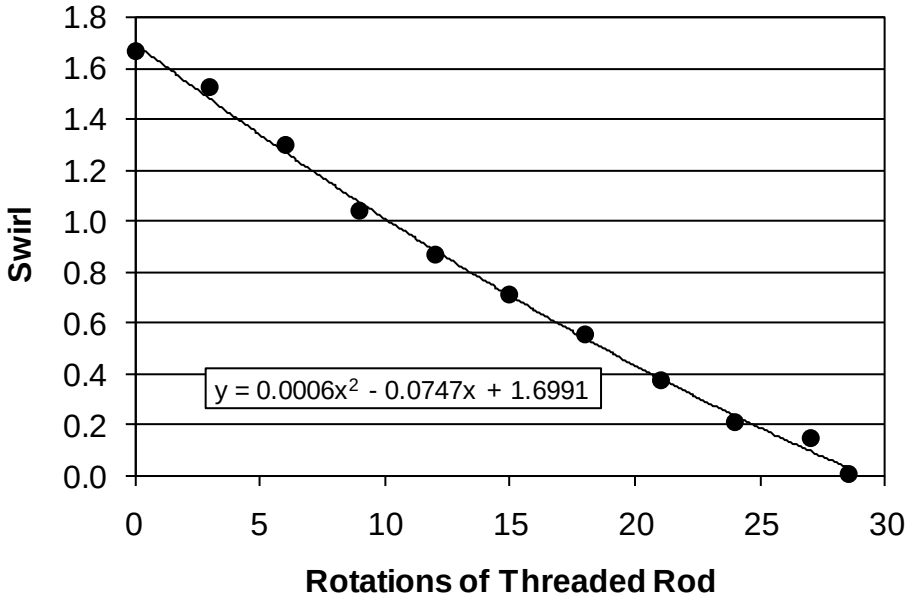

Figure 7: Correlation of Swirl and Rotations of Threaded Rod on the Dual Fuel Burner.

The upper plenum of the feeder is designed with secondary air entering from opposing sides of the burner in an attempt to produce an even distribution of air and create flow symmetry. After collecting several sets of data, it was determined that largest contribution to flow asymmetry was an uneven distance between the center and annular fuel tubes. Following this

discovery, before each experiment, the flame was visually inspected for symmetry. If the flame was not symmetric, the fuel tubes were adjusted slightly to correct the flame's direction. When swirl is low (0.1 – 0.25), however, the flame is in transition from a straight flame to a recirculating structure, and the stagnation point of the flow becomes much less stable, moving from side to side in the BFR.

Table 4: Swirl According to Any Number of Rod Rotations.

Rotations	Swirl	Rotations	Swirl
0	1.70	15	0.71
1	1.63	16	0.66
2	1.55	17	0.60
3	1.48	18	0.55
4	1.41	19	0.50
5	1.34	20	0.45
6	1.27	21	0.40
7	1.21	22	0.35
8	1.14	23	0.30
9	1.08	24	0.25
10	1.01	25	0.21
11	0.95	26	0.16
12	0.89	27	0.12
13	0.83	28	0.08
14	0.77	28.5	0.00

Table 5: Characteristics of the Burner.

Burner Geometry	Dimension
Center tube I.D. (in)	1.342
Annulus Inner I.D. (in)	1.50
Annulus Outer I.D. (in)	1.842
Secondary Air Inner I.D. (in)	2.00
Secondary Air Outer I.D. (in)	3.68
Center Tube Area (in^2)	1.414
Annulus Tube Area (in^2)	0.8977
Secondary Air Tube Area (in^2)	7.495
Swirl Plate Thickness	0.25

3.2 Coal Delivery System

To facilitate the long term (10-30 hours) experiments required in this project, a new coal feed system was installed. This system consists of a bulk bag unloader and loss-in-weight feeder, as shown in Figure 8. The system also includes a platform to hold a bulk bag in place and pneumatic massage paddles to help discharge the coal. The bulk bag is approximately 49”x38”x38” in dimension and can hold up to 682 kg (1500 lb) of pulverized coal. After discharge, the coal is fed through an agitator hopper that fills the feeder hopper on demand. A pneumatic line was installed to convey the pulverized coal from the feeder to the BFR. This integrated system allows the coal feed rate to be held somewhat constant for an extended period of time. The system typically holds the feed rate to within 5% of the set point over a period of 1 minute and within 1% over a period of an hour. The feeder also maintains the flow rate to within 5% of the set point during a refill. The feeder system was purchased through National Bulk Equipment (NBE) but includes parts from both NBE and K-Tron.

Coal exits the feeder as it is pushed out of a tube by the twin augers. As with all auger systems, the coal tends to exit in clumps which can be exaggerated by the coal moisture content and the tendency of the coal to cake together. It was found to be very effective to place a wire mesh screen over the exit of the feeder to break up the coal clumps as they leave the feeder tube. Unfortunately, the wire mesh is also a collector for foreign material mixed with the coal. On two occasions, testing was interrupted by plugging at this wire mesh and therefore the mesh had to be removed. A larger mesh with holes of approximately 1 cm^2 was placed on the feeder exit and has proved to work very well.

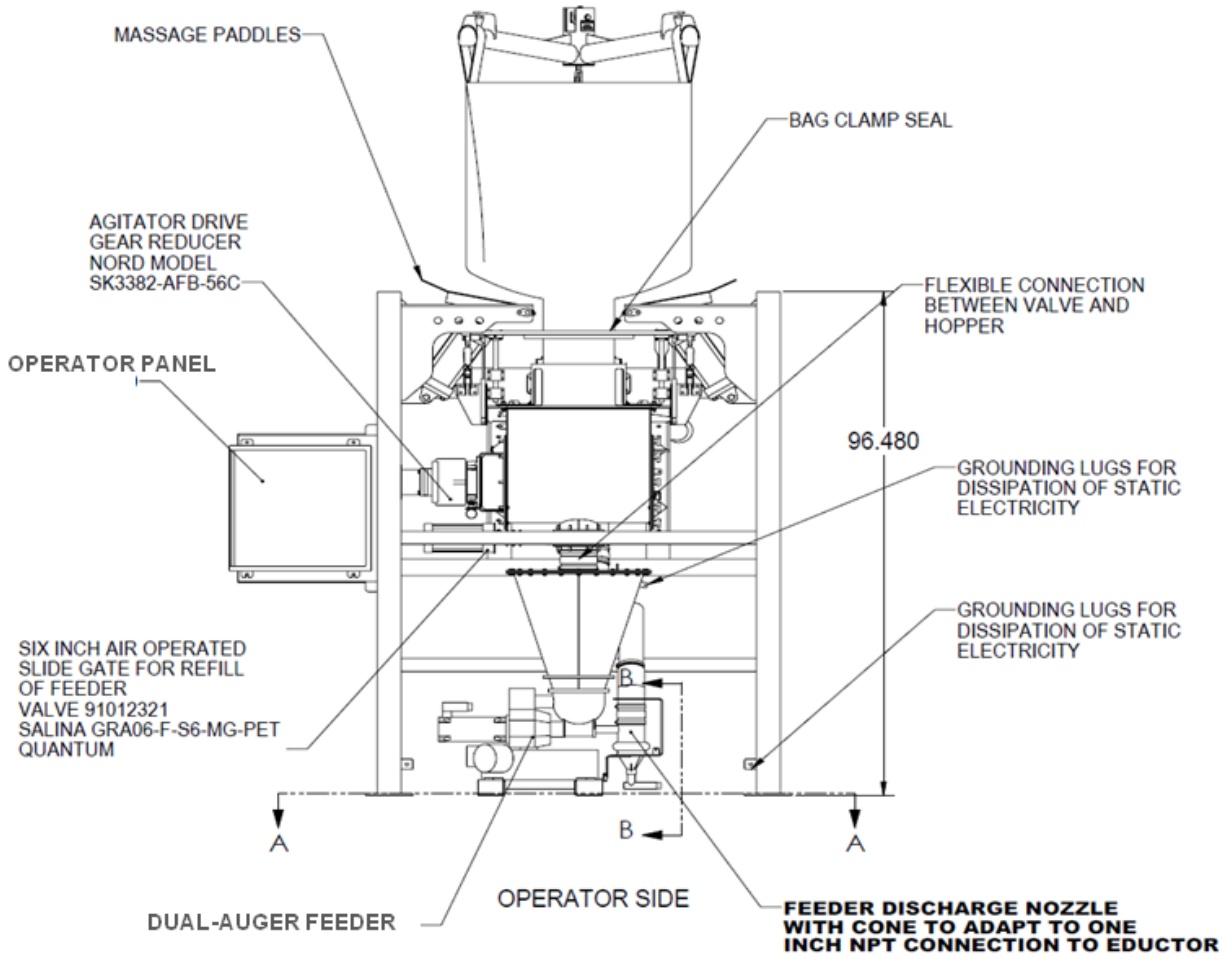

Figure 8: Schematic of the Bulk Bag Unloader and Feeder (Riemersma, 2010).

Another problem encountered with the feed system is the caking of coal to the feeder hopper. The feeder hopper walls are almost vertical and yet, moist coal can still stick to the walls and occasionally cause the center of the auger to be uncovered by coal. This problem only occurs for the high moisture low rank coals. The problem was averted by the placement of vibrators mounted to the hopper lid.

3.2.1 Coal Procurement and Analysis

All eight coals were selected by B&W and are representative of common coals used in commercial boilers around the nation. Each coal was pulverized by Headwaters Energy Services

Table 6. Ultimate, Proximate, and Ash Analyses for Each Coal.

Proximate Analysis, As Received	Ill. #6-1	Ill. #6-2	PRB-1	PRB-2	Beulah Zap	Mahoning	Indiana	Gatling	Pitt 8	Kentucky
Moisture	5.40	3.68	24.59	21.23	27.33	2.22	7.25	3.77	1.05	3.39
Ash	8.65	10.45	5.14	5.53	8.66	9.92	7.20	11.34	10.45	8.46
Vol. Matter	35.68	33.70	37.00	33.76	33.77	40.79	30.87	40.73	18.61	36.97
Fixed Carbon	50.27	52.17	33.27	39.48	30.24	47.07	54.68	44.16	69.89	51.18
Total	100.00	100.00	100.00	100.00	100.00	100.00	100.00	100.00	100.00	100.00
Ultimate Analysis, As Received										
Moisture (%)	5.40	3.68	24.59	21.23	27.33	2.22	7.25	3.77	1.05	3.39
Hydrogen (%)	3.74	3.14	2.55	2.06	2.03	4.18	4.02	4.07	3.86	4.34
Carbon (%)	70.16	67.66	54.75	54.39	46.56	74.67	69.48	67.11	77.37	70.89
Nitrogen (%)	1.04	0.95	0.83	0.86	0.86	0.93	1.36	0.94	1.44	1.23
Sulfur (%)	2.69	2.96	0.25	0.26	0.67	1.96	1.14	4.31	1.03	3.64
Oxygen (%)	8.32	11.16	11.89	15.67	13.89	6.12	9.55	8.46	4.80	8.05
Ash (%)	8.65	10.45	5.14	5.53	8.66	9.92	7.20	11.34	10.45	8.46
Total (%)	100.00	100.00	100.00	100.00	100.00	100.00	100.00	100.00	100.00	100.00
Heating Value (Btu/lb)	12,575	12,464	9,156	9,479	7,792	13,404	12,400	12,191	13,715	12,905
Ash Analysis										
Silicon Dioxide, % as SiO2	48.12	49.13	36.04	37.42	32.25	42.65	55.14	40.35	56.77	41.70
Aluminum Oxide, % as Al2O3	19.65	18.55	16.84	17.18	12.23	29.07	21.10	22.56	29.28	18.40
Iron Oxide, % as Fe2O3	17.64	16.38	5.86	5.50	7.45	20.45	12.93	28.33	6.63	26.09
Calcium Oxide, % as CaO	4.28	5.49	21.61	17.41	19.91	1.76	2.48	2.62	0.90	4.80
Magnesium Oxide, % as MgO	0.95	1.07	5.06	3.94	6.47	0.52	0.86	0.69	0.56	0.90
Sodium Oxide, % as Na2O	1.08	0.66	1.69	1.08	3.29	0.34	1.25	0.41	0.65	0.53
Potassium Oxide, % as K2O	2.59	2.34	0.50	0.57	0.82	1.61	2.40	1.28	2.30	2.43
Titanium Dioxide, % as TiO2	1.05	0.93	1.32	1.20	0.65	1.41	1.30	1.04	1.53	0.96
Manganese Dioxide, % as MnO2	0.07	0.04	0.02	0.02	0.08	0.00	0.03	0.05	0.05	0.03
Phosphorus Pentoxide, % as P2O5	0.08	0.09	1.00	0.54	0.27	0.76	0.35	0.22	0.56	0.31
Strontium Oxide, % as SrO	0.03	0.03	0.35	0.25	0.64	0.12	0.08	0.09	0.12	0.05
Barium Oxide, % as BaO	0.05	0.05	0.62	0.43	0.73	0.07	0.06	0.11	0.12	0.18
Sulfur Trioxide, % as SO3	4.41	5.24	9.09	14.46	15.21	1.24	2.02	2.25	0.53	3.62
Alkalies as Na20	2.79	2.20	2.02	1.46	3.83	1.40	2.83	1.25	2.17	2.13
Base to Acid Ratio	0.39	0.38	0.64	0.51	0.84	0.34	0.26	0.52	0.13	0.57
Silica Ratio	0.68	0.68	0.53	0.58	0.49	0.65	0.77	0.56	0.88	0.57
T250, °F	2429	2439	2228	2302	2130	2497	2624	2295	>2900	2263
Chloride (%) (dry basis)	0.3892	0.283	0.0012	0.001	0.001	0.1989	0.2121	0.0387	0.0045	0.2057
Rank	Bitum.	Bitum.	Sub-bit.	Sub-bit.	Lignite	Bitum.	Bitum.	Bitum.	Bitum.	Bitum.

in Kennesaw, Georgia and delivered to BYU. The coal arrived at BYU in bulk bags, sometimes known as supersacks. A proximate, ultimate, and ash analysis were obtained for each coal, the results of which are summarized in Table 6. The particle size of the pulverized coal has been specified as 75% passing through a number 200 mesh, but the particle size distribution has not been measured. The original proximate, ultimate, and ash analyses can be seen in Appendix B.

The initial deliveries of Illinois No. 6 and Powder River Basin (PRB) coals were consumed during testing in 2009. Additional coal was ordered and received in the third and fourth quarters of 2009. The additional PRB coal had not been tested at the time of this writing but the additional Illinois #6 coal had. For clarity in understanding the data, the two deliveries of Illinois #6 coals will be called Illinois #6-1 and Illinois #6-2, respectively. Although similar, differences in the composition of the two deliveries of coal are larger than expected. The Illinois #6-2 coal has significantly less chlorine and sodium, and higher ash content than the Illinois #6-1 coal. Therefore, significant differences can be expected when comparing product gas data between the two coals.

3.3 Fuel and Air Flow Rates

Coal and air flow rates used for each of the five tests completed to date are shown in Table 7. The feed rate of coal for the Illinois #6 test was selected based on prior experience as the amount of heat required to maintain the BFR at a high enough temperature to produce ignition and burnout (150 kW). The flow rates of coal for the other fuels were selected to maintain the heating rate of the Illinois #6 coal.

Air flow rates were selected in order to produce a fuel-rich reducing zone of S.R. = 0.85 followed by burnout air and an oxidizing zone of S.R. = 1.15. The ultimate and proximate

analyses of each coal were used to calculate a stoichiometric air-fuel ratio. Due to an error in the program used to calculate the stoichiometric A/F ratio, the values actually used in some of the experiments are slightly leaner than they should have been for three of the coal tests (Illinois-2009, PRB, and Beulah Zap). The actual S.R. based on the fuel and air flow rates are also listed. The uncertainty of the fuel and air flow rates was estimated to be approximately 2%. The uncertainty of the calculated stoichiometric air-fuel ratio is also 2%, primarily based on the uncertainty of moisture content. Thus, the total uncertainty of the S.R. is on the order of 3%.

Table 7: Coal and Air Flow Rates Used in the Gas Sampling Tests.

	Illinois #6-1	PRB	Beulah Zap	Mahoning	Indiana	Illinois #6-2	Gatling
Coal (kg/hr)	20	30	32	19.30	20.28	20.18	20.63
Primary Air (kg/hr)	18.8	27	22	28.54	28.94	27.28	28.07
Secondary Air (kg/hr)	139.8	148	135	132.8	124.09	119.8	127.13
Tertiary Air (kg/hr)	50.4	62.2	51.8	45.7	54.37	51.72	54.84
Secondary Air Temp. (°C)	138	138	138	138	138	138	138
Swirl Number	0.66	1.09	1.67	0.77	0.77	0.77	0.77
Stoichiometric A/F	9.01	6.63	5.46	9.80	8.97	8.47	8.90
Ave. S.R., Reducing Zone	0.88	0.88	0.89	0.85	0.84	0.86	0.85
Ave. S.R., Oxidizing Zone	1.16	1.19	1.19	1.14	1.14	1.16	1.14

The swirl number of each test was chosen based on a sparse matrix of preliminary gas data and visual observations of the flame. The O_2 concentration near the BFR exit was measured as the swirl ratio was changed. At zero swirl, the Illinois #6 coal produced a lifted flame that penetrated slightly off-axis of the centerline almost the entire length of the BFR. Initially, the flame shortened and the O_2 concentration at the BFR exit decreased as swirl was increased. After reaching a swirl of 0.6 or higher, the flame shape appeared stable and the O_2 no longer decreased with increasing swirl. Regions of high CO, along with other gases typically found in a reducing region, such as H_2S, were found in the near-burner region. The swirl for Illinois #6 was therefore selected at 0.66 as the lowest swirl to produce a swirl stabilized, attached flame.

A similar process was used to determine the swirl number used for the other coals. The swirl ratio was varied and near-burner gas composition was measured. The lower rank coals visually appeared to require a higher swirl ratio to produce a stable recirculating flame. This can be attributed to the higher momentum of the primary flow relative to the secondary flow in the lower rank coals. As can be seen in Table 7, the lower rank coals required approximately the same total flow of air to complete the combustion and thus secondary air flow and secondary momentum is similar for all coals. The primary air and fuel flow rates are both increased with the low rank coals increasing the ratio of primary to secondary momentum. Thus the swirl ratio of PRB was 1.09 and Beulah Zap, 1.67. The last four tests (Mahoning, Indiana, Illinois-2010, and Gatling) were similar coals (all the same rank with similar moisture contents; see Table 6) and a swirl of 0.77 created the desired conditions for all four.

3.4 Gas Sampling System

The goal of the gas sampling system is to deliver gases to the analyzers that are free of solid particles and are unaltered chemically from those sampled in the BFR. This requires the removal of particulate from the gas stream to protect the optical components in the gas analyzers and rapid cooling of the gas to 180°C to prevent chemical reactions, and avoid condensation of water and acids. A total of eleven gas species were measured, including CO, CO_2, H_2, H_2O, H_2S, COS, HCl, NO, O_2, SO_2, and SO_3. Three different analyzers were used to collect all of the desired gases.

The analyzer used to measure most of the gases was a Fourier transform infrared (FTIR) gas spectrometer. The FTIR, manufactured by MKS Online Products, was used to measure CO, CO_2, H_2O, H_2S, COS, HCl, NO, SO_2, and SO_3 which includes all gases of interest except H_2 and

O_2. Though more detail on FTIR theory will be given later, each gas is measured by the amount of infrared light it absorbs. Some gases absorb light very well and the accuracy for these gas measurements is high. Some gases, such as H_2S, HCl, and SO_3, are not strong absorbers and are therefore more difficult to measure. The steps taken to ensure proper measurement of these gases are discussed later.

The gas chromatograph (GC), manufactured by Agilent Technologies (model 3000 Micro GC), operates by separating gases according to the time it takes to travel through a separation column. Once separated, the thermal conductivity of the gas at the column exit is used to determine the gas concentrations. The GC was purchased primarily for the measurement of H_2, but the same column that measures H_2 can also be used to measure O_2, N_2, and CO.

The Horiba PG-250 is a five gas analyzer built to measure common combustion product gases including CO, CO_2, NO, O_2, and SO_2. Three of the gases are measured using infrared absorption (CO, SO_2 and CO_2). NO is measured using chemiluminescence and O_2 is measured using a zirconium oxide cell. Before passing into the analyzer, gas must pass through a desiccant as the instrument cannot handle excessive amounts of moisture. Experience has shown that the desiccant and water trap influence the SO_2 concentration in the gas and therefore the Horiba analyzer was not used to measure SO_2. Additionally, CO has a maximum detection limit of 5000 ppm which is too low for most measurement locations in the reducing region of the BFR studied in this work. Because all ten gases of interest are measured by the FTIR and GC, the Horiba PG-250 was only used to obtain redundant measurements and wasn't always necessary for recording data.

A schematic diagram of the current sampling system is shown in Figure 9, where all bolded items are heated to prevent condensation. A water cooled tube is inserted into the BFR

through a circular port in an access door. The water-cooled tube acts as a housing to protect an electrically heated probe (heating jacket and sample tube) from the combustion gases inside the BFR. The heating element in the probe is connected to a temperature controller which maintains the heated sample line at 180°C. The heated sample line is available commercially as Teflon or stainless steel. Both materials have been evaluated in this study with preference for Teflon due to its chemical stability with the combustion gases, as will be discussed shortly. The water-cooled tube and heated sample line are nominally 5 ft in length which is long enough to traverse the diameter of the BFR. Outside of the BFR, a second heated line, 25 ft in length, is used to carry the gases from the BFR to the analyzers.

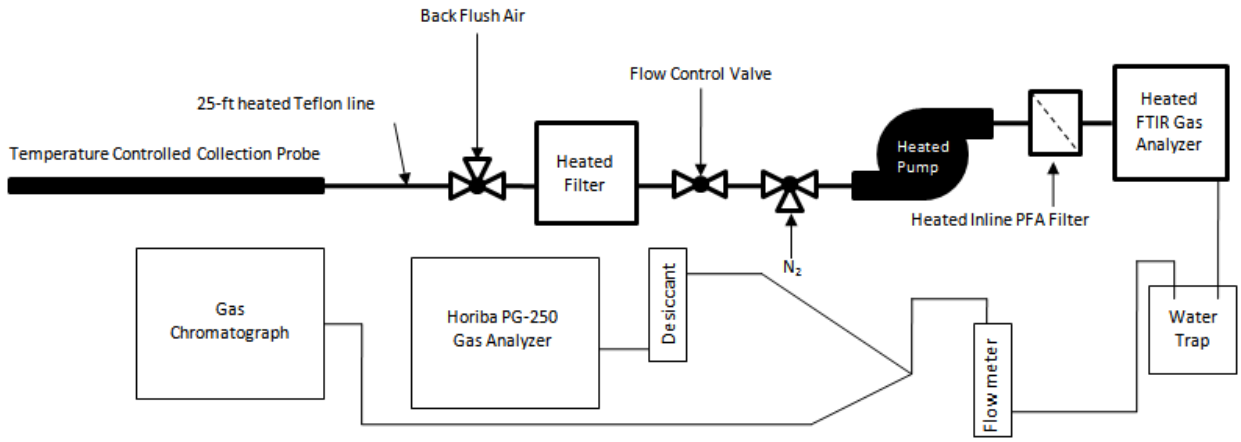

Figure 9: Schematic Diagram of the Components and Analyzers of the Gas Sampling System.

Just before reaching the analyzers, the gas sample travels through a series of components necessary for proper measurement. The first is a 3-way valve that, turned one direction, allows gas to continue toward the analyzers or, turned the other way, allows high pressure air to back flush the probe; clean air travels backward through the 25-ft heated line and heated probe to free them of any debris. After the 3-way valve, the sample passes through a heated Teflon filter. This filter is controlled to 180°C and contains no metallic components on any surfaces in contact with the gases. Upon exiting the heated Teflon filter, the gas travels through two more valves. The

first valve, a needle valve, is in place strictly to control the flow through the sampling system. When the valve is closed, the pump cannot draw any gases from the BFR whereas if the valve is completely open, the pump is not restricted (except for line and filter pressure losses) in its ability to sample gases from the BFR. The second valve, a three-way valve, controls the source of the gas that passes into the gas analyzers. The valve is used to switch between nitrogen from a compressed gas cylinder and the sample line. The nitrogen is used as a zero reference point for the FTIR and a calibration point for the Horiba PG-250. The gas subsequently travels through a heated pump that is oil-less and uses a Teflon diaphragm. The pump head and valve body are made of 316 stainless steel but are Teflon coated. The final component the gas must travel through before entering the FTIR is an in-line Teflon-PFA (perfluoroalkoxy**)** filter with a single 47 mm-diameter Whatman qualitative (grade 5) filter paper (Whatman No. 1005 047).

While in the FTIR, the sample is maintained at a temperature of 150°C and a pressure as close to one atmosphere (1 atm) as possible. The FTIR can accurately compensate for pressure variations that are within ± 10% of 1 atm. After exiting the FTIR, the gas passes through a water trap located in an ice bath, reducing the water vapor to the saturation pressure at 0°C, thus reducing moisture in the lines prior to the subsequent analyzers. After the water trap, the gas sample passes through a rotometer containing a needle valve used to control the FTIR pressure and then the flow is split with one line going to the GC and the second going to the Horiba PG-250.

The configuration of components discussed above and shown in Figure 9 was not always as shown. Various items were added throughout the duration of the project that made gas sampling easier and/or more repeatable. The changes made were such that the system worked more reliably for longer periods of time but not necessarily more accurately. Anyone attempting

to sample gases with a similar setup is encouraged to follow the above configuration to avoid unnecessary troubleshooting that has already been corrected for during this research.

A major challenge for the sampling system was preventing Teflon from melting at the probe tip. A detailed drawing of the sampling probe that was initially used for this project, designed by Damstedt (2007), is shown in Figure 10. The flow of water in the cooling jacket is indicated by the arrows with the heating element shown by the shaded area. Combustion gases enter the probe from the left into a Teflon tube inside the heating jacket. The problem encountered with this probe design was that the Teflon tube tip can melt due to the high temperatures of combustion gases and occasional flame impingement. Once the Teflon tube was melted, a new heated probe assembly had to be ordered to replace it because the Teflon tube was not designed to be removable.

In consultation with the manufacturer of the heated line, a new design was produced as shown in Figure 11. The new heated line is similar to the original design with the only significant difference being that the center tube is a larger 3/8”-OD stainless steel tubing. The 3/8”-OD tubing allows a ¼”-OD Teflon tube to be inserted through the ID. The Teflon tubing could be easily replaced when damaged from overheating without the need to change the entire heating element.

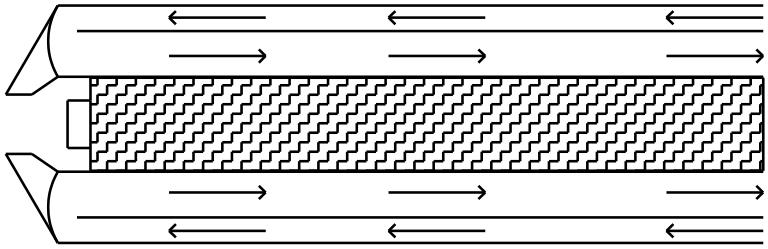

Figure 10: Schematic Diagram of the Sample Line Inlet Including the Water Cooled Tube and Heated Sample Line (dark region), Taken from Damstedt (2007).

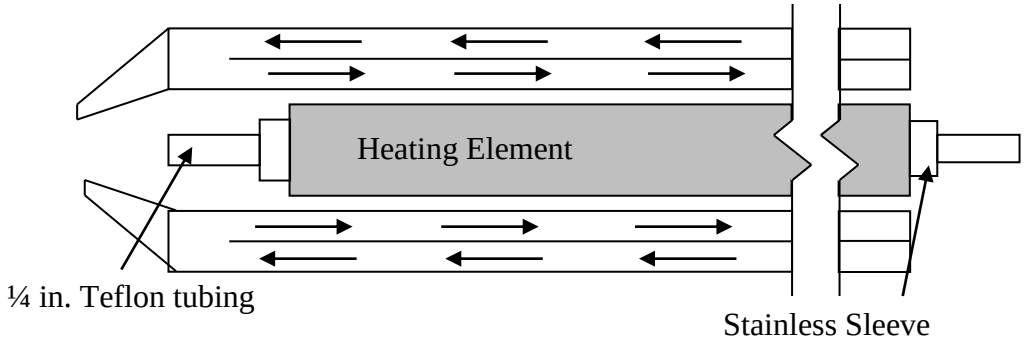

Figure 11: New Heated Probe Design with Replaceable 1/4-inch Teflon Tubing.

This modified probe design has been used with a short stainless steel tube and compression fitting as shown in Figure 12. The stainless tubing approximately 50 mm (2 inches) in length protruded approximately 25 mm (1 inch) into the combustion chamber. Pressure inside the BFR was always positive while data were being collected, nevertheless if the end of the sample tube was located inside the water cooled tube and not out in the combustion gases, air would leak into the sample. Therefore, a metal piece protruding into the combustion gas was necessary.

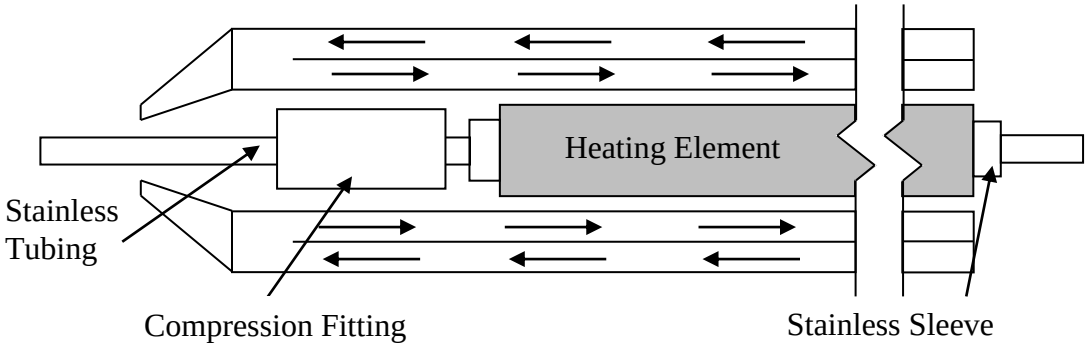

Figure 12: Heated Probe Design with a 1-inch Stainless Steel Tube Inserted into the Sample Gas.

3.4.1 Leak Testing

During warm up for each experiment, a mass balance was completed on the oxygen which allowed a check on the fuel, air, and O_2 measurements. The mass balance was necessary each time to ensure there were no leaks in the gas sampling system. It was performed by

calculating the excess oxygen for the fuel/air flow under lean conditions assuming complete combustion. For example the methane, air, and fuel flows were set to an S.R. of 1.15. The appropriate oxygen concentration for the mixture assuming complete combustion of natural gas to CO_2 and H_2O was calculated. Agreement between the measured and calculated O_2 was generally within 0.4% which means that the S.R. was being measured within approximately 0.02. This is within the combined uncertainty of 2% in the fuel and air flow. When disagreement was greater than 0.5% O_2, the source of error was identified before continuing with the test. The most common sources of errors were (1) the BFR pressure was not positive and thus air was leaking into the BFR, (2) there was a leak in the sample line, and (3) the gas analyzer was out of calibration.

A similar test was performed after the beginning of coal flow. The overall stoichiometry was set to an S.R. of 1.15 and the exit oxygen concentration is measured and compared to the expected value of 3% O_2. If the O_2 concentration is not within 0.5%, sources of error were investigated. In addition to the most common errors found with natural gas and air flow, additional errors can occur with the mass flow rate of the coal, primary air flow, and incomplete combustion of the coal.

3.4.2 FTIR Theory

The FTIR spectrometer, model number MG2030 manufactured by MKS Online Instruments was used to measure CO, CO_2, H_2O, H_2S, COS, HCl, NO, SO_2, and SO_3. The FTIR has a 5.11 m, long-pass gas cell and a maximum resolution of 0.5 cm^{-1}. The instrument transmits an infrared light through the sample gas and collects a measurement of the absorption of light as a function of wave number (WN). Each gas has a known spectral absorption pattern which can be quantified when compared to calibration spectra taken at the same temperature and pressure.

Absorption of gases follows Beer's law which states that the amount of transmitted light through a gas is exponentially proportional to the product of absorption coefficient, κ_η, and path length through the gas, s (Modest, 2003). Mathematically, this is expressed as Equation 3, where τ is the amount of transmitted light and s is the optical path length the light has taken through the gas. For simplicity, absorbance is defined as the negative logarithm of τ as shown in Equation 4 (Bosch-Charpenay, 2010).

$$\tau = \frac{I}{I_0} = 10^{-\kappa_\eta s} \tag{3}$$

$$A_\eta = -\log_{10}(I / I_0). \tag{4}$$

This implies that absorbance is directly proportional to the absorption coefficient of a gas and the optical path length. Since the absorption coefficient can be expressed in terms of molar absorptivity, ε_η, and gas concentration, c, absorbance can be expressed as shown in Equation 5.

$$A_\eta = \varepsilon_\eta c s\,. \tag{5}$$

When measuring combustion products, the total absorbance is the sum of the absorbance of all gases in the mixture. Though each gas absorbs in a large range of wave numbers, an analysis band is specified for each individual gas by which the concentration of the gas is calculated. For example, though H_2S has a spectrum spanning from 400 – 3000 cm^{-1}, the region selected as the analysis band is only a small portion of the total spectrum (2670 – 2700 cm^{-1}). This region was selected because it contained the least interference from other gases. The rest of the spectrum is still very important, however, because it is used in calculating the concentrations of other gases that absorb in different regions. The MKS software attempts to determine the concentration of gases by interpolating between the calibration spectra to match the measured spectrum. In the H_2S example, the data between 2670 – 2700 cm^{-1} are used to calculate the H_2S

concentration while the rest of the H_2S spectrum is used to determine the absorption contribution of H_2S in other spectral regions so that other gases can be properly calculated.

H_2S is a particularly difficult gas to measure because of its low signal to noise ratio using IR spectroscopy. It is advantageous to use the FTIR for H_2S measurements because it is a continuous measurement and can be made simultaneously with the other gas measurements, but the poor signal to noise ratio can cause low accuracy in the FTIR measurements. Because of the importance of analyzing H_2S, particular care has been taken to characterize the accuracy of this measurement. The spectral absorption pattern for 1000 ppm of H_2S is shown in Figure 13. Note the maximum absorbance is about 0.012 absorbance units (AU), where absorbance is measured according to Equation (4). This low magnitude corresponds to a transmitted IR intensity of $0.973I_0$, meaning at that specific wave number (1292.8 cm^{-1}), 2.7% of the IR light was absorbed by H_2S.

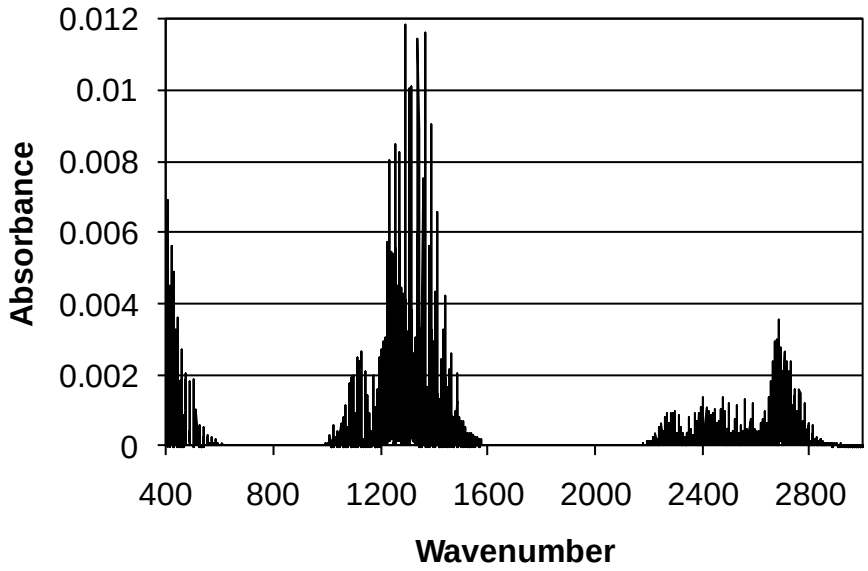

Figure 13: H_2S Absorption Spectrum for 1000 ppm of H_2S in Nitrogen.

As stated above, the FTIR software interpolates among the calibration spectra, creating a calculated spectrum that closely matches the measured spectrum. The error, *E*, in a gas measurement is determined by Equation 6 (Bosch-Charpenay, 2010),

$$E = \frac{\sqrt{\sum_{0}^{n} \left(meas_i - calc_i \right)^2}}{\sum_{0}^{n} calc_i} \times conc \tag{6}$$

where *i* refers to each wave number, and *n* is the amount of wave numbers in a given analysis region. The terms *meas* and *calc* refer to the absorbance value of the measured and calculated spectra, respectively, and *conc* is the measured concentration of the gas. To be clear, this calculation assumes that the difference between the measured and calculated spectra, or residual, is only noise. Therefore, it is strictly a measure of precision and not accuracy or complete uncertainty.

It is possible that gases can be interfered with by other gases absorbing in the same spectral region, causing the reported value to deviate from the actual value. Some possible gases that have interfered with the H_2S measurement are water and acetylene, but this interference has been found to be less than 150 ppm. Combining possible interference with the precision of the H_2S measurement, the overall accuracy is approximately ±250 ppm. This should be seen as a worst case scenario, as the interference from other gases is not always present. Averaging several spectra can decrease the uncertainty to a worst case of about ±125 ppm. Although the uncertainty in H_2S is significant, reasonable data have been recorded at levels well above the uncertainty level and prove to be very valuable in considering the behavior and evolution of sulfur. These data are presented in Chapter 4 and Appendix A.

3.4.3 Analyzer Comparison and Calibration

Certified calibration gases were used to calibrate the Horiba PG-250 and GC. The calibrations were done routinely, usually in the morning of each day before data collection. The calibration gases used to calibrate the Horiba and GC are listed in Table 8. It should be mentioned that the GC was only calibrated with a CO concentration expected in fuel-lean regions and the Horiba cannot measure CO above 5000 ppm.

Table 8: Calibration Gases Used for the Analyzers.

Analyzer	Gas	Concentration (Nominal)
GC	O_2	0, 0.1, 22 (%)
	H_2	0, 0.1, 2.0(%)
	CO	0, 0.1 (%)
Horiba	O_2	0, 22 (%)
	CO_2	0, 18 (%)
	CO	0, 4500 (ppm)
	NO	0, 1000 (ppm)
FTIR	H_2S	800 (ppm)
	HCl	100 (ppm)

For the FTIR, rather than producing a new spectral absorption curve, the results from the manufacturer's (MKS) calibration curve were used and compared with certified calibration gases. The calibration gases, found in Table 8, were fed directly into the FTIR as shown in Figure 14. Results of the measurements for H_2S and HCl are shown in Table 9. The results show excellent agreement between the measured and actual concentrations with a 3% or less variation. SO_3 is very toxic and difficult to purchase. It is also highly reactive and would be difficult to maintain in a gas cylinder. It should be noted that the existing calibration for SO_3, obtained by MKS, was obtained by producing a reaction with the products being fed into the FTIR. MKS has expressed confidence in the spectral shape but not the magnitude. All other gases measured by

the FTIR are more common and easier to measure because of their IR absorption properties. It was therefore unnecessary to compare these gases with calibration gases.

Table 9: Results of HCl and H_2S Calibrations.

Gas	Cylinder Concentration (ppm)	FTIR Measurement (ppm)	Error
H_2S	817	827	+ 2%
HCl	96	93	- 3%

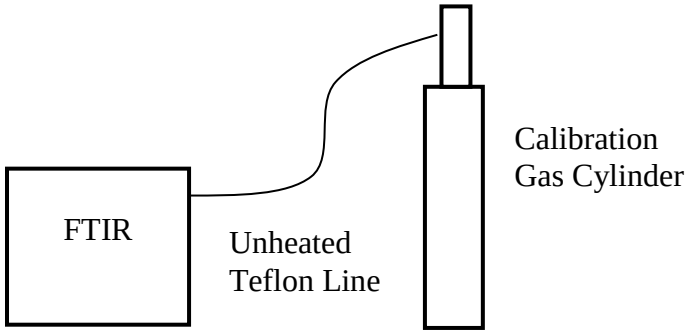

Figure 14: Setup for Calibration of the FTIR.

3.4.4 Reactivity Testing

Several combustion gases of interest, including H_2S, HCl, and SO_3, are chemically reactive and can condense out in the sampling line when the temperatures fall below their respective dew points. In order to determine the loss of H_2S and HCl in the sampling line, calibration gases were passed through individual and multiple components of the sampling system. A diagram of the sampling line used for the reactivity testing is shown in Figure 15. This sample system differs from the one currently used (Figure 9) because the testing was done prior to the current set-up. Four components of interest for this test included (1) a 2-m heated stainless steel sample line, (2) a heated stainless steel filter, (3) a 7.6-m heated Teflon sample line, and (4) a heated pump.

Results of the measured concentrations after passing through various components are listed in Table 10. Results are compared to those when the gases were fed directly into the FTIR through a short 2 m Teflon line (see Table 9). Although not all of the components were tested, a trend is evident. When either calibration gas was passed through Teflon lines (components 3 and 5), losses were minimal or negligible. However, when the gases were passed through stainless steel tubing (component 1), the loss became significant, around 10%. Losses in the filter which was housed in stainless steel were also significant at 10%. Following these tests, it was decided that stainless steel components in the sampling train needed to be eliminated as much as possible. A Teflon filter and Teflon heated lines have been used to replace the stainless steel components.

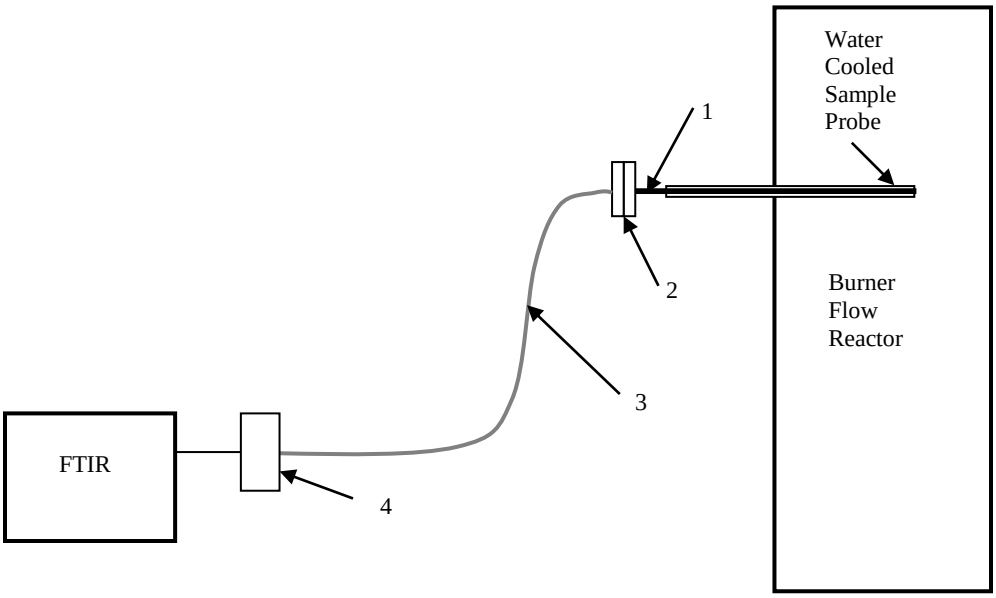

Figure 15: Diagram of Gas Sampling System Including: (1) a 2-m Heated Sample Line, (2) a Heated Filter, (3) a 7.6-m Heated Teflon Sample Line, and (4) a Heated Pump.

Also of interest is the variability seen in the sample line data for H_2S. Although the average H_2S concentration measured is in good agreement with the standard, a variation of ~100 ppm occurred from sample to sample, as shown in Figure 16. While all of the gases show some

degree of variability from one scan to the next, the scattering of H_2S concentration is higher compared to its average. Reasons for variability in the H_2S sample are discussed earlier in Chapter 3.4.2. In this case, there were no other gases to interfere with H_2S and the scattering was simply caused by the low absorbance of the H_2S gas. Averaging the data based on 16 data points has produced an average value of 744 ppm for H_2S, a 95% confidence at $\pm$12 ppm.

Table 10: Results of Measured Gas Concentrations after Passing through One or More of the Components in Sample Line.

Gas (concentration)	Components	FTIR Measurement	Difference From Direct Delivery (%)
H_2S (817 ppm)	3	821 ppm	- 6 ppm (-0.7%)
H_2S (817 ppm)	1, 2, 3, 4	744 ppm	- 83 ppm (-10%)
HCl (96 ppm)	3	91 ppm	- 2 ppm (-2%)
HCl (96 ppm)	5	91 ppm	-2 ppm (-2%)
HCl (96 ppm)	2, 5	80 ppm	-13 ppm (-14%)
HCl (96 ppm)	1, 4, 5	80 ppm	-13 ppm (-14%)

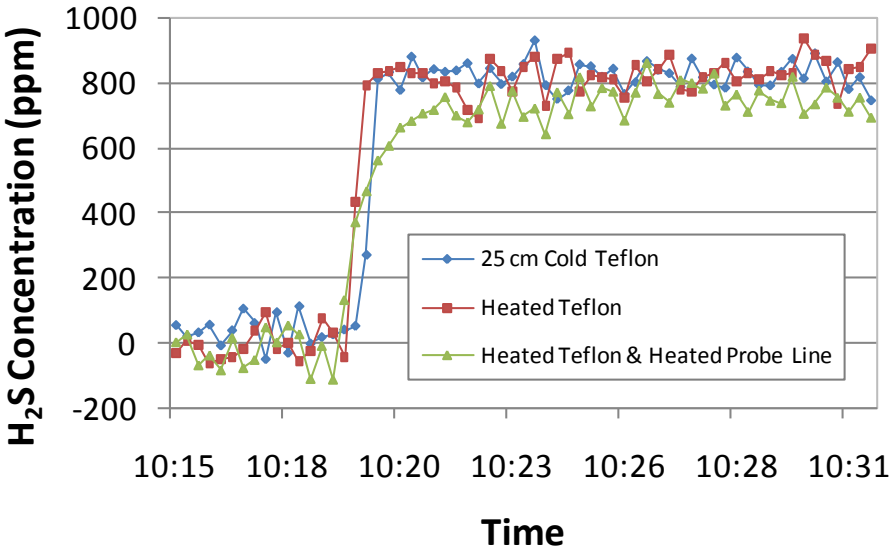

Figure 16: FTIR Measurement of 817-ppm H_2S Calibration Gas.

Another potential loss of H_2S, HCl, and SO_3 can be associated with condensation in the sampling line. The specified line temperature of 180°C is sufficiently high to prevent condensation of acids and water. The challenge was to maintain this temperature in the sample

line throughout the testing. The heated filter was thought to be the lowest temperature point in the sampling train and was upgraded. The lowest temperatures then appeared to be in the water cooled tube or at a fitting connection between the heated lines. The line temperatures were carefully monitored at different line locations. In addition to maintaining the line temperatures, several other species sensitive to condensation, such as NH_3 and HCN, were also monitored. Condensation in the line would reduce their concentrations. Therefore, lower than expected values in these species would have also served as an indication for condensation. Experience suggests that HCl is the first of the measured species to condense.

4 RESULTS

This chapter presents experimental results, discussing important characteristics and trends in the data. The reported data are directly useful for understanding the gas phase distribution of potentially corrosive elements in the coal such as sulfur and chlorine and as empirical results for use in corrosion analyses. Additional discussion will be provided in Chapter 5 where equilibrium calculations are presented and compared with the measured data. The FTIR contains data for numerous gas species that were not of specific interest to corrosion such as NH_3 and HCN. These data are reported in Appendix A. Although only two tables (one reducing and one oxidizing) of data for each coal are presented in this chapter, all acquired data can be found in Appendix A.

For reference in reviewing the data, Figure 17 illustrates the dimensions of the BFR. The BFR is 265 cm axially, as measured from the fuel injection tube outlet located at the bottom of the burner, and has a 75 cm inner diameter. The tertiary air was inserted about half way down the BFR, near 140 cm. Accordingly, some of the tertiary air penetrates up into the lower part of the reducing zone, having been injected slightly upwards. Because of this, reducing zone gas species were sampled well above the tertiary air insertion point (usually at 63 – 97 cm axially).

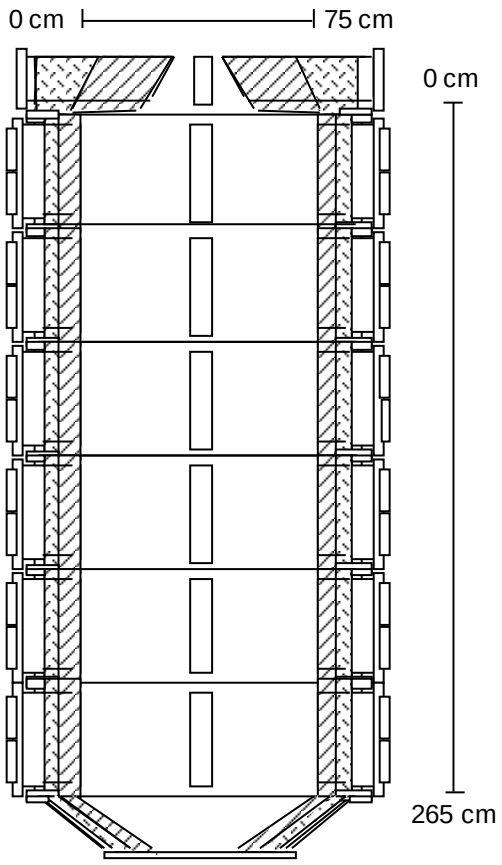

Figure 17: Gases Can Be Sampled 23 - 257 cm Below the Annular Fuel Tube of the Burner.

4.1 Reducing Zone Gas Sampling Results

Gas species data of each coal for the reducing zone are shown in Table 11 – Table 17. The data are shown in the chronological order in which they were taken. The radial position given is measured from the north wall of the BFR. When viewing the tabulated gas concentration data it should be remembered that the largest single gas species in the mixture is nitrogen (N_2) which is 78% of the incoming air. The concentration of other gases can be significantly influenced by dilution with air in fuel lean regions and can be very high in regions where gases evolve from the coal at a faster rate than the coal is mixed with or reacts with air. The data reported in this chapter are raw data and are not corrected to an equivalent O_2 concentration to

allow the absolute magnitudes to be evaluated but in some cases to aid the discussion, the data will be normalized to 3% O_2.

It should also be remembered that the FTIR (used to measure all reported species except O_2 and H_2) is a heated, wet measurement while the O_2 and H_2 are dry measurements being obtained with the GC after cooling the product gases to 0 ^oC and removing the water. These data have not been adjusted to the same basis (i.e. they are reported as they were measured).

4.1.1 Carbon Monoxide

The first column containing CO is useful for identifying fuel rich and fuel lean regions within and between the reducing and oxidizing zones. The CO concentrations show that a similar fuel rich stoichiometry was produced in the near burner fuel-rich zone for each coal. Maximum CO concentrations vary from 3-5% among all the tests. The CO concentration shows the symmetry or lack thereof for each flame. For the Illinois #6 and PRB coals, the flame was richest south of the centerline at 50-60 cm. The asymmetry was eventually found to be caused by the primary fuel tube being off center from the annular secondary air tube and could be adjusted prior to collecting data. The CO concentrations (and other gas concentrations) are more symmetric in the latter five coal tests after it became a practice to visually center the flame before starting a test. The flame symmetry can however be difficult to assess visually leading to asymmetric gas phase data being collected. This lack of symmetry shifted the location of the richest region of the BFR from the centerline toward the walls of the reactor but did not appear to have a significant impact on the magnitude or trends of the gases being measured.

4.1.2 Carbon Dioxide & Water

The second and third columns show CO_2 and H_2O. These species give some indication of the completeness of combustion and the amount of mixing with air. The highest values of CO_2 and H_2O will occur in stoichiometric regions where the carbon content of the coal is burned out and there is little or no dilution from excess air. In fuel rich regions, CO_2 is lower with some of the carbon being split between CO and CO_2, but the sum of CO and CO_2 is approximately constant. CO_2 is highest when O_2 and CO concentrations are both low indicating a near-stoichiometric location. These locations occur between the fuel rich center and the fuel lean wall regions.

When comparing CO_2 concentrations for different coals, CO_2 is expected to be highest in coals of low stoichiometric air fuel ratio because of the lower dilution of the products with air nitrogen. The Beulah Zap and PRB coals have the lowest stoichiometric air fuel ratios due to their higher oxygen content. As expected, the total CO_2 plus CO concentrations of these two coals are higher than the other coals.

When comparing coals, the differences in H_2O concentration in the product gases are dominated by the amount of moisture in the coal. The PRB coal and Beulah Zap are both high moisture coals and therefore have higher H_2O concentrations at a given S.R. This can be seen in the data where the highest H_2O concentrations for PRB Beulah Zap are 15 and 21 % respectively while H_2O concentrations for the other coals are on the order of 10% or less.

Table 11: Illinois #6-1 – Axial Distance 77 cm.

Dist. (cm)	CO (ppm)	CO_2 (%)	H_2O (%)	H_2S (ppm)	HCl (ppm)	NO (ppm)	SO_2 (ppm)	SO_3 (ppm)	COS (ppm)	H_2 (%)	O_2 (%)
10	642	15.44	7.35	18	180	296	2129	44	0	0.95	4.07
20	1574	16.29	7.78	20	224	275	2253	36	4	0.33	3.31
30	7619	15.85	8.91	10	244	230	2529	39	-7	0.04	1.35
40	22414	14.76	9.77	788	157	96	1773	37	57	0.17	0.69
50	17264	15.07	9.88	376	187	141	2258	37	41	0.65	0.10
60	32254	14.40	10.47	991	144	99	1497	23	132	0.89	0.07
70	22070	14.47	10.12	671	129	148	1828	33	118	0.67	0.06

Table 12: PRB – Axial Distance 90 cm.

Dist. (cm)	CO (ppm)	CO_2 (%)	H_2O (%)	H_2S (ppm)	HCl (ppm)	NO (ppm)	SO_2 (ppm)	SO_3 (ppm)	COS (ppm)	H_2 (%)	O_2 (%)
10	5130	14.17	12.16	-41	1	301	190	11	7	0.03	4.35
20	5116	13.96	11.20	-81	1	311	179	12	6	0.08	4.08
30	6642	14.04	11.43	-27	0	321	171	11	7	0.12	3.46
40	38487	14.11	15.17	203	0	215	149	6	13	1.32	0.41
50	34866	14.48	14.32	180	0	288	141	7	13	1.13	0.66
60	15135	15.24	12.58	53	0	311	168	9	11	0.35	1.85
70	1835	13.72	10.65	-35	0	360	149	10	7	0.03	4.33

Table 13: Beulah Zap – Axial Distance 77 cm.

Dist. (cm)	CO (ppm)	CO_2 (%)	H_2O (%)	H_2S (ppm)	HCl (ppm)	NO (ppm)	SO_2 (ppm)	SO_3 (ppm)	COS (ppm)	H_2 (%)	O_2 (%)
10	11617	17.79	16.94	54	4	454	781	12	20	0.32	2.89
20	39181	17.86	18.91	170	3	227	629	15	71	1.51	0.90
30	47406	16.21	20.50	571	3	174	298	13	108	2.07	0.96
40	42536	16.05	21.29	465	2	211	419	10	75	2.06	0.86
50	29380	17.39	19.14	98	2	287	666	19	45	0.90	1.26
60	6640	17.24	16.64	-43	1	410	719	18	21	0.18	3.01
70	1030	16.25	15.01	-32	1	510	668	19	11	0.07	3.36

Table 14: Mahoning – Axial Distance 83 cm.

Dist. (cm)	CO (ppm)	CO_2 (%)	H_2O (%)	H_2S (ppm)	HCl (ppm)	NO (ppm)	SO_2 (ppm)	SO_3 (ppm)	COS (ppm)	H_2 (%)	O_2 (%)
10	3001	17.59	6.79	-62	4	373	1585	36	-26	0.02	2.20
20	7813	17.71	9.38	7	10	381	1746	36	-7	0.11	1.58
30	20719	17.23	10.39	-52	12	410	1861	42	1	0.37	0.92
40	35154	16.34	11.97	88	19	330	1708	30	33	0.80	0.62
50	17333	17.45	11.53	-47	14	337	1836	36	4	0.78	0.64
60	2295	17.54	9.56	-28	14	356	1642	33	-7	0.92	0.84
70	481	16.50	7.98	-2	15	390	1447	31	-1	3.51	0.02

Table 15: Indiana No. 6 – Axial Distance 70 cm.

Dist. (cm)	CO (ppm)	CO_2 (%)	H_2O (%)	H_2S (ppm)	HCl (ppm)	NO (ppm)	SO_2 (ppm)	SO_3 (ppm)	COS* (ppm)	H_2 (%)	O_2 (%)
10	652	11.69	6.79	-41	44	375	800	29	-9	0.00	4.44
20	17225	11.79	9.27	93	66	212	910	23	16	0.87	0.81
30	42635	10.63	10.56	303	188	76	522	8	42	2.56	0.59
40	39253	10.75	10.46	423	184	66	436	7	13	3.18	0.56
50	30262	11.22	10.13	318	132	80	432	14	19	2.19	0.56
60*	16239	14.42	9.44	-27	16	280	1237	30	0	0.10	0.80
70*	10105	14.46	8.49	-76	12	349	1133	26	-2	0.19	0.73

* These data were collected on a different day than other data in the same table.

Table 16: Illinois #6-2 – Axial Distance 97 cm.

Dist. (cm)	CO (ppm)	CO_2 (%)	H_2O (%)	H_2S (ppm)	HCl (ppm)	NO (ppm)	SO_2 (ppm)	SO_3 (ppm)	COS (ppm)	H_2 (%)	O_2 (%)
10	8256	15.82	9.20	-1	30	213	2402	53	15	1.10	0.53
20	23505	14.85	9.77	491	262	49	1098	30	93	1.04	0.50
30	28591	14.63	9.81	578	255	36	748	22	108	1.16	0.53
40	25197	14.71	9.83	646	242	42	802	25	109	1.32	0.52
50	13365	15.46	9.62	477	177	83	2049	47	101	0.61	0.52
60	6764	15.93	8.63	20	90	192	3456	68	14	0.23	0.54
70	6993	15.98	7.82	43	44	227	2675	64	1	0.07	0.74

Table 17: Gatling – Axial Distance 97 cm.

Dist. (cm)	CO (ppm)	CO_2 (%)	H_2O (%)	H_2S (ppm)	HCl (ppm)	NO (ppm)	SO_2 (ppm)	SO_3 (ppm)	COS (ppm)	H_2 (%)	O_2 (%)
10	18168	16.79	10.43	353	15	164	2861	54	98	0.30	0.77
20	20853	16.73	10.15	404	53	115	2614	58	124	0.40	1.62
30	27136	14.65	10.49	760	15	92	2154	52	57	2.24	0.02
40	21515	16.66	10.23	680	10	107	2606	57	71	2.32	0.02
50	13377	17.22	10.20	307	5	125	3112	62	53	0.23	0.34
60	10594	17.39	10.49	305	4	127	3146	64	4	0.07	0.92
70	6111	17.66	9.43	-69	3	190	3643	80	4	0.03	1.59

4.1.3 Oxygen

Staying with the major species, the O_2 concentrations are shown in the final column. Though both the Horiba PG-250 and GC measure O_2, the GC values were selected for use because they were more closely correlated with the timing of the FTIR data. The Horiba produces a running average of the concentration in the measurement cell while the GC provides

the concentration of a small amount of gas in the sample line at a particular instant in time. O_2 is generally seen to change inversely with CO as would be expected. The O_2 concentration is higher near the walls where CO is low and lowest near the center where CO is a maximum. The O_2 is very low (less than 0.5%) in the richest regions of the flame (CO above 25,000) and significantly higher near the walls with values on the order of 2-5%. This is an indication that burnout air is flowing up along the walls from the tertiary air injector or is available from the recirculating secondary air. In some of the later experiments, the tertiary air injector was inverted to inject air downward in the BFR. In spite of this change, O_2 was still prominent near the walls indicating that the O_2 present was primarily originating from the secondary air.

The O_2 values in the reducing and oxidizing zone for Beulah Zap are slightly higher than would be expected when compared to the other coals. It was initially thought there was a leak in the sample line causing the high readings but it was later determined that air was being entrained in the primary air line at the feeder. A correction was made for the entrained O_2 as can be seen in results for the subsequent tests. Because of the leak, the S.R. of the reducing zone as evidenced by higher O_2 values, was higher (S.R = 0.89) than the target value (S.R. = 0.85).

4.1.4 Sulfur-containing Species

The sulfur-bearing species of H_2S, SO_2, COS, and SO_3 are critical to fireside corrosion and therefore are of particular interest. H_2S and COS are seen to follow the same trend as the CO being highest in the reducing zone and lowest or zero near the walls where O_2 is present. At the same locations where H_2S and COS are relatively high, the concentration of SO_2 is low. An exception to this result is the data for the Mahoning coal where SO_2 is seen to be high across the entire BFR profile and H_2S and COS are only measurable at the richest measured test point at a radial position of 40 cm. As will be seen in the discussion, the trend of increasing H_2S and COS

with decreasing S.R. is consistent with equilibrium trends where sulfur is preferentially formed as H_2S and COS under reducing conditions and SO_2 under oxidizing conditions. The concentration of SO_2 deceases slightly near the walls where oxygen is present because of dilution with the air. The concentration of SO_3 is seen to be very low compared to the other sulfur species, typically on the order of 2-3 percent of the total sulfur.

The sum of H_2S, SO_2, SO_3, and COS for each coal as a function of radial position in the reducing zone is shown in Figure 18. The sum is relatively constant across the diameter of the BFR with a deviation of typically less than 10 percent across the diameter. The least constant data seems to be from Illinois #6-1 and Gatling coals. This non-uniform data may be due to incomplete combustion, unsteady conditions in the BFR during the measurement or measurement uncertainty. The uncertainty in the measurements is dominated by the uncertainty of the H_2S measurement and is considered to be approximately ±100 ppm.

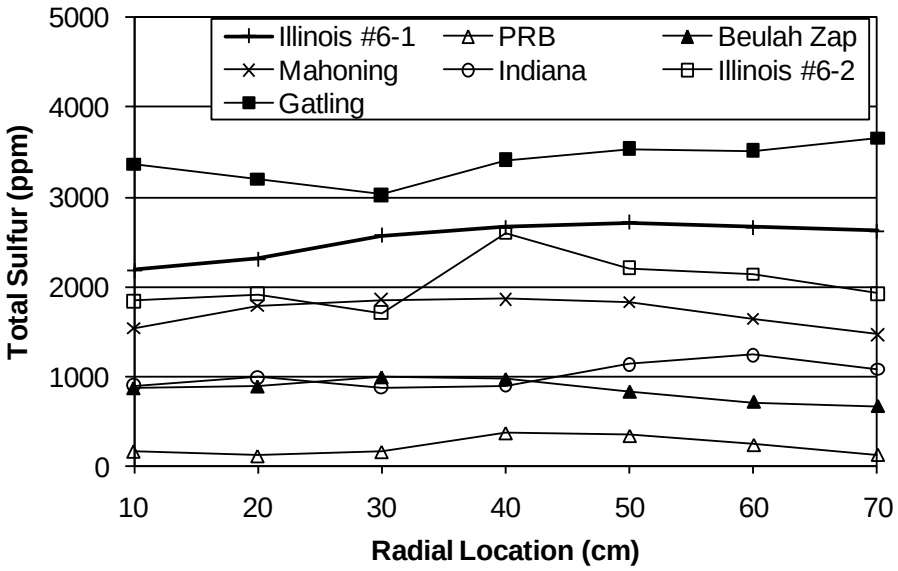

Figure 18: Sum of H_2S, SO_2, & SO_3 in the Reducing Zone for Each Coal.

The average sum of H_2S, SO_2, SO_3, and COS in the reducing zone are compared to the total sulfur in the coal in Table 18. In the table, the magnitudes of measured sulfur-containing gases are seen to scale linearly with the sulfur content in the coal. This trend is illustrated more clearly in Figure 19, where the parent coal sulfur is plotted against the average total measured sulfur-containing gases for each coal. The data appear to have a linear relationship, showing that a relatively constant amount of sulfur is released from each coal in the reducing zone. The maximum possible sulfur was determined with equilibrium calculations and is also plotted in Figure 19.

When comparing the measured values with the maximum sulfur possible, the Illinois #6-2 and Gatling coals appeared to release a smaller fraction of sulfur into the gas phase than the other five coals. One possible explanation of this disparity in sulfur release is that gases are reacting with a part of the sampling line for the Illinois #6-2 and Gatling coals but not for the others. This is possible because the flow rate of gases was decreased for the Illinois #6-2 and Gatling tests to mitigate particulate accumulation in the filters. The decreased flow rate caused the gases to be in contact with each component of the gas sampling system for a longer amount of time. At the tip of the gas sampling probe—the first component the gases enter—is a small (1-3 inches long) piece of stainless steel. This stainless steel is necessary to prevent hot gases from melting the Teflon sampling lines. As discussed in Chapter 3.4.2, stainless steel is known to react with H_2S (and possibly other sulfur-containing gases). Though the stainless steel tip is small, it is possible that gases were reacting with it at lower flow rates. This theory is discussed in more detail in Chapter 4.1.5.

Table 18: Correlation between Coal Sulfur and Measured Sulfur Species.

Coal	Sulfur wt%, As Received	Total Measured Sulfur Avg. (ppm)
Illinois #6-1	2.69	2534
PRB	0.25	219
Beulah Zap	0.67	846
Mahoning	1.96	1709
Indiana	1.14	1018
Illinois #6-2	2.96	2048
Gatling	4.31	3388

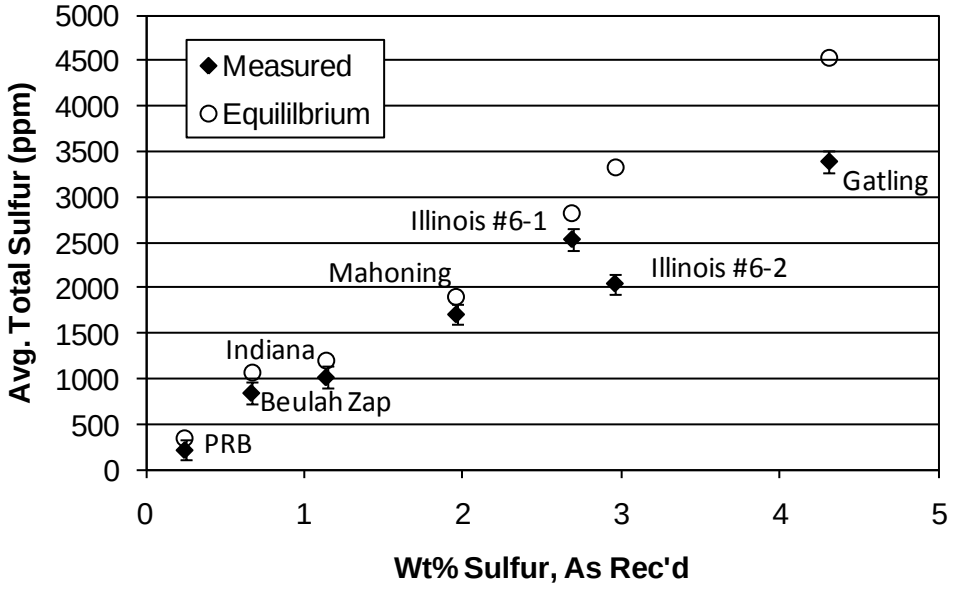

Figure 19: Comparison of As Rec'd Sulfur and Total Measured Sulfur in the Reducing Zone.

A clear trend is seen for all of the coals measured—when CO increases, H_2S and COS increase and SO_2 decreases. The highest values of H_2S and lowest values of SO_2 occur where CO is a maximum. This is consistent with equilibrium considerations which predict that H_2S is formed in reducing conditions. The correlation of H_2S and SO_2 values with equilibrium predictions is a topic worthy of additional investigation and will be discussed in the next chapter. H_2S is a particularly difficult species to measure because of the low signal to noise ratio, as mentioned in Chapter 3.4.2. The uncertainty of the H_2S measurement when the instrument is clean is on the order of ±50 ppm. Therefore, negative values on the order of 50-100 ppm are

sometimes encountered and can be interpreted as near zero H_2S. Generally, at a given axial location, the increase in H_2S is seen to be approximately equal to the decrease in SO_2 from one location to the next. Plots showing these trends are shown for each coal in Figure 20. CO is also included in each plot to elucidate how fuel rich the gas mixture is at each location. More information regarding these plots and the data is found in the next chapter where equilibrium calculations are discussed.

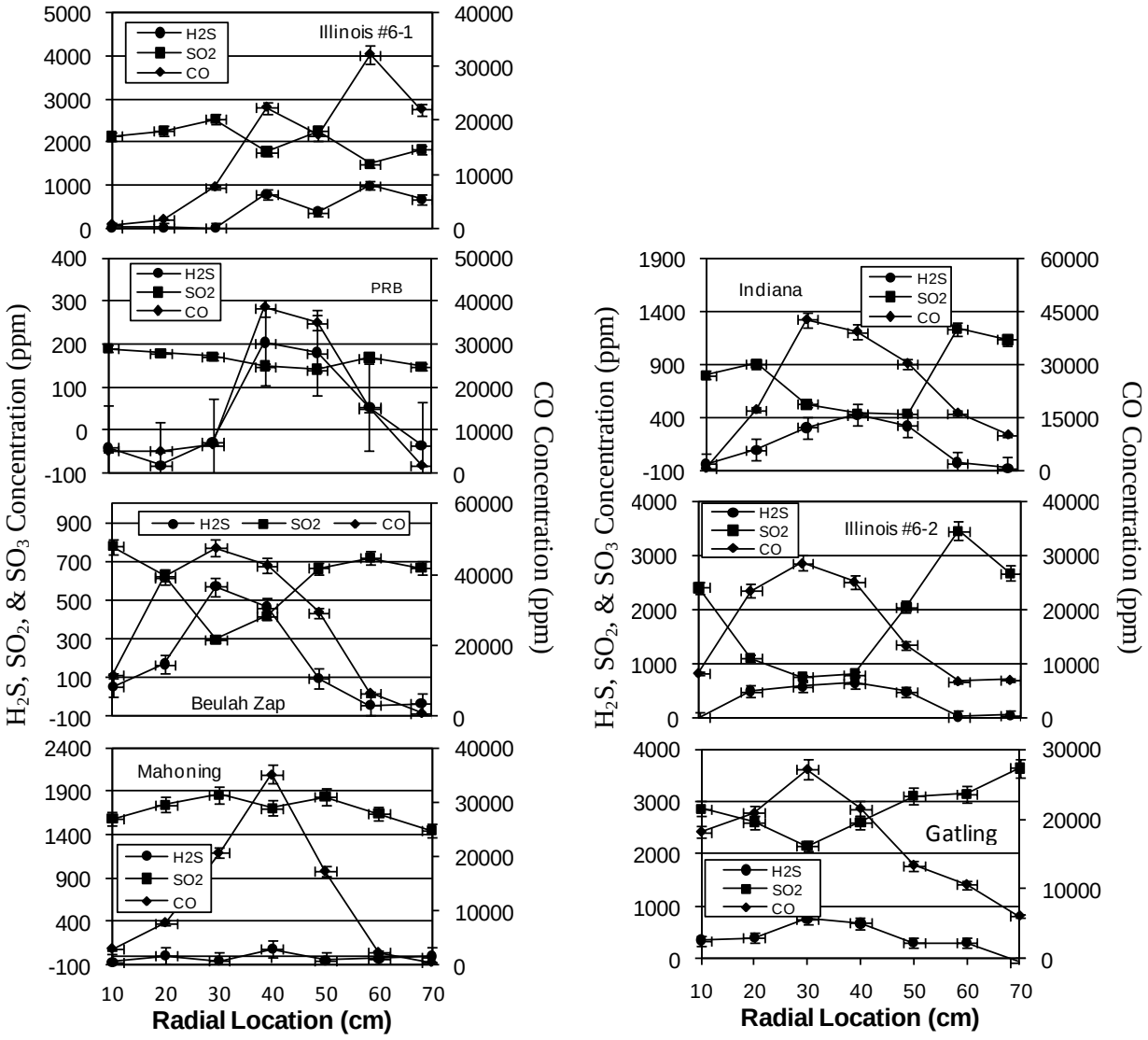

Figure 20: Trends in H_2S, SO_2, & SO_3 for Each Coal.

4.1.5 Hydrogen Chloride

HCl is another species critical to fireside corrosion. The literature suggests (Gibb, 1983) that chlorine is loosely bonded in the coal with 90-100% of it being released rapidly and forming HCl. The chloride concentration in the PRB and Beulah Zap coals is very low—0.0012 and 0.0010 wt%, respectively. For these coals the concentration of HCl of 1-2 ppm (essentially zero) in the reducing zone is at the instrument detection limit. The Illinois #6-1 coal on the other hand has a chloride concentration of 0.39 wt% (see Table 6) and thus produced measurable amounts of HCl in the reducing zone on the order of 150-250 ppm. The Mahoning and Indiana coals both had chloride contents of approximately 0.20 wt%, about half the amount found in the Illinois #6-1 coal. While the Indiana coal produced HCl in line with the Illinois coals, Mahoning produced a maximum of only 19 ppm—far less than half that of the Illinois #6-1 coal. Both Illinois #6-2 and Gatling coals produced results consistent with a linear relationship between HCl and coal chlorine. Figure 21 compares the measured HCl concentration with the amount of chloride in the coal for the reducing zone. With the exception of the Mahoning data (open marker), a somewhat linear trend is seen in the data.

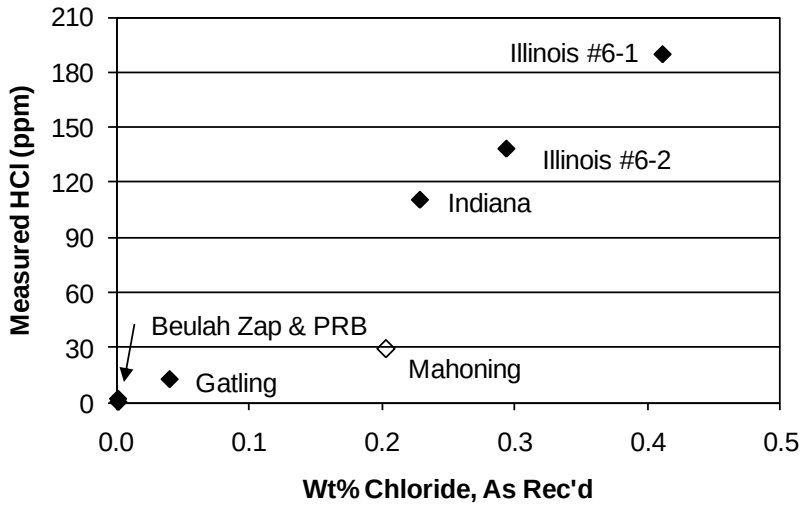

Figure 21: Comparison of Measured HCl to As Received Wt% Chloride for the Reducing Zone.

It was noted during some of the Indiana tests that HCl was slow to respond to changes in radial sampling location in the BFR. When CO and other gases would increase, HCl would rise only slowly. Some of these occurrences can be seen in Appendix A. It was later determined that the HCl concentration is affected greatly by the flow rate of gases through the sampling line. With low sampling flow rates, the HCl concentration would decrease and respond slowly to changes in radial sampling location. With high flow rates, the HCl concentration was higher and responded to sampling location changes just like other gases did. It is theorized that the HCl was reacting within the sampling line at the lower flow rates because of the increased residence time prior to quenching to 180°C. This same phenomenon of low HCl occurred in all the Mahoning tests, possibly creating the anomaly in the reported data above. The reason for the low HCl was not determined until after the Mahoning tests were completed. It is suggested that future work include repeating the Mahoning tests to determine if a low flow rate was indeed the cause of the lower measured HCl concentration.

In addition to chlorine forming HCl in the reducing zone, chlorine reportedly remains as HCl unless reacting with a metal surface where it forms $FeCl_2$. Gibb's findings correlate well with the measured HCl data. HCl is formed in the reducing zone and remains as HCl in the oxidizing zone. This appears consistent with the measured data with Indiana and Mahoning coals being the exceptions. For both of these coals, low sampling flow rates in the oxidizing zone are suspected.

4.1.6 Hydrogen Gas

Hydrogen is the final species given in the tables and is the only species in addition to O_2 that was obtained with the GC. The H_2 is highest in the richest locations and drops to zero in fuel-lean locations. In equilibrium calculations, hydrogen concentrations are typically on the

order of about half the concentration of CO. The ratio of H_2 to CO varies from approximately 1/4 to 1/2 for the majority of the measured data.

4.2 Oxidizing Zone Gas Sampling Results

This section presents the combustion gas species for the oxidizing region where the target S.R. was 1.15. Results from the oxidizing region for the seven tested coals are shown in Table 19 – Table 25.

4.2.1 Carbon Monoxide and Carbon Dioxide

Ideal combustion concludes that all carbon will eventually become CO_2. In the oxidizing region, combustion is more complete than in the reducing zone and the CO is almost completely converted to CO_2. Because of the addition of burnout air, on the order of ~30% by volume to the mixture, the concentration of CO_2 should decrease in the oxidizing zone compared to the reducing zone unless additional CO_2 is formed. The data are consistent with CO being converted to CO_2 between the reducing and oxidizing zones.

4.2.2 Water

The reduction in water concentration between the reducing and oxidizing zones can also be explained by dilution from the tertiary air. In all cases, the water concentration decreases when traveling from the reducing to oxidizing zone. If the mass of water were to remain the same between the two combustion zones, the addition of tertiary air in the oxidizing zone should decrease the water concentration by about 30% on a relative basis. Like carbon, not all of the hydrogen is immediately oxidized in the reducing zone and some water is formed between the two measurement locations. For example, H_2 measured in the reducing zone is converted to H_2O

in the oxidizing zone. Other hydrocarbons are also present in the reducing zone, seen in Appendix A. When comparing the percent change in the H_2O measurement between reducing and oxidizing zones for each coal, it varies widely. One possible reason for this inconsistency is the completeness of combustion in both the reducing and oxidizing zones.

4.2.3 Oxygen

The O_2 measurements in the oxidizing region are more uniform, indicating better mixing than in the reducing section. O_2 tends to average close to three percent in the oxidizing region for most coals. Beulah Zap is one exception because, as previously discussed, there was air entrainment in the primary air line that allowed excess oxygen into the reactor during that test. The data are correct according to the conditions they were recorded in; there was not an issue with the instruments used to obtain the measurements).

Table 19: Illinois #6-1 – Axial Distance 217 cm.

Dist. (cm)	CO (ppm)	CO_2 (%)	H_2O (%)	H_2S (ppm)	HCl (ppm)	NO (ppm)	SO_2 (ppm)	SO_3 (ppm)	H_2 (%)	O_2 (%)
10	92	13.66	6.09	9	152	147	1834	36	0.00	5.69
20	163	15.91	6.83	2	179	153	2114	43	0.00	3.31
30	2129	16.45	7.82	15	247	146	2381	46	0.00	1.46
40	96	16.91	7.65	-53	185	131	2281	42	0.00	1.81
50	306	16.98	7.92	10	190	140	2333	43	0.00	1.92
60	423	16.24	7.76	0	182	153	2233	38	0.00	2.45
70	690	13.40	6.78	27	196	168	1902	33	0.00	2.92

Table 20: PRB – Axial Distance 243 cm.

Dist. (cm)	CO (ppm)	CO_2 (%)	H_2O (%)	H_2S (ppm)	HCl (ppm)	NO (ppm)	SO_2 (ppm)	SO_3 (ppm)	H_2 (%)	O_2 (%)
10	11	14.93	10.83	54	2	272	115	6	0.00	3.52
20	21	14.53	10.91	-44	1	237	120	6	0.00	2.73
30	23	17.01	12.67	11	2	251	182	10	0.00	2.36
40	59	17.26	13.10	-3	2	243	203	8	0.00	1.41
50	50	17.60	13.02	28	3	254	193	10	0.00	1.80
60	24	16.77	12.57	40	3	270	162	8	0.00	2.41
70	20	13.33	10.94	4	3	257	102	7	0.00	3.82

Table 21: Beulah Zap – Axial Distance 243 cm.

Dist. (cm)	CO (ppm)	CO_2 (%)	H_2O (%)	H_2S (ppm)	HCl (ppm)	NO (ppm)	SO_2 (ppm)	SO_3 (ppm)	H_2 (%)	O_2 (%)
10	9	10.67	8.57	59	2	304	273	2	0.00	5.31
20	22	13.69	11.03	178	2	264	458	9	0.00	7.33
30	20	13.74	11.20	172	2	269	481	11	0.00	5.18
40	16	13.64	11.28	191	2	264	494	12	0.00	5.31
50	15	13.26	11.17	162	2	261	476	10	0.00	5.97
60	23	12.85	11.17	135	1	253	453	7	0.00	6.69
70	40	12.46	12.68	201	1	250	402	7	0.00	6.69

Table 22: Mahoning – Axial Distance 243 cm.

Dist. (cm)	CO (ppm)	CO_2 (%)	H_2O (%)	H_2S (ppm)	HCl (ppm)	NO (ppm)	SO_2 (ppm)	SO_3 (ppm)	H_2 (%)	O_2 (%)
10	324	16.36	7.88	-56	7	234	1546	37	0.00	2.54
20	193	16.39	10.52	-10	9	229	1692	38	0.00	2.70
30	321	16.58	11.61	72	10	230	1668	35	0.00	2.86
40	83	15.43	10.03	-50	12	251	1501	31	0.00	4.55
50	82	15.31	8.50	-48	11	254	1434	34	0.00	3.89
60	220	15.89	7.81	-31	13	266	1466	37	0.00	4.05
70	149	15.41	6.94	-11	14	282	1374	33	0.00	4.89

Table 23: Indiana – Axial Distance 250 cm.

Dist. (cm)	CO (ppm)	CO_2 (%)	H_2O (%)	H_2S (ppm)	HCl (ppm)	NO (ppm)	SO_2 (ppm)	SO_3 (ppm)	H_2 (%)	O_2 (%)
10	607	13.32	8.45	-4	7	110	889	29	0.00	2.77
20	465	13.28	7.97	-13	9	143	882	26	0.00	3.12
30	701	13.25	7.32	-5	16	154	870	28	0.00	3.71
40	769	13.23	7.24	-27	19	148	868	25	0.00	3.57
50	750	13.10	7.13	35	24	152	853	25	0.00	3.60
60	118	12.91	6.91	-47	23	153	813	25	0.00	3.95
70	389	12.79	6.99	-5	26	147	803	24	0.00	3.81

Table 24: Illinois #6-2 – Axial Distance 257 cm.

Dist. (cm)	CO (ppm)	CO_2 (%)	H_2O (%)	H_2S (ppm)	HCl (ppm)	NO (ppm)	SO_2 (ppm)	SO_3 (ppm)	H_2 (%)	O_2 (%)
10	493	14.01	6.77	7	136	182	2094	54	0.00	2.63
20	95	13.86	6.29	-91	128	154	1989	49	0.00	3.55
30	152	13.67	6.45	28	146	192	1970	46	0.00	3.62
40	237	13.55	6.44	-11	146	177	1962	54	0.00	3.53
50	608	13.22	6.64	-33	148	174	1949	54	0.00	3.31
60	464	14.80	6.88	-15	134	186	2208	46	0.00	1.88
70	1300	15.13	7.41	14	158	177	2284	54	0.00	1.39

Table 25: Gatling – Axial Distance 243 cm.

Dist. (cm)	CO (ppm)	CO_2 (%)	H_2O (%)	H_2S (ppm)	HCl (ppm)	NO (ppm)	SO_2 (ppm)	SO_3 (ppm)	H_2 (%)	O_2 (%)
10	74	15.00	6.83	59	-2	113	2788	54	0.00	3.79
20	74	14.96	6.97	59	1	108	2823	60	0.00	3.68
30	106	15.09	7.00	52	5	112	2828	56	0.00	3.86
40	74	14.36	6.74	26	6	118	2650	53	0.00	4.83
50	73	13.79	6.55	36	6	115	2497	46	0.00	5.42
60	93	14.82	6.85	97	6	109	2711	50	0.00	4.22
70	71	14.26	6.71	58	7	116	2574	52	0.00	4.67

4.2.4 Sulfur-containing Species

As mentioned, H_2S is expected to become SO_2 in the oxidizing zone. This result is observed in the data where H_2S is typically within a range from negative to positive 50 ppm, or essentially zero for each coal. Figure 22 illustrates this for the Illinois #6-1 coal and very similar data can be seen for each coal in Table 19 – Table 25. The uncertainty of the SO_2 measurement in Figure 22 is within 1% of the measured value.

As SO_3 is transported from the reducing to oxidizing condition, it remains a small (1-3%) fraction of the total sulfur. The amount of SO_3 increases with increasing sulfur in the coal. Both of these results are in agreement with the cited literature (Srivastava et al, 2004).

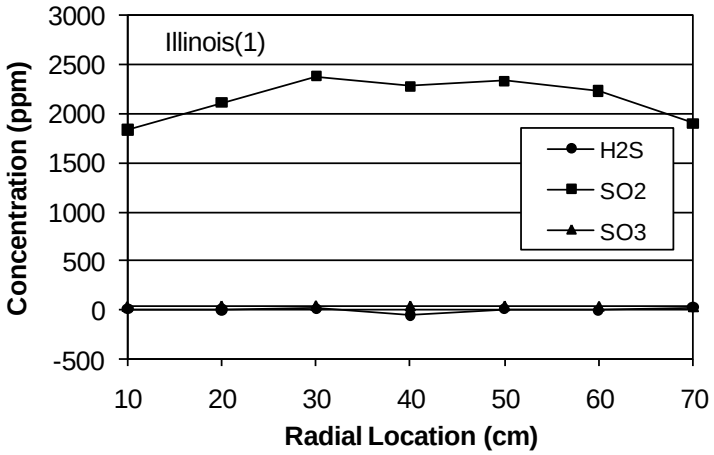

Figure 22: Concentrations of H_2S, SO_2, & SO_3 for Illinois #6-1 Coal - Axial Location 217 cm.

The SO_2 values in the oxidizing zone are similar in magnitude to those in the reducing zone; however, as noted earlier the tertiary air is added between the two measurements diluting the rich mixtures by approximately 30%. Since the measured SO_2 values in the oxidizing zone are not lower there is clearly an indication of sulfur release between the reducing and oxidizing zone measurements. In order to determine how much sulfur was released, the total sulfur in the reducing zone gases was multiplied by the ratio of the reducing zone air flow rate to the total air flow rate to correct the reducing zone concentrations to the equivalent concentration in the oxidizing zone. The total sulfur release was compared to the maximum possible according to equilibrium calculations. Table 26 shows the percent increase in total measured sulfur between the reducing and oxidizing zone (absolute basis). The Beulah Zap data shows a slight decrease in total sulfur between the two zones that is within the measurement uncertainty. The other coals all show an increase in gas phase sulfur between the two measurement locations. The change in sulfur for both low rank coals, Beulah Zap and PRB, is small. The high rank coals showed a sulfur increase of 5-20%.

Table 26: Comparison of Total Measured Sulfur in the Reducing and Oxidizing Zones. The Reducing Zone Sulfur Data was Normalized to be on the Same Dilution Basis as the Oxidizing Zone.

Coal	Reducing Zone Sulfur (ppm)	Oxidizing Zone Sulfur (ppm)	Percent Increase
Illinois #6-1	1723	2196	10
PRB	164	175	1
Beulah Zap	634	599	-8
Mahoning	1283	1542	14
Indiana	716	871	8
Illinois #6-2	1739	2102	20
Gatling	2541	2804	5

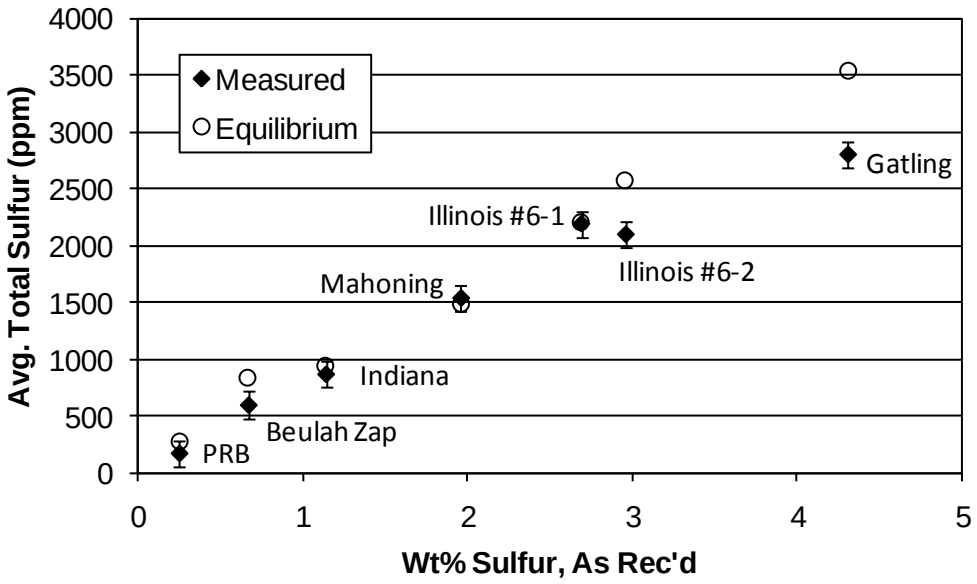

Figure 23: Comparison of As Rec'd Sulfur and Total Measured Sulfur in the Oxidizing Zone.

In the reducing zone, the fraction of coal sulfur released to the four measured sulfur containing gases was relatively constant. Since the gases are better mixed and more complete combustion has occurred, the same trend is expected in the oxidizing zone. Figure 23 shows the comparison of as received sulfur with the sum of H_2S, SO_2, and SO_3 for each coal in the oxidizing zone. The apparent linear trend seen in the reducing zone is even clearer in the oxidizing zone.

4.2.5 Hydrogen Chloride

A plot of measured HCl in the coal as a function of coal chlorine is shown in Figure 24. As discussed in the literature review, chlorine is expected to form HCl rapidly in a reducing environment and stay in that form throughout oxidation unless interacting with a surface or particles (Gibb 1983). Data from Illinois #6-1 and Illinois #6-2 coals appear to support Gibb's conclusion. The average HCl concentration of the Illinois #6-1 coal in the oxidizing zone was

measured to be 190 ppm and that of Illinois #6-1 measured 143 ppm, similar to the results of the reducing zone (167 and 157 ppm, respectively). The same argument can be made here as with the sulfur that the oxidizing concentrations should be lower than the reducing zone concentrations due to dilution of the tertiary air. Thus there is an indication of additional HCl formation between the reducing and oxidizing zones. The concentrations of HCl in the oxidizing zone are much lower for Indiana and Gatling than in the reducing zone. As discussed in Chapter 4.1.5, it was determined during additional testing that HCl was significantly affected by the flow rate of gases traveling through the sampling line. These flow rates were definitely lowered during the Indiana and Mahoning tests. Gatling is uncertain, but the HCl data in the oxidizing zone appears too low to fit a linear trend. Therefore, the accuracy of the HCl measurements is questionable and needs to be determined more accurately by performing repeat tests on at least the Mahoning and Indiana coals.

In addition to labeling each data point in Figure 24, the HCl data that is suspect has been plotted with open markers. If the data are taken to be correct, there appears to be a nonlinear relationship between coal chlorine and HCl. These data suggest a threshold level of coal chlorine required before significant amounts of gas phase HCl is produced. Given the problems encountered with the HCl measurement, such a conclusion would be inappropriate at this time. Additional insights will be given in the discussion of the data in the next chapter and additional data will be needed to provide a strong conclusion.

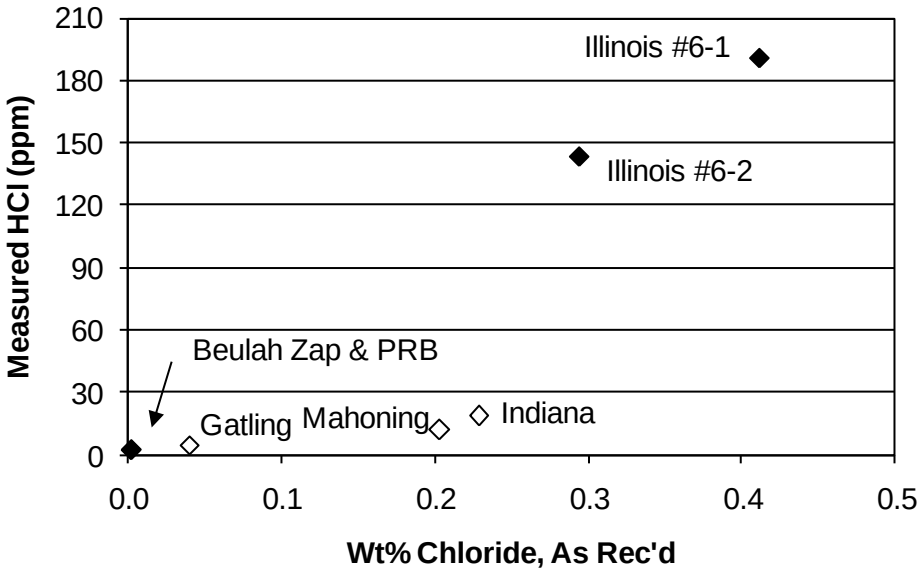

Figure 24: Comparison of Measured HCl to As Received Wt% Chloride for the Oxidizing Zone.

4.2.6 Hydrogen Gas

Hydrogen gas is not expected in the oxidizing region because it is expected to oxidize when the staged air is added. Recorded data match this expectation with no H_2 recorded in the oxidizing zone. In some cases, small amounts of H_2 (2-17ppm) were measured in the oxidizing region. They cannot be seen in the tabulated results because H_2 is reported in %, not ppm and should be considered background noise.

5 DISCUSSION OF RESULTS – SULFUR AND CHLORINE GAS DATA

Two of the most significant coal elements relative to fireside gas corrosion are sulfur and chlorine. Sulfur and chlorine containing gas species are difficult to measure and detailed combustion zone measurements of H_2S, SO_2, SO_3, COS, and HCl are a unique contribution of this work. This chapter will discuss these species measurements in detail.

Equilibrium calculations can serve as a guide for the interpretation of measured gas concentrations. Equilibrium calculations are presented for three coals, including Illinois #6, PRB, and Gatling. These coals were selected because they differ substantially in chlorine and sulfur content. Additionally, PRB is a lower rank coal with relatively high moisture content. Equilibrium calculations were completed using a publically available equilibrium code written by McBride and Gordon (1994; 1996) at NASA-Glenn. An equilibrium calculation requires the elemental composition of the fuel and oxidizer, temperature, and pressure to be defined. The elemental composition of the coal was obtained through an ultimate analysis and a standard ash analysis for each coal, as reported in Chapter 3.2.1. In the calculations, both average and local S.R.'s have been used to make comparisons with equilibrium results.

5.1 Equilibrium Trends for Sulfur Containing Gases

Equilibrium products greater than 10^{-14} in concentration produced by the NASA equilibrium program for the Illinois #6 coal include: COS, CS_2, CaS(cr), H_2S, S, SH, SN, SO, SO_2, SO_3, S_2, S_2O, S_3, and SiS. Note that this list is incomplete to cover all the possible sulfur

containing species that can form or that were considered by the equilibrium program. Of all available species, only five were significant (> 1 ppm) over a range of 0.8 – 1.0 S.R. and a temperature range of 1300 – 2400 K which represents the range of gas temperatures thought to be possible in the reducing region of the BFR. The five significant and measurable gases are COS, H_2S, SO_2, SO_3, and CaS(cr). CaS(cr) is a solid phase sulfur bearing compound that was not measurable with the instruments used in this research.

5.1.1 Reducing Zone Equilibrium Trends for H_2S, COS and SO_2

In order to understand the major trends produced by equilibrium, H_2S and SO_2 are shown in Figure 25 for two stoichiometries over a range of temperatures with the Illinois #6-2 coal. At S.R. = 0.9 and temperatures above 1800 K, sulfur is seen in the figure to be primarily in the form of SO_2 with little or no sulfur as H_2S. As temperature is decreased, sulfur is converted from SO_2 to H_2S such that the two concentrations are approximately equal at 1300 K. Lowering the gas temperature at a fixed fuel rich stoichiometry therefore shifts the equilibrium from SO_2 to H_2S. A second trend seen in this figure is that decreasing the S.R. from 0.9 to 0.8 shifts the transition of SO_2 to H_2S to a higher temperature. At an S.R. of 0.8, the crossover point where the equilibrium concentration of H_2S approximately equals that of SO_2 is at 1500 K. Equilibrium calculations show that H_2S can be created by decreasing the S.R. or decreasing temperature under reducing conditions. The trend of increasing H_2S with decreasing S.R. is seen in all of the fuel rich gas data for all of the coals shown in Table 11 – Table 17.

The equilibrium results for all sulfur species from the Illinois #6 coal greater than 1 ppm are shown in Figure 26 as a function of S.R. at 1400 K. This figure again shows that decreasing the S.R. decreases SO_2 and increases H_2S. As the S.R. decreases to 0.80, approximately 60 percent of the sulfur is in the form of H_2S while the remaining 40 percent appears to be divided

evenly among the other four gases. In addition to H_2S, several other sulfur species including COS, S_2, and CaS(cr) are predicted. This result shows that a decrease in SO_2 in fuel rich regions will not be matched by an equal increase in H_2S because additional species are being formed. This trend also agrees with the measured data.

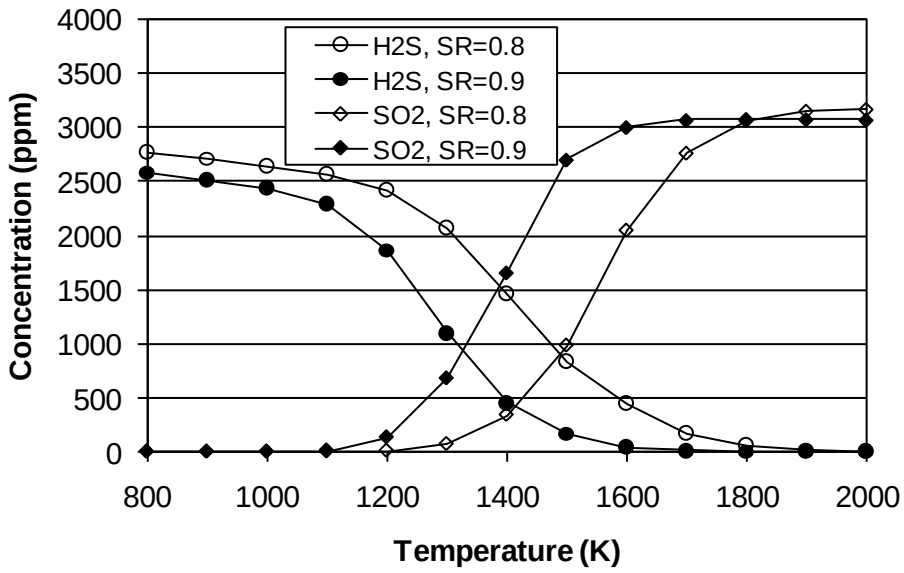

Figure 25: Equilibrium Concentrations of H_2S and SO_2 for an Illinois #6-2 Coal at Two Stoichiometries.

The equilibrium data from the Gatling coal (Figure 27) is similar to that of Illinois #6, except the magnitudes of all species are greater as would be expected by the higher sulfur content of the Gatling coal. The PRB equilibrium and measured gas data showed some differences from the Illinois #6 and Gatling coals. Equilibrium results for the PRB coal are shown in Figure 28. The magnitude of the y-axis is approximately one tenth that of the Illinois #6 coal (Figure 26) as would be expected with approximately an order of magnitude less sulfur in the coal. Under fuel rich conditions, the amount of S_2 and CaS remain negligible for the PRB coal while for the Illinois #6 and Gatling coals they were similar in magnitude to COS. The PRB equilibrium results suggest that the ratio of H_2S to SO_2 would be greater than those of

Illinois #6 and Gatling coals. From the data, this appears to be true although the uncertainty of the H_2S measurement is clearly too large to draw any strong conclusions. The maximum H_2S to SO_2 ratio for the PRB coal is 1.36 whereas it is only 0.72 and 0.34 for Illinois #6 and Gatling, respectively.

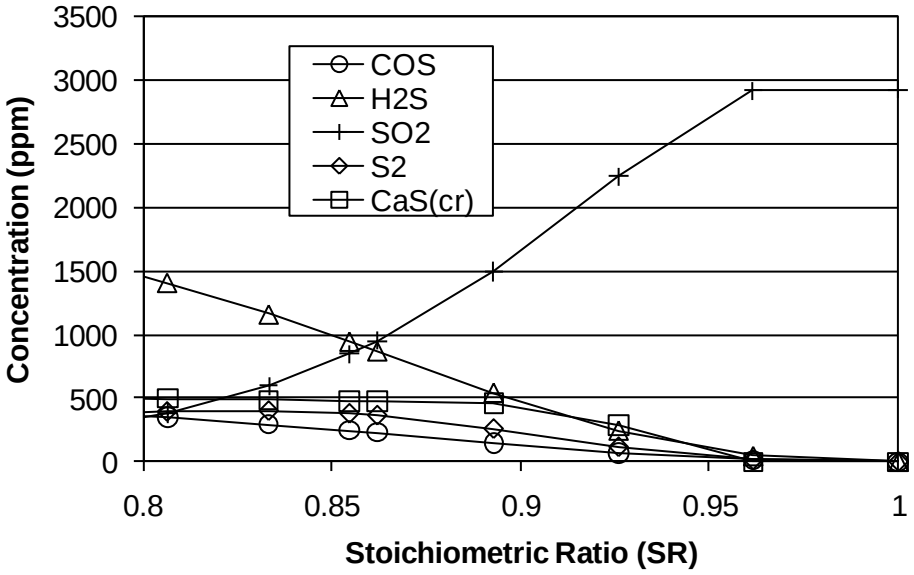

Figure 26: Illinois #6-2 coal. Significant Sulfur-bearing Equilibrium Species at 1400 K.

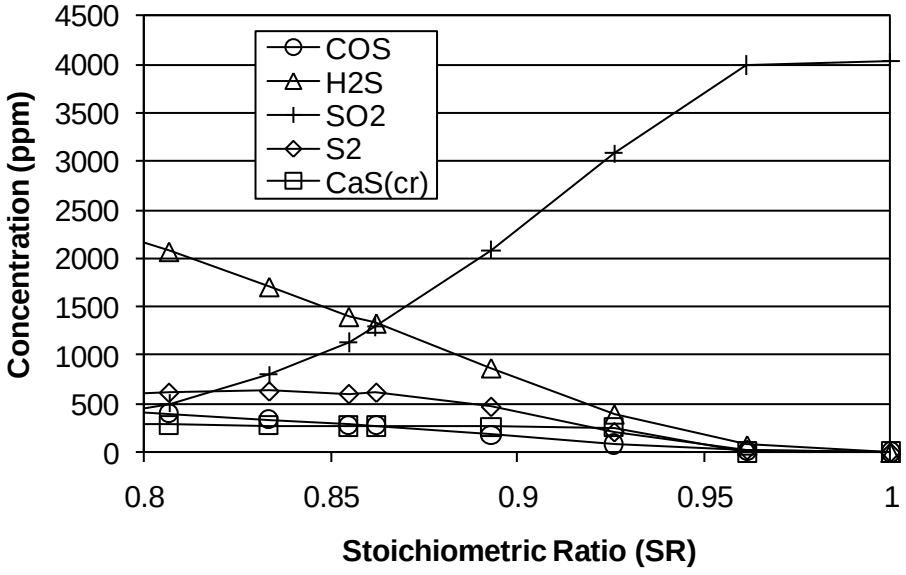

Figure 27: Gatling coal. Significant Sulfur-bearing Equilibrium Species at 1400 K.

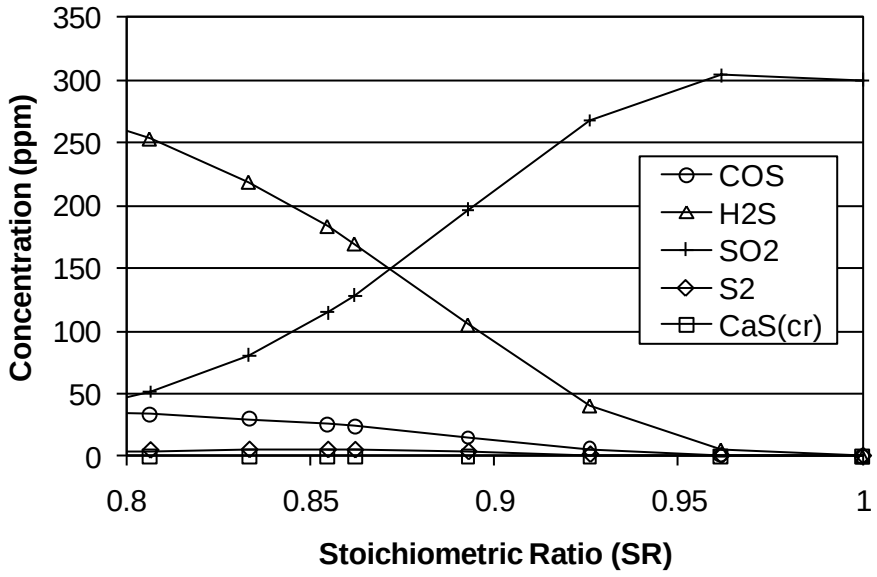

Figure 28: PRB Coal. Significant Sulfur-bearing Equilibrium Species at 1400 K.

5.1.2 Comparison of Total Coal and Gas Phase Sulfur

Given the fairly comprehensive measurement of gas phase sulfur species that were measured, an estimation of the fraction of total sulfur in the gas phase becomes possible. It is very difficult to produce an accurate determination of the total mass of sulfur in the gas phase because of the difficultly of converting a concentration measurement into a mass measurement. To do so requires the density of the gas, which is unknown. Damstedt (2007) used a method for estimating the mass flux of measured elements by integrating the product of the local mass flux and the measured mass fraction of a species. Doing so required the assumption that mass flux was uniform radially across the reactor and that the gas species concentrations were symmetrical. Both of these assumptions are suspect in our particular data although such an approach could be used to provide an estimate.

An alternative method is to compare the measured gas concentrations from an equilibrium calculation with the measured data. The same basic difficulties arise in making the comparison—the temperature and local stoichiometric ratio of the measured locations are not known. An average S.R. of 0.85 in the reducing zone and 1.15 in the oxidizing zone were used in conjunction with an estimated temperature of 1400 K to make the comparison.

The average of the total of all measured sulfur-bearing gas species are compared with the total determined by equilibrium for the three coals at an S.R of 0.85 and temperature of 1400 K in Table 27. The table shows that a large fraction (62-79%) of the coal sulfur is found in the four measured gas species (SO_2, H_2S, COS, and SO_3) for all three coals.

Table 27: Comparison of Total Measured Sulfur Species and Total Equilibrium Sulfur Species at S.R. = 0.85 and 1400K.

Coal	Measured (ppm)	Equilibrium (ppm)	% of Equilibrium
PRB	209	324	65
Illinois #6-2	2035	3259	62
Gatling	3388	4303	79

Because of the uncertainty of the measurement associated with the unknown temperature and local S.R.'s discussed above, it can only be concluded that a large fraction of the coal sulfur is being released. Clearly, some of the sulfur from the coal ends up in the solid phase in the deposit and ash. Deposit analyses from coal-fired boilers in the near burner region suggest not all pyritic sulfur in the coal is available for reaction which may account for some of the sulfur not being measured. Additional insight could be gained by sampling particles at multiple axial locations in the BFR and analyzing them for sulfur content. This analysis was not performed as part of this work but is a suggestion for future work.

5.2 Comparison of Local Measured Sulfur Gas Species with Equilibrium

5.2.1 Local Stoichiometric Ratio Calculation

To compare measured data with equilibrium calculations, the local stoichiometric ratio (S.R.) and temperature of each sampling location must be known. As discussed previously, the S.R. values are nominally 0.85 and 1.15 in the reducing and oxidizing regions, respectively. However, the S.R. is not constant within each region since the fuel and air are clearly not yet mixed, especially in the reducing region.

It is possible to estimate the local S.R. by using the measured product concentrations to determine the mixture fraction. A formal derivation of these calculations can be found in Appendix D but a brief overview will be discussed here. A similar method was introduced by Damstedt (2007).

The mixture fraction, *f*, is defined as the mass of the originating fuel divided by the total mass in the system. Mathematically, this is expressed as

$$f = \frac{m_f}{m_f + m_{air}} \tag{7}$$

where *m* is mass and the subscripts '*f*' and '*air*' refer to the fuel and air, respectively.

Next, the stoichiometric ratio (S.R.) is defined as the actual ratio of air to fuel $(A/F)_{act}$ divided by the stoichiometric ratio of air to fuel $(A/F)_{stoich}$. This is expressed as

$$SR = \frac{\left(\frac{m_{air}}{m_f}\right)_{act}}{\left(\frac{m_{air}}{m_f}\right)_{stoich}}. \tag{8}$$

These two equations can be manipulated and combined to produce the following:

$$f = \frac{1}{1 + SR\left(\frac{m_{air}}{m_f}\right)_{stoich}}. \tag{9}$$

Damstedt (2007) shows how the mass for fuel and air identified in Equation 7 can be related to the measured carbon containing species in the gas phase and the molecular weight of the mixture as shown in Equation 10. A derivation of Equation 10 can be found in Damstedt (2007).

$$f = \frac{MW_c \sum X_i C_i}{Y_c MW_{mix}}, \tag{10}$$

where MW_c and Y_c are the molecular weight and mass fraction (of the fuel) of carbon respectively and MW_{mix} is the molecular weight of the complete product gas mixture. X_i is defined as the mole fraction of each species while C_i is the number of carbon atoms in each species. Setting Equations (9) and (10) equal to one another yields an equation for the local S.R. value at any sampling location, expressed mathematically as

$$SR = \frac{\left[\frac{Y_c MW_{mix}}{MW_c \sum X_i C_i} - 1\right]}{\left(\frac{m_{air}}{m_f}\right)_{stoich}}. \tag{11}$$

A derivation, similar to Damstedt's (2007), of Equation 11 can be found in Appendix D. The derivation assumes the following:

1. The mass fraction of carbon in the fuel, Y_c, remains constant as the coal is burned (i.e., the coal burns as a homogenous mixture). A constant mass fraction requires for example that volatiles and char have the same composition. Though the amount of

carbon burned with each of these components is different, this disparity is not accounted for in the equations.

2. The molar density of the sampled mixture is constant during the sampling process. This would require the temperature of the sampled gas to remain constant.
3. The measured gases can produce an accurate approximation of the total gas molecular weight. The concentration of nitrogen is calculated as the difference of all measured gases and unity. If a significant amount of unmeasured gas is different in MW than nitrogen, the mixture molecular weight will be in error.

The CO_2 concentration is an important species for this calculation given the large amount of carbon contained in this gas. Unfortunately there is a considerable amount of uncertainty involved in this measured gas concentration. After correcting for differences in the dry and wet measurements of CO_2 obtained with the Horiba PG-250 and FTIR respectively, the two measurements were found to differ by about 10% (relative). The FTIR is capable of better resolution but CO_2 was not a matter of focus during FTIR calibration and analysis. The PG-250 is calibrated with calibration standard gases before each use and there is less reason to believe that its measurements are incorrect. The PG-250 was not used for all experiments however, so the FTIR measurements were used in reporting the data to maintain consistency.

The local temperature of gases at the measurement locations is also not known. This makes a direct comparison of the gas data and equilibrium calculations more difficult and less conclusive. Previous temperature measurements have been obtained by Nazeer et al (1999); and Tree and Clark (2000) in the BFR under similar conditions but with a different coal and a different burner. These measurements obtained with a suction pyrometer show maximum temperatures from 1500-1600 K.

Energy balance calculations to determine the gas temperature suggest temperatures above 1600 K are likely. If 1600 K is selected as the best estimate for the gas temperature, Figure 25 shows that the equilibrium sulfur will be almost exclusively in the form of SO_2. This equilibrium prediction is in conflict with the measured data which show substantial amounts of COS and H_2S. Possible explanations for this conflict are discussed below.

An investigation was made to determine at what temperature the equilibrium calculation could be made to best match the measured data. A comparison at 1300 K between the measured and equilibrium data for the Illinois #6 coal is shown in Figure 29. At this lower gas temperature, the measured H_2S, COS, and SO_2 appear to be in good agreement with the equilibrium calculation. Results for Gatling at 1500 K and PRB at 1300 and 1400 K are shown in Figure 30 and Figure 31, respectively. As with the Illinois #6 coal, PRB and Gatling trends can be matched with equilibrium calculations. One data point in the Gatling results (30 cm) did not match the trend of the other Gatling data. The S.R. calculated for this point was high because of an abnormally low CO_2 measurement. It is unknown why the CO_2 measured 2% lower than the previous and subsequent data and therefore this data point is seen as an outlier.

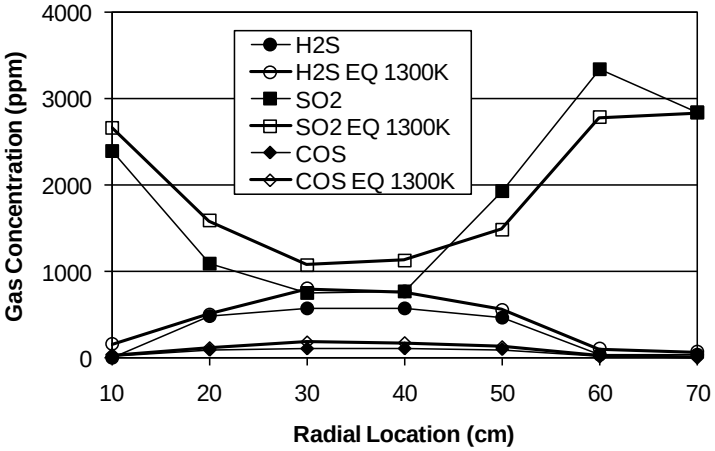

Figure 29: Illinois #6-2 Coal; Measured H_2S, SO_2, and COS vs. Equilibrium Calculations at 1300 K.

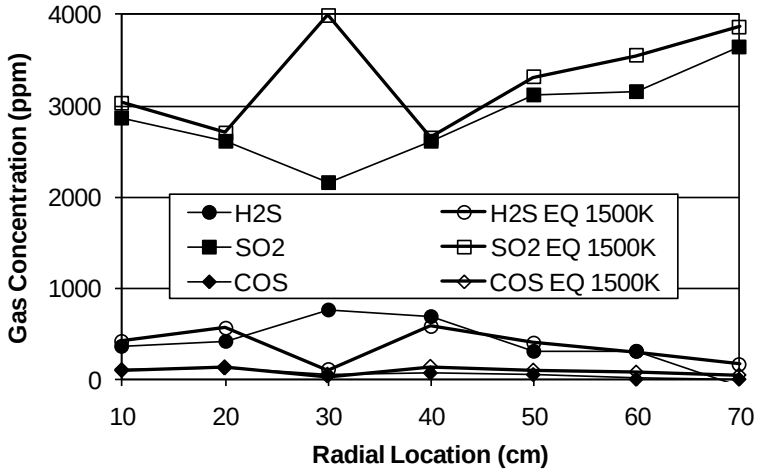

Figure 30: Gatling Coal; Measured H_2S, SO_2, and COS vs. Equilibrium Calculations at 1500 K.

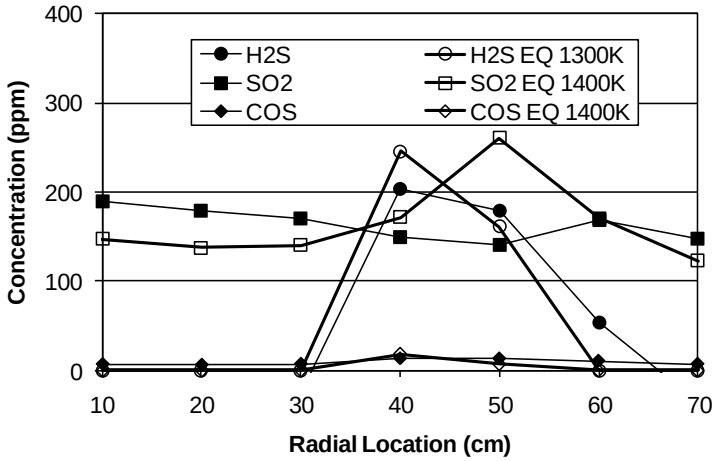

Figure 31: PRB Coal; Measured H_2S, SO_2, and COS vs. Equilibrium Calculations at 1300 & 1400 K.

The disparity in gas temperatures required to produce a match between measured and equilibrium concentrations cannot be explained by trends in adiabatic flame temperature or heating rates. The adiabatic flame temperature of each coal air mixture is within 50 K and all coals were fired at the same heating rate. These two factors should produce similar gas temperatures among the different coals.

At least two possible explanations exist for why the equilibrium temperature must be lower than the expected gas temperature in order to match the data. The first is that the gas composition is moving towards but is simply not in equilibrium. As noted in the literature

review, sulfur is thought to decompose from the coal primarily as H_2S and COS, but conversion from H_2S and COS to SO_2 and other species may be too slow to reach equilibrium making the ratio of H_2S to SO_2 higher than would be predicted by equilibrium. Regions which are fuel rich may be slower to move toward equilibrium leaving more H_2S and COS in these regions while fuel lean regions move more rapidly toward SO_2. Another possibility is that the gas temperature is decreasing during sampling and the equilibrium is shifted to lower temperatures during the sampling process. Knowing the flow rate through the gas sampling system and the area of the sampling line, the time required to quench the gas from the temperature at the sampling location down to 180 °C in the sampling probe was estimated to be 50-100 ms. The sample flow rate was not seen to influence sulfur measurements but it has been found to influence HCl values. If sulfur is still reactive during the sampling process and can shift from SO_2 to H_2S and COS while cooling, a similar process may be possible within a boiler as combustion gases approach boiler tubes.

SO_3 was not included in the equilibrium comparison because the data were too close to zero to be distinguished from the zero line and would have made the graph more cluttered and difficult to read. Equilibrium values for SO_3 are less than one ppm under fuel rich conditions at these temperatures. The measured values are higher than predicted by equilibrium, suggesting that SO_3 is formed rapidly from sulfur in the coal; however, reactions of SO_3 to the equilibrium products of H_2S, SO_2, and COS are too slow to reach equilibrium.

5.2.2 Oxidizing Zone

In the oxidizing zone, based on reported flue gas measurements, sulfur is expected to be primarily in the form of SO_2. This is in fact the case as seen in Table 19 – Table 25. When the Illinois #6-2, Gatling, and PRB coal data are compared with equilibrium calculations in the

oxidizing zone, trends match very well. This can be seen for any one of the coals in Figure 32 – Figure 34. The uncertainty of the SO_2 measurement is within 1% of the measured value.

Though not as strong as in the reducing zone, SO_2 is a mild function of temperature in the oxidizing zone according to equilibrium calculations. The Illinois #6-2 and Gatling coal sulfur is predicted to be SO_2 above 1400 K. Between 1000-1400 K, a fraction (5% at 1400 K and 20-30% at 1000 K) of the sulfur begins to be predicted in the form of SO_3 and CaSO4(solid). Even at temperatures as low as 1000 K, most Illinois #6-2 and Gatling sulfur is predicted to be SO_2.

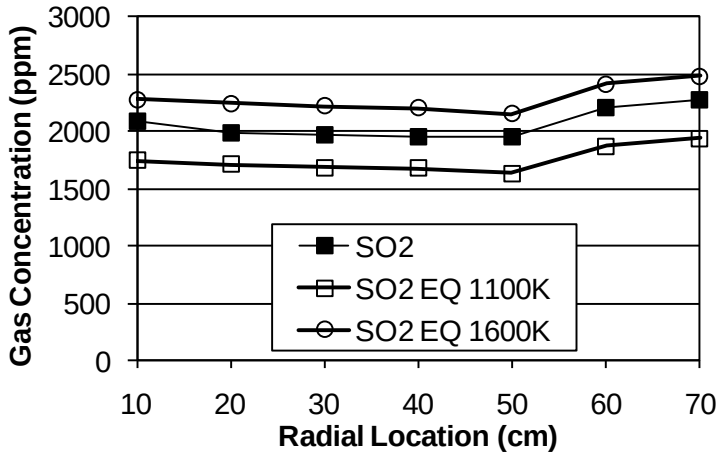

Figure 32**: Illinois #6-2 Coal; Measured SO_2 vs. Equilibrium Calculations at 1100 and 1600 K.**

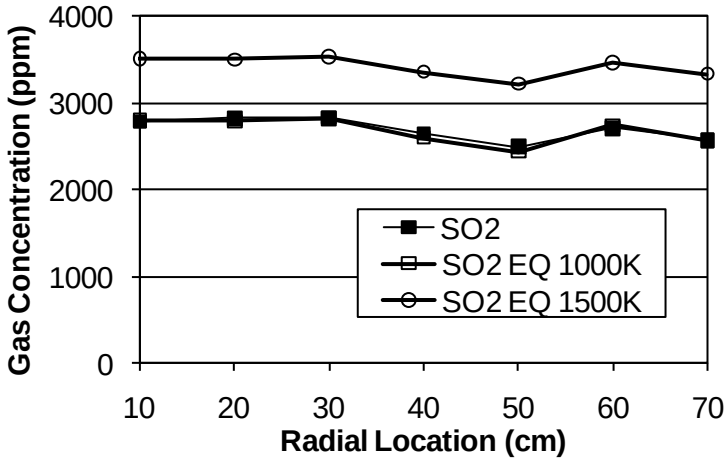

Figure 33: Gatling Coal; Measured SO_2 vs. Equilibrium Calculations at 1000 and 1500 K.

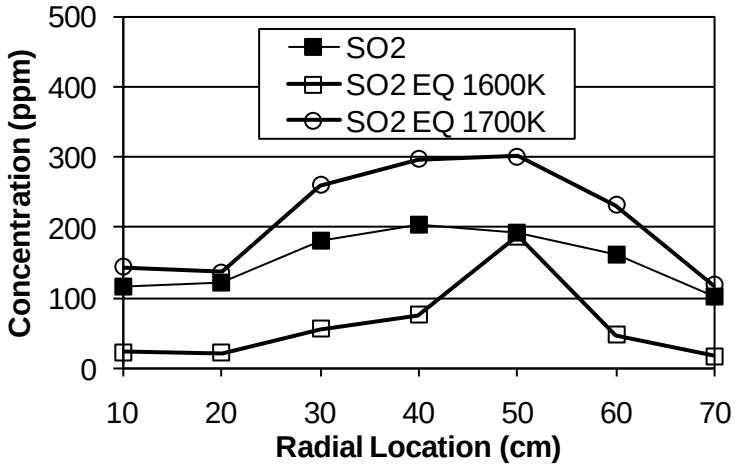

Figure 34: PRB Coal; Measured SO_2 vs. Equilibrium Calculations at 1600 and 1700 K.

PRB sulfur, however, is predicted to be SO_2 only at temperatures of 1700 K and above. As the temperature drops below 1700 K, equilibrium predicts PRB sulfur to be in the form of calcium sulfate ($CaSO_4$). $CaSO_4$ even dominates SO_2 at some fuel lean stoichiometries at 1700 K. Table 20 and Figure 34 show that PRB SO_2 data are between 100-200 ppm in the oxidizing zone. This large change in SO_2 between the locations close to the wall and the center of the BFR follow the equilibrium suggestion that some of the sulfur has been converted to $CaSO_4$.

The fact that SO_2 matches equilibrium trends does not indicate that the gas is actually in equilibrium. The PRB results, which matched equilibrium trends at a temperature much higher than expected, are a good example of this. From Nazeer's (1997) work, the temperature in the oxidizing zone is expected to be near 1300 K. It is possible that the gas mixture in the oxidizing zone is at the expected temperatures but the kinetics related to SO_2 converting to $CaSO_4$ could be slow enough to keep much of the sulfur in the gas phase. Regardless of the varying temperatures among the equilibrium comparisons of SO_2 in the oxidizing region, the trends match very well.

5.3 Chlorine

5.3.1 Reducing Zone

As mentioned previously, chlorine also participates in corrosion and is therefore of high interest. The only chlorine species measured in this research was hydrogen chloride, or HCl. According to Gibb (1983), 90-100% of evolved chlorine is in the form of HCl. Since less than 10% of the evolved chlorine is reportedly in other species, measuring only HCl appears to be reasonable when attempting to account for chlorine evolution as was done with sulfur.

When equilibrium calculations are performed for any of the coals with the as received constituents, the chlorine is predicted to be in the form of iron chloride ($FeCl_3$). It has been suggested by Baxter (2010) that only a small fraction of the iron is available for reaction because it is in stable forms within the coal. If iron is removed from the equilibrium input, the chlorine is calculated to be primarily in the form of KCl, NaCl, and HCl. However, according to Baxter (2010), not all the sodium (Na) and potassium (K) in coal are available for reaction either.

It has already been stated that some gases, such as SO_3, do not match equilibrium trends and it is clear that HCl does not match equilibrium calculations either since several elements had to be altered to achieve results similar to Gibb's findings. After altering the inputs for the coals used in the equilibrium comparison (Illinois #6-2, Gatling, and PRB) so that all chlorine was predicted to be in the form of HCl, no strong correlation can be drawn between measured and equilibrium values for any of the three coals, as shown in Figure 35 – Figure 37, respectively. Of the three coals, PRB matched equilibrium values the best but the low concentration of measured HCl (always less than 1 ppm) is well below the uncertainty of the HCl measurement and no quantitative conclusions can be drawn from this comparison.

Initially, equilibrium values at different temperatures were compared to the measured data. However, the equilibrium values from multiple temperatures were so similar that only one temperature (1500 K) was used. It is possible that, unforced, equilibrium calculations predict HCl to behave differently at different temperatures.

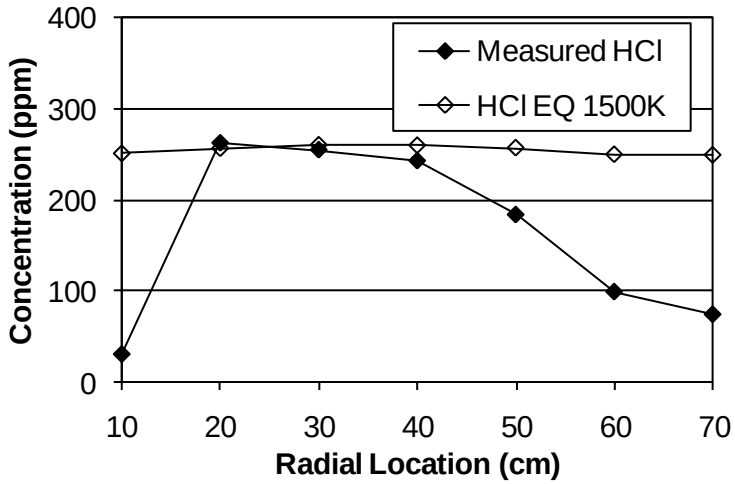

Figure 35: Measured and Equilibrium HCl at 1500K for the Illinois #6-2 Coal at an Axial Distance of 83 cm.

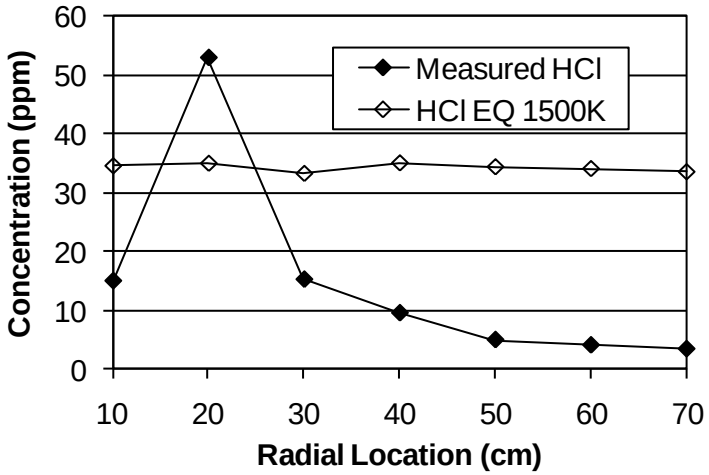

Figure 36: Measured and Equilibrium HCl at 1500K for the Gatling Coal at an Axial Distance of 97 cm.

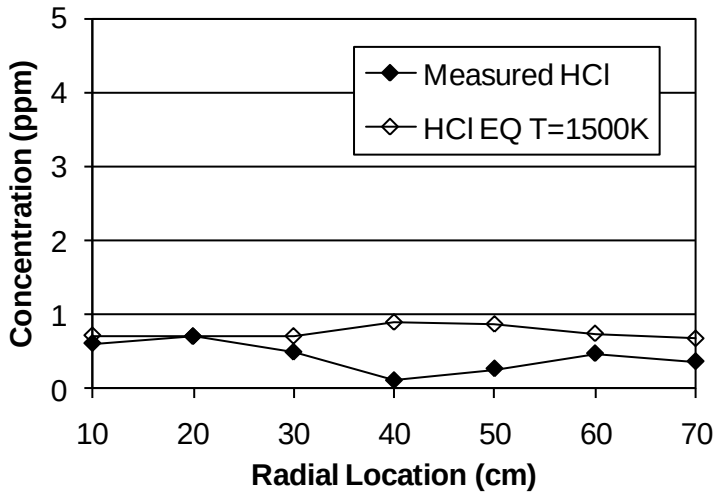

Figure 37: Measured and Equilibrium HCl at 1500K for the PRB Coal at an Axial Distance of 90 cm.

Recent findings have provided insight into the HCl measurements obtained in this research. It was discovered that the flow rate of gases through the sampling system causes wide variation in the HCl reading. As the flow of gases through the FTIR is increased, the measured HCl concentration increases also. Likewise, as the flow is decreased, the HCl concentration decreases. For a Kentucky #11 (Warrior) coal at the lowest (reasonable) flow rate through the FTIR, an HCl concentration was recorded that was 40% lower than the measurement obtained with a higher flow rate. This new discovery causes past HCl measurements to become suspect and could easily account for the poorly matched measured and equilibrium values shown for the Illinois #6-2, Gatling, and PRB coals.

5.3.2 Oxidizing Zone

In the oxidizing zone of the BFR, the gas mixture is more homogeneous because of the extra time given the gases to react and mix. Accordingly, the HCl concentrations in the oxidizing zone are more constant across the diameter of the BFR. This is seen in Table 19 – Table 25 and is easily seen with the Illinois #6-2 HCl data in Figure 38. The measured HCl data for the

Gatling and PRB coals is also somewhat constant but is at lower concentrations which cause the graphs of the data (Figure 39 & Figure 40) to appear otherwise. As discussed previously, HCl is considered neutral when considering its preferential existence in reducing and oxidizing stoichiometries. Because of this, HCl is expected to be present at similar concentrations as the reducing zone, with the dilution effect creating a slightly lower concentration.

The Illinois #6-2 HCl data accounts for approximately 75% of the total chlorine in the coal. The PRB data is relatively low and not adequate for proper comparison, but the Gatling HCl data is lower than expected. These data may have been affected by the flow rate of the gases through the sampling line, as discussed previously.

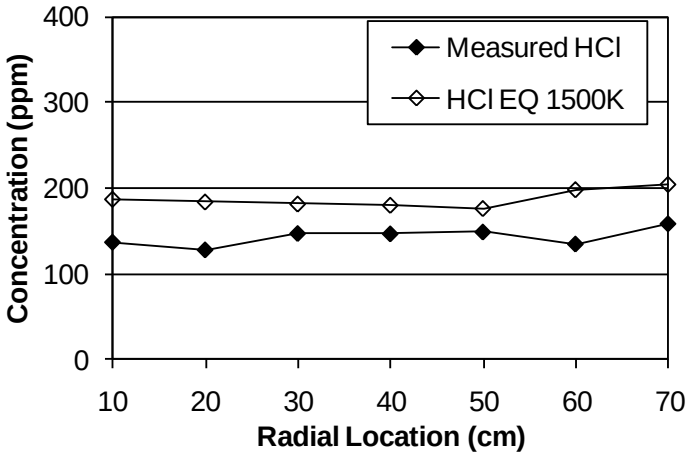

Figure 38: Measured and Equilibrium HCl at 1500K for the Illinois #6-2 Coal at an Axial Distance of 257 cm.

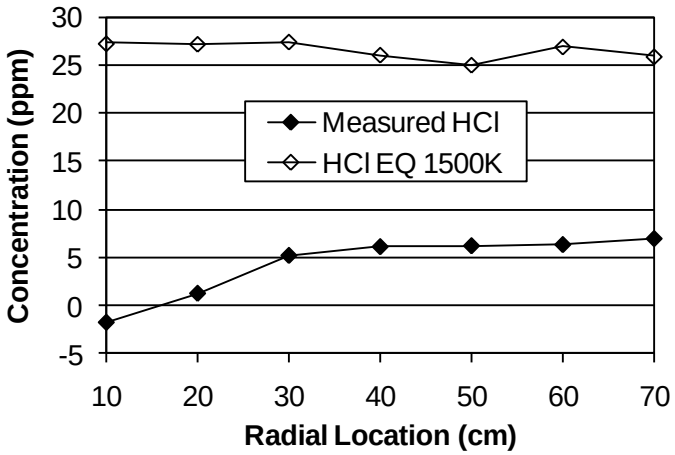

Figure 39: Measured and Equilibrium HCl at 1500K for the Gatling Coal at an Axial Distance of 243 cm.

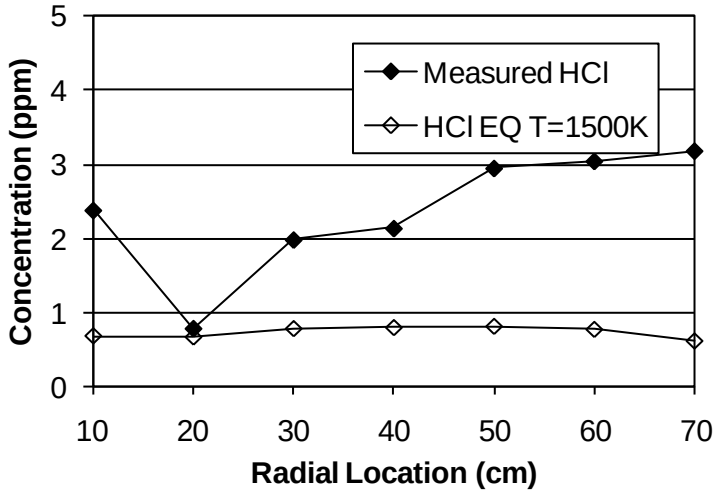

Figure 40: Measured and Equilibrium HCl at 1500K for the PRB Coal at an Axial Distance of 243 cm.

6 SUMMARY AND CONCLUSIONS

Knowing the boiler gas phase composition is critical to understanding and minimizing the corrosion rates of water walls and superheater tubes. Sulfur- and chlorine-bearing species are of particular interest because of their significant contribution to these corrosion rates. Combustion in the BFR was staged to simulate both near-burner (S.R. = 0.85) and superheater (S.R. = 1.15) conditions.

Measurements of eleven species under both reducing and oxidizing conditions are reported. Deposit samples were obtained adjacent to the gas samples but are not reported. For all coals, the gas measurements showed a low-S.R. reducing zone in the center of the BFR near the burner, transitioning to an oxidizing environment near the walls. CO values were in the range of 2.5 – 4% in the richest regions. Oxygen was near but typically not zero (0.5 – 1%) in regions of relative high CO. In the oxidizing zone, the gas mixture was somewhat mixed with relatively flat profiles for all measured gases. O_2 concentrations ranged from 2.5 – 5% depending of the coal and/or location. The gas species data are self-consistent showing expected trends between the major species.

More than 60% of the sulfur for each coal was released into the gas phase while in the reducing zone. Additional sulfur, dependent of coal rank, was released between the reducing and oxidizing zones during char burnout. Total sulfur release between the reducing and oxidizing zones varied among the coals but was greater for the higher rank coals. The total measured sulfur (sum of H_2S, SO_2, SO_3, and COS) was relatively linear with the as received coal sulfur in both

the reducing and oxidizing zones. In the oxidizing zone, most of the sulfur converted to SO_2 with a small (1-3%) fraction remaining as SO_3.

In the reducing zone, H_2S, SO_2, and COS follow equilibrium trends at temperatures of 1300 – 1500K. The highest values of H_2S and COS were recorded in low-S.R. conditions. SO_2 was lowest in these same locations, increasing with higher S.R.'s. The gas temperatures were not measured in this research but from Nazeer (1997), they are expected to be near 1500 – 1600 K in the reducing zone. There are two possible reasons that explain why the measured data match equilibrium at lower than expected temperatures: 1. The quench time down to 180 °C is long (50-100 ms) relative to the kinetics and the gases continue to react, creating concentrations of H_2S and SO_2 consistent with lower temperatures. 2. Fuel sulfur when released originally forms H_2S and is slow to transition to SO_2 which is the preferred equilibrium state at higher temperatures.

In the oxidizing zone, SO_2 matched equilibrium trends but at varying temperatures. Expected temperatures in the BFR for the oxidizing zone are near 1300 K. The temperature of equilibrium calculations that matched the measured data best were lower than expected for the Illinois #6-2 and Gatling coals. For the PRB coal, the temperature of equilibrium calculations that matched the measured data best was higher than expected.

Equilibrium calculations show the most stable forms of chlorine are, in order: $FeCl_2$, KCl, HCl, and NaCl. When HCl is compared to the total amount of gaseous chlorine possible, the measured Illinois #6-2 data reports that 75% of the chlorine in the coal was in the form of HCl in the oxidizing zone. Therefore, the measured HCl does not match equilibrium unless iron and potassium are made unavailable. Even with these two elements unavailable, HCl is predicted to be somewhat constant in similar stoichiometric conditions. Most of the HCl data do not match

this equilibrium trend, and a possible reason for HCl not matching better with the total chlorine possible is the fact that the HCl concentration is greatly affected by the flow rate of gases through the gas sampling line.

It is anticipated that these results will be valuable to the energy industry. The conditions in which they were obtained cause the data to be directly applicable to pulverized coal combustion with air, in both rich and lean stoichiometries. Such a comprehensive set of data have not yet been measured in a coal-fired boiler or boiler-like conditions. With the data, correlations between coal chemistry, gaseous combustion products, and corrosion can be created. With this increased understanding the amount of corrosion incident in a commercial boiler may be reduced, allowing for increased efficiencies and, in turn, increased boiler availability and reliability.

REFERENCES

Babcock & Wilcox Company (2010). "Boilers." Available from http://www.babcock.com/products/boilers/. Internet; accessed 02 February 2010.

Bassilakis, R., Y. Zhao, P.R. Solomon, M.A. Serio, (1993). "Sulfur and Nitrogen Evolution in the Argonne Coals: Experiment and Modeling." *Energy & Fuels*, 7(6), 710-720.

Baxter, L., Personal Communication. Brigham Young University 04Apr2010.

Beér, J.M., N.A. Chigier. *Combustion Aerodynamics*. London: Applied Science Publishers Ltd, 1972, pp. 113-114.

Boll, R.H., H.C. Patel, (1961). "The Role of Chemical Thermodynamics in Analyzing Gas-side Problems in Boilers." *Transactions of the American Society of Mechanical Engineers, Journal of Engineering for Power, series A*, 83(4), 451-467.

Bosch-Charpenay, S. Personal Communication. MKS Online Products, 18Feb2010.

Boudou, J.P., M. Nip, J.J. Boon, J. Boulegue, J.W. de Leeuw, L. Malechaux, (1987). "Identification of Some Sulphur Species in a High Organic Sulphur Coal." *Fuel*, 66(11) 1558-1569.

Brunner, D.R., (2011). *Deposit Composition for a Suite of Coals in Staged Combustion*. Master's Thesis, Brigham Young University. Thesis Expected April 2011.

Calkins, W.H., (1987). "Investigation of Organic Sulfur-containing Structures in Coal by Flash Pyrolysis Experiments." *Energy & Fuels*, 1, 59-64.

Chou, S.F., P.L. Daniel, A.J. Blazewicz, R.F. Daniel, (1986). "Hydrogen Sulfide Corrosion in Low-NO_X Combustion Systems." *Journal of Materials for Energy Systems*, 7(4), 361-369.

Clarke, F., C.W. Morris, (1983). "Combustion Aspects of Furnace Wall Corrosion." *Corrosion-resistant Materials for Coal Conversion Systems*, London, New York, 47.

Damstedt, B.D., (2007) *Structure and Nitrogen Chemistry in Coal, Biomass, and Cofiring Low-NOx Flames*. PhD Dissertation, Brigham Young University.

Daybell, G.N., W.J.S. Pringle, (1958). "The Mode of Occurrence of Chlorine in Coal." *Fuel*, 37, 283-292.

DeVito, M.S., D.L. Smith, (1991). "Controlled Condensation Method: New Option for SO_3 Sampling." *Power*, 135(2).

Duan, L., C. Zhao, W. Zhou, C. Qu, X. Chen, (2009). "Investigation on Coal Pyrolysis in CO_2 Atmosphere." *Energy & Fuels*, 23(7), 3826-3830.

Edgecombe, L.J., (1956). "State of Combination of Chlorine in Coal." *Fuel*, 35, 38-48.

Energy Information Administration (2009). *Annual Energy Outlook 2009*.

Ershov, Yu.B., V.G. Meshcheryakov, Yu.P. Enyakin, (1992). "Formation of Hydrogen Chloride in Pulverized Coal Flare During Combustion of Coal with High Content of Chlorine." *Thermal Engineering*, 39(7), 61-64.

Fukuchi, T., H. Ninomiya, (2006). "SO_3 Concentration Measurement Using Ultraviolet Absorption Spectroscopy and Thermal Conversion." *IEEJ Transactions on Fundamentals and Materials*, 126(10), 977-982.

Gibb, W.H., (1983). "The Nature of Chlorine in Coal and its Behaviour During Combustion." *Corrosion Resistant Materials for Coal Conversion Systems*, Ch. 2, 25-45. London: Applied Science Publishers, 1983.

Giuriati, C., M.C. Cristofori, A. Gorni, F. Abballe, (2003). "Ion Chromatography Applications in the Determination of HF, HCl, NO_X, SO_X, on Stationary Emissions." *Annali dell'Istituto superiore di sanità*, 39(2), 223-228.

Gorbaty, M.L, G.N. George, S.R. Kelemen, (1990). "Direct Determination and Quantification of Sulphur Forms in Heavy Petroleum and Coals 2. The Sulphur K Edge X-ray Absorption Spectroscopy Approach." *Fuel*, 69(8), 945.

Hack, H., A. Seltzer, G. Stanko, (2008). "Design Considerations for Advanced Materials in Oxygen-fired Supercritical and Ultra-supercritical Pulverized Coal Boilers." *Advances in Materials Technology for Fossil Plants – Proceedings from the 5th International Conference*, 993-1000.

Himes, R., (2006). "Keeping an Eye on SO_3." *Power Engineering*, 110(4), 24, 27-28, 30, 32.

Huffman, G.P., S. Mitra, F.E. Huggins, N. Shah, S.Vaidya, F. Lu, (1991). "Quantitative Analysis of All Major Forms of Sulfur in Coal by X-ray Absorption Fine Structure Spectroscopy." *Energy & Fuels*, 5, 574-581.

Ivanova, I.P, L.A. Svistanova, (1971). "Corrosion of 12Kh1MF Steel and Different Corrosion-Resistant Coatings in an Atmosphere of Flue Gases when Burning Anthracite Culm." *Thermal Engineering (English Translation of Teploenergetika)*, (1), 60-63.

Jaworowski, R.J., S.S. Mack, (1979). "Evaluation of Methods for Measurement of SO_3/H_2SO_4 in Flue Gas." *Journal of Air Pollution Control Association*, 29(1), 43-46.

Kaminskii, V.P., (1996). "The Mechanism of How Several Components of the Flame Form and Act on the Tube Metal of the Waterwalls of Power Boilers when Burning Anthracite Culm." *Thermal Engineering*, 43(6), 505-510.

Kelemen, S.R., G.N. George, M.L. Gorbaty, (1990). "Direct Determination and Quantification of Sulphur Forms in Heavy Petroleum and Coals 1. The X-ray Photoelectron Spectroscopy (XPS) Approach." *Fuel*, 69(8), 939.

Kihara, S., K. Nakagawa, A. Ohtomo, H. Aoki, S. Ando, (1985). "Simulating Test Results for Fireside Corrosion of Superheater and Reheater Tubes Operated at Advanced Steam Condition in Coal-Fired Boilers." *High Temperature Corrosion in Energy Systems*, 361-376.

Kitto, J.B., S.C. Stultz, editors (1992). *Steam, its generation and use: Edition 40*, The Babcock & Wilcox Company, a McDermott company, ISBN 09634570-0-4.

Kung, S.C., (2006). *Fireside Corrosion in Coal- and Oil-Fired Boilers*, ASM Handbook, 13C.

LaCount, R.B., D.K. Walker, R.B. LaCount Jr., R.K. Walker, A.L. Stewart, T.K. Trulli, D.G. Kern, et al. (1993). "Advances in Coal Characterization by Programmed-temperature Oxidation." *Fuel*, 72(8), 1203-1208.

Linnerud, I., P. Kaspersen, T. Jæger, (1998). "Gas Monitoring in the Process Industry Using Diode Laser Spectroscopy." *Applied Physics B: Lasers & Optics*, 67, 297-305.

Manolescu, A.V., P. Mayer, (1979). "Influence of Hydrogen Chloride on Corrosion of Boiler Steels in Synthetic Flue Gas." *Corrosion*, B35(12-16 Mar), 9 pages.

McBride, B.J., S. Gordan, (1994). *Computer Program for Calculation of Complex Chemical Equilibrium Compositions and Applications*. Cleveland, Ohio, USA, Lewis Research Center, pts. I.

McBride, B.J., S. Gordan, (1996). *Computer Program for Calculation of Complex Chemical Equilibrium Compositions and Applications*. Cleveland, Ohio, USA, Lewis Research Center, pts. II.

Modest, M.F. Radiative Heat Transfer, Second Edition. California: Academic Press, 2003.

Nazeer, W.A., (1997) *Species and Temperature Measurements in a Pulverized Coal Controlled Profile with Natural Gas Reburning*. Master's Thesis, Brigham Young University.

Nazeer, W.A., R.E. Jackson, J.A. Peart, and D.R. Tree, (1999). "Detailed Measurements in a Pulverized Coal Flame With Reburning," Fuel, 78(6), 689-699.

Oppenheimer, C., P. Bani, J.A. Calkins, M.R. Burton, G.M. Sawyer, (2006). "Rapid FTIR Sensing of Volcanic Gases Released by Strombolian Explosions at Yasur Volcano, Vanuatu." Applied Physics B: Lasers & Optics, 11(2/3), 453-460.

Riemersma, K., Personal Communication. National Bulk Equipment, Inc., 11Feb2010.

Srivastava, R.K., C.A. Miller, C. Erickson, R. Jambhekar, (2004). "Emissions of Sulfur Trioxide from Coal-fired Power Plants." Journal of the Air & Waste Management Association, 54(6), 750-762.

Tree, D.R., A.W. Clark, (2000). "Advanced Reburning Measurements of Temperature and Species in a Pulverized Coal Flame." Fuel,79(13), 1687-1695.

United States Department of Energy (2007). "Coal." Available from http://www.energy.gov/energysources/coal.htm; Internet; Accessed October 25, 2008.

APPENDIX A: ALL RECORDED DATA

In addition to the data presented in the Results chapter, other data were recorded for each coal. These data, along with additional measured gas species, are presented here. The axial distance of each data set is shown in the upper left cell of each table. For reference, the dimensions of the BFR are shown below. The reducing zone nominally consisted of the top three sections (0 – 140 cm) while the oxidizing zone consisted of the bottom three sections (140 – 265 cm).

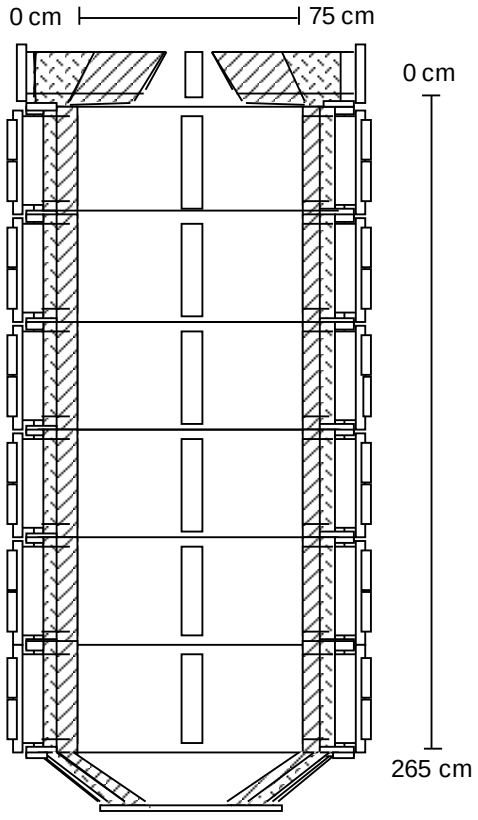

Figure 41: Dimensions of the BFR for Use in Analyzing Data.

A.1 Illinois #6-1

Table 28: Illinois #6-1 Coal – Axial Distance 77 cm.

Radial Dist. (cm)	10	20	30	40	50	60	70
The following eight gases were measured by the FTIR							
CO (ppm)	642	1574	7619	22414	17264	32254	22070
CO_2 (%)	15.44	16.29	15.85	14.76	15.07	14.40	14.47
H_2O (%)	7.35	7.78	8.91	9.77	9.88	10.47	10.12
H_2S (ppm)	18	20	10	0	376	991	671
HCl (ppm)	180	224	244	157	187	144	129
NO (ppm)	296	275	230	96	141	99	148
SO_2 (ppm)	2129	2253	2529	1773	2258	1497	1828
SO_3 (ppm)	44	36	39	37	37	23	33
The following four gases were measured by the Horiba PG-250							
NO (ppm)	255	210	177	79	119	107	139
CO (ppm)	1059	1220	> 5000	> 5000	> 5000	> 5000	> 5000
CO_2 (%)	14.97	16.10	17.37	16.94	17.13	16.82	16.97
O_2 (%)	4.07	3.07	1.35	0.82	0.95	0.98	1.07
The following two gases were measured by the GC							
H_2 (%)	0.95	0.33	0.04	0.17	0.65	0.89	0.67
O_2 (%)	0.18	3.31	2.60	0.69	0.10	0.07	0.06
The following were additional species measured by the FTIR							
Acetylene (ppm)	12	33	160	326	194	304	148
Aldehyde (ppm)	4	3	9	20	14	20	12
Dodecane (ppm)	-1	-1	0	-1	-1	-1	-1
Ethanol (ppm)	1	5	1	30	2	25	6
Ethylene (ppm)	0	4	62	92	23	20	7
Formaldehyde (ppm)	1	1	4	2	2	2	1
HCN (ppm)	3	6	23	65	47	78	48
MeOH (ppm)	-1	-1	-1	-2	-1	-1	0
Methane (ppm)	18	91	482	1546	955	1506	814
NH_3 (ppm)	0	0	1	1	1	1	1
NO_2 (ppm)	-3	-4	-4	0	-2	2	-1
N_2O (ppm)	7	7	4	-4	-2	-4	-3
Phosgene (ppm)	0	0	1	2	1	1	1
Propane (ppm)	3	3	3	-2	1	-2	-3
Propylene (ppm)	0	0	5	1	0	-2	-1
Toluene (ppm)	8	-1	-48	-67	-56	-75	-47

Table 29: Illinois #6-1 Coal – Axial Distance 217 cm.

Radial Dist. (cm)	10	20	30	40	50	60	70
The following eight gases were measured by the FTIR							
CO (ppm)	92	163	2129	96	306	423	690
CO_2 (%)	13.66	15.91	16.45	16.91	16.98	16.24	13.40
H_2O (%)	6.09	6.83	7.82	7.65	7.92	7.76	6.78
H_2S (ppm)	9	2	15	-53	10	0	27
HCl (ppm)	152	179	247	185	190	182	196
NO (ppm)	147	153	146	131	140	153	168
SO_2 (ppm)	1834	2114	2381	2281	2333	2233	1902
SO_3 (ppm)	36	43	46	42	43	38	33
The following four gases were measured by the Horiba PG-250							
NO (ppm)	100	140	137	123	131	177	156
CO (ppm)	102	150	1951	82	300	369	790
CO_2 (%)	17.94	15.67	17.13	16.47	16.89	16.36	15.80
O_2 (%)	4.81	3.84	2.50	3.13	2.77	3.38	3.74
The following two gases were measured by the GC							
H_2 (%)	0.00	0.00	0.00	0.00	0.00	0.00	0.00
O_2 (%)	5.69	3.31	1.46	1.81	1.92	2.45	2.92
The following were additional species measured by the FTIR							
Acetylene (ppm)	-10	6	7	6	6	6	0
Aldehyde (ppm)	-2	-1	0	-2	-1	0	1
Dodecane (ppm)	-1	0	-1	-1	-1	-1	-1
Ethanol (ppm)	-1	-1	3	0	-2	-2	-2
Ethylene (ppm)	0	0	0	0	0	1	0
Formaldehyde (ppm)	2	1	1	1	1	3	3
HCN (ppm)	1	1	8	1	1	2	3
MeOH (ppm)	0	-1	0	-1	-1	-1	-1
Methane (ppm)	4	3	5	5	5	7	4
NH_3 (ppm)	0	0	0	0	0	0	0
NO_2 (ppm)	-3	-3	-3	-4	-4	-4	-4
N_2O (ppm)	5	8	5	6	3	5	9
Phosgene (ppm)	0	0	0	0	0	0	0
Propane (ppm)	2	2	2	2	3	3	2
Propylene (ppm)	2	1	1	0	0	1	1
Toluene (ppm)	5	6	11	1	6	5	-2

Table 30: Illinois #6-1 Coal – Axial Distance 50 cm.

Radial Dist. (cm)	10	20	30	40	50	60	70
The following eight gases were measured by the FTIR							
CO (ppm)	717	4554	34731	58660	24343	3286	2332
CO_2 (%)	12.15	11.62	12.54	10.35	14.13	16.17	16.30
H_2O (%)	6.24	7.00	9.40	11.20	10.97	8.53	8.36
H_2S (ppm)	19	64	281	1782	267	52	13
HCl (ppm)	155	148	147	113	140	183	189
NO (ppm)	321	383	390	174	306	396	343
SO_2 (ppm)	1788	1909	2582	2005	2392	2376	2309
SO_3 (ppm)	41	41	38	21	45	45	50
The following four gases were measured by the Horiba PG-250							
NO (ppm)	302	362	384	212	310	313	331
CO (ppm)	682	3400	> 5000	> 5000	> 5000	2700	2500
CO_2 (%)	12.32	12.10	14.49	13.12	16.69	16.48	16.66
O_2 (%)	6.45	6.73	2.16	1.13	1.26	3.02	2.92
The following two gases were measured by the GC							
H_2 (%)	0.00	0.04	0.98	3.36	0.52	0.02	0.03
O_2 (%)	6.18	6.04	1.54	0.21	0.33	1.99	1.98
The following were additional species measured by the FTIR							
Acetylene (ppm)	-11	44	1368	2010	242	23	18
Aldehyde (ppm)	2	4	73	204	16	1	1
Dodecane (ppm)	-1	0	4	-24	-1	0	-1
Ethanol (ppm)	-4	-1	78	292	9	4	-4
Ethylene (ppm)	0	6	334	969	19	1	0
Formaldehyde (ppm)	1	4	17	15	5	3	2
HCN (ppm)	3	17	195	450	62	9	7
MeOH (ppm)	-1	0	-1	-10	0	-1	-1
Methane (ppm)	8	106	2948	4913	778	35	32
NH_3 (ppm)	0	0	0	1	1	0	0
NO_2 (ppm)	0	-1	0	2	2	-1	-2
N_2O (ppm)	14	17	2	-7	0	9	8
Phosgene (ppm)	0	0	3	10	0	0	0
Propane (ppm)	2	2	7	12	0	2	2
Propylene (ppm)	1	2	22	71	0	0	0
Toluene (ppm)	4	-3	-28	84	-72	-1	4

Table 31: Illinois #6-1 Coal – Axial Distance 77 cm.

Radial Dist. (cm)	10	20	30	40	50	60	70
The following eight gases were measured by the FTIR							
CO (ppm)	704	3301	23104	32355			
CO_2 (%)	14.24	14.53	14.17	14.06			
H_2O (%)	6.31	6.77	9.38	10.73			
H_2S (ppm)	53	-25	293	533			
HCl (ppm)	136	130	173	144			
NO (ppm)	353	291	232	167			
SO_2 (ppm)	1932	2015	2408	2142			
SO_3 (ppm)	41	29	32	32			
The following four gases were measured by the Horiba PG-250							
NO (ppm)	301	274	234	166			
CO (ppm)	716	2095	> 5000	> 5000			
CO_2 (%)	13.82	14.63	16.34	15.65			
O_2 (%)	5.29	4.60	1.94	1.70			
The following two gases were measured by the GC							
H_2 (%)	0.00	0.00	0.05	0.46			
O_2 (%)	5.33	5.43	4.47	2.11			
The following were additional species measured by the FTIR							
Acetylene (ppm)	9	83	942	1026			
Aldehyde (ppm)	2	6	52	49			
Dodecane (ppm)	-1	-1	0	1			
Ethanol (ppm)	1	2	68	66			
Ethylene (ppm)	0	5	195	188			
Formaldehyde (ppm)	1	2	5	3			
HCN (ppm)	2	14	136	168			
MeOH (ppm)	-1	-1	-3	-4			
Methane (ppm)	9	180	2252	2575			
NH_3 (ppm)	0	0	0	1			
NO_2 (ppm)	-2	-2	2	3			
N_2O (ppm)	5	8	0	-5			
Phosgene (ppm)	0	0	2	3			
Propane (ppm)	2	3	6	4			
Propylene (ppm)	1	2	8	7			
Toluene (ppm)	5	-5	-25	-28			

A.2 PRB

Table 32: PRB Coal – Axial Distance 243 cm.

Radial Dist. (cm)	10	20	30	40	50	60	70
The following eight gases were measured by the FTIR							
CO (ppm)	11	21	23	59	50	24	20
CO_2 (%)	14.93	14.53	17.01	17.26	17.60	16.77	13.33
H_2O (%)	10.83	10.91	12.67	13.10	13.02	12.57	10.94
H_2S (ppm)	54	-44	11	-3	28	40	4
HCl (ppm)	2	1	2	2	3	3	3
NO (ppm)	272	237	251	243	254	270	257
SO_2 (ppm)	115	120	182	203	193	162	102
SO_3 (ppm)	6	6	10	8	10	8	7
The following four gases were measured by the Horiba PG-250							
NO (ppm)	270	210	250	230	260	290	278
CO (ppm)	10	220	26	170	50	14	41
CO_2 (%)	14.90	17.20	17.39	18.41	18.03	17.32	16.08
O_2 (%)	4.80	2.62	3.00	2.20	2.63	3.25	4.30
The following two gases were measured by the GC							
H_2 (%)	0.00	0.00	0.00	0.00	0.00	0.00	0.00
O_2 (%)	3.52	2.73	2.36	1.41	1.80	2.41	3.82
The following were additional species measured by the FTIR							
Acetylene (ppm)	6	3	6	6	6	6	-3
Aldehyde (ppm)	-1	-2	-1	-2	-2	-2	-1
Dodecane (ppm)	-1	-1	-1	-1	-1	0	0
Ethanol (ppm)	8	4	7	2	5	5	7
Ethylene (ppm)	0	0	0	0	0	0	0
Formaldehyde (ppm)	0	0	0	0	0	0	1
HCN (ppm)	0	0	0	0	0	0	0
MeOH (ppm)	0	0	0	0	0	0	0
Methane (ppm)	3	2	1	1	1	1	2
NH_3 (ppm)	5	2	3	3	4	4	6
NO_2 (ppm)	2	2	3	2	1	3	2
N_2O (ppm)	0	2	-1	-1	-1	-1	0
Phosgene (ppm)	0	0	0	0	0	0	0
Propane (ppm)	0	0	0	0	1	0	0
Propylene (ppm)	0	0	0	0	0	0	0
Toluene (ppm)	7	0	1	-3	-3	4	3

Table 33: PRB Coal – Axial Distance 90 cm.

Radial Dist. (cm)	10	20	30	40	50	60	70
The following eight gases were measured by the FTIR							
CO (ppm)	2443	2415	9340	29916	35315	36802	14792
CO_2 (%)	14.09	14.43	14.42	14.02	14.50	14.83	14.50
H_2O (%)	11.29	11.23	13.03	15.76	15.46	14.98	13.64
H_2S (ppm)	57	71	95	228	297	170	65
HCl (ppm)	1	1	1	0	0	0	1
NO (ppm)	324	319	307	308	259	205	314
SO_2 (ppm)	149	159	151	118	105	108	158
SO_3 (ppm)	10	9	10	8	11	6	14
The following four gases were measured by the Horiba PG-250							
NO (ppm)	315	319	315	323	257	240	313
CO (ppm)	2540	2069	> 5000	> 5000	> 5000	> 5000	> 5000
CO_2 (%)	14.69	14.33	16.42	17.36	17.45	17.83	17.71
O_2 (%)	5.27	5.64	3.50	1.76	1.47	1.26	2.24
The following two gases were measured by the GC							
H_2 (%)	0.04	0.04	0.24	0.97	1.39	1.09	0.23
O_2 (%)	4.93	5.22	2.89	0.88	0.40	0.21	2.24
The following were additional species measured by the FTIR							
Acetylene (ppm)	3	2	138	678	670	254	61
Aldehyde (ppm)	-1	-1	7	40	38	17	-1
Dodecane (ppm)	-1	0	-1	0	1	0	0
Ethanol (ppm)	-3	-3	-4	22	31	5	-3
Ethylene (ppm)	0	1	31	266	253	48	6
Formaldehyde (ppm)	0	0	1	5	3	1	2
HCN (ppm)	1	1	7	24	25	16	5
MeOH (ppm)	0	0	0	-4	-5	-3	0
Methane (ppm)	22	26	275	1343	1528	919	214
NH_3 (ppm)	10	8	23	174	273	261	61
NO_2 (ppm)	0	0	1	0	1	3	1
N_2O (ppm)	0	0	0	-1	-1	-2	-1
Phosgene (ppm)	0	0	0	1	2	1	0
Propane (ppm)	1	0	1	2	1	1	0
Propylene (ppm)	-1	0	0	7	0	-5	-2
Toluene (ppm)	2	0	-29	-56	-62	-79	-32

Table 34: PRB Coal – Axial Distance 243 cm.

Radial Dist. (cm)	10	20	30	40	50	60	70
The following eight gases were measured by the FTIR							
CO (ppm)	59	22	80	35	55	158	
CO_2 (%)	17.56	16.68	17.65	16.33	16.36	16.72	
H_2O (%)	12.90	12.31	13.00	12.07	12.09	12.36	
H_2S (ppm)	94	81	109	59	66	90	
HCl (ppm)	1	1	1	1	1	1	
NO (ppm)	248	265	247	268	271	259	
SO_2 (ppm)	200	185	213	180	176	186	
SO_3 (ppm)	13	9	12	9	9	10	
The following four gases were measured by the Horiba PG-250							
NO (ppm)	255	251	248	274	275	201	
CO (ppm)	63	63	69	33	53	28	
CO_2 (%)	18.15	18.11	18.16	16.56	16.64	19.25	
O_2 (%)	2.75	2.86	2.87	4.20	4.12	1.91	
The following two gases were measured by the GC							
H_2 (%)	0.00	0.00	0.00	0.00	0.00	0.02	
O_2 (%)	2.02	1.38	1.51	2.93	3.18	1.25	
The following were additional species measured by the FTIR							
Acetylene (ppm)	6	6	6	6	6	7	
Aldehyde (ppm)	-3	-1	-1	-1	-2	-1	
Dodecane (ppm)	-1	0	-1	-1	-1	-1	
Ethanol (ppm)	-2	-5	-6	-4	-5	-4	
Ethylene (ppm)	0	0	0	0	0	0	
Formaldehyde (ppm)	1	1	0	0	0	0	
HCN (ppm)	0	0	0	0	0	0	
MeOH (ppm)	0	0	0	0	0	0	
Methane (ppm)	3	2	2	2	2	2	
NH_3 (ppm)	20	9	6	5	5	5	
NO_2 (ppm)	1	1	0	2	1	1	
N_2O (ppm)	-1	-1	-1	-1	-1	-1	
Phosgene (ppm)	0	0	0	0	0	0	
Propane (ppm)	1	1	1	1	1	1	
Propylene (ppm)	-1	-1	-1	0	0	0	
Toluene (ppm)	3	5	3	7	5	5	

Table 35: PRB Coal – Axial Distance 90 cm.

Radial Dist. (cm)	10	20	30	40	50	60	70
The following eight gases were measured by the FTIR							
CO (ppm)	4934	4929	6790	38157	34748	14738	1675
CO_2 (%)	15.03	14.75	14.61	14.77	14.64	14.40	14.54
H_2O (%)	12.09	11.24	11.49	15.18	14.35	12.56	10.58
H_2S (ppm)	-44	-61	-21	202	165	68	-30
HCl (ppm)	1	1	0	0	0	0	0
NO (ppm)	303	312	321	215	284	313	360
SO_2 (ppm)	189	179	172	149	142	168	147
SO_3 (ppm)	6	8	8	2	5	13	7
The following four gases were measured by the Horiba PG-250							
NO (ppm)	319	313	316	215	302	317	359
CO (ppm)	2402	3752	> 5000	> 5000	> 5000	> 5000	1570
CO_2 (%)	15.24	15.46	16.15	17.84	17.52	17.44	15.18
O_2 (%)	5.16	4.41	4.19	1.45	1.89	2.92	5.41
The following two gases were measured by the GC							
H_2 (%)	0.03	0.08	0.12	1.32	1.13	0.35	0.03
O_2 (%)	4.35	4.08	3.46	0.41	0.66	1.85	4.33
The following were additional species measured by the FTIR							
Acetylene (ppm)	17	13	43	674	535	76	1
Aldehyde (ppm)	-2	-3	-1	37	31	1	-3
Dodecane (ppm)	-1	0	-1	3	0	-1	-1
Ethanol (ppm)	-5	-4	-3	28	7	-8	-1
Ethylene (ppm)	0	1	5	369	149	12	0
Formaldehyde (ppm)	0	1	1	6	3	1	1
HCN (ppm)	1	1	3	27	24	7	1
MeOH (ppm)	0	0	0	-4	-3	0	0
Methane (ppm)	57	50	110	1654	1222	254	13
NH_3 (ppm)	12	11	16	200	201	64	18
NO_2 (ppm)	0	1	1	-1	3	1	-1
N_2O (ppm)	-1	0	0	-1	-2	-1	0
Phosgene (ppm)	0	0	0	1	1	0	0
Propane (ppm)	1	1	1	2	2	1	1
Propylene (ppm)	0	0	0	14	-1	-1	0
Toluene (ppm)	8	3	0	-28	-64	-49	4

Table 36: PRB Coal – Axial Distance 137 cm.

Radial Dist. (cm)	10	20	30	40	50	60	70
The following eight gases were measured by the FTIR							
CO (ppm)	6279	20920	45780	29266	20285	34633	18623
CO_2 (%)	16.00	15.19	15.14	14.76	14.64	15.04	14.68
H_2O (%)	12.33	12.96	13.02	13.08	12.51	12.74	12.32
H_2S (ppm)	-66	49	181	-12	63	64	20
HCl (ppm)	1	1	0	0	0	0	0
NO (ppm)	261	228	97	220	243	216	244
SO_2 (ppm)	206	209	113	193	191	165	174
SO_3 (ppm)	9	7	9	9	12	11	12
The following four gases were measured by the Horiba PG-250							
NO (ppm)	261	231	91	224	248	221	250
CO (ppm)	> 5000	> 5000	> 5000	> 5000	> 5000	> 5000	> 5000
CO_2 (%)	18.14	18.31	17.56	18.11	17.92	17.76	17.85
O_2 (%)	2.73	1.84	1.27	1.81	2.38	1.97	2.55
The following two gases were measured by the GC							
H_2 (%)	0.17	0.47	1.94	0.79	0.48	0.99	0.51
O_2 (%)	1.36	0.79	0.06	0.66	1.61	0.65	1.32
The following were additional species measured by the FTIR							
Acetylene (ppm)	14	45	188	156	66	100	43
Aldehyde (ppm)	-3	-2	7	3	0	2	-3
Dodecane (ppm)	-1	-1	0	0	0	0	0
Ethanol (ppm)	-6	-7	-9	-10	-7	-9	-7
Ethylene (ppm)	0	1	14	14	4	5	2
Formaldehyde (ppm)	1	1	1	1	1	1	1
HCN (ppm)	1	5	18	12	7	12	6
MeOH (ppm)	0	0	-4	-1	-1	-2	-1
Methane (ppm)	50	239	1191	618	322	616	293
NH_3 (ppm)	19	49	304	142	92	168	101
NO_2 (ppm)	0	1	2	1	0	0	1
N_2O (ppm)	-1	-2	-2	-2	-1	-2	-1
Phosgene (ppm)	0	0	0	0	0	0	0
Propane (ppm)	1	1	1	1	1	1	1
Propylene (ppm)	0	0	-5	-2	-1	-2	-1
Toluene (ppm)	-1	-12	-50	-47	-25	-23	-19

Subsequent PRB data was recorded with a different swirl (~0.45)

Table 37: PRB Coal – Axial Distance 90 cm.

Radial Dist. (cm)	10	20	30	40	50	60	70
The following eight gases were measured by the FTIR							
CO (ppm)	18460	48017	59196	39082	6457	878	509
CO_2 (%)	12.45	14.15	13.92	14.25	14.17	14.57	11.44
H_2O (%)	11.40	13.87	15.13	13.58	10.72	10.32	8.09
H_2S (ppm)	-46	160	312	95	-35	-62	-65
HCl (ppm)	0	0	0	0	0	0	0
NO (ppm)	280	217	117	251	280	294	248
SO_2 (ppm)	128	94	59	106	121	136	123
SO_3 (ppm)	10	8	15	10	10	10	7
The following four gases were measured by the Horiba PG-250							
NO (ppm)	270	228	131	257	280	291	300
CO (ppm)	> 5000	> 5000	> 5000	> 5000	4200	770	680
CO_2 (%)	15.14	19.49	16.44	16.90	15.09	14.85	14.87
O_2 (%)	4.57	2.11	1.47	2.30	5.38	5.77	5.86
The following two gases were measured by the GC							
H_2 (%)	0.55	1.76	2.55	1.21	0.11	0.02	0.01
O_2 (%)	3.56	0.91	0.30	1.21	4.70	4.50	4.75
The following were additional species measured by the FTIR							
Acetylene (ppm)	81	536	1045	488	22	7	2
Aldehyde (ppm)	6	35	60	31	1	2	0
Dodecane (ppm)	0	2	6	0	-1	-1	-1
Ethanol (ppm)	-2	16	69	8	-2	0	1
Ethylene (ppm)	9	96	396	117	3	0	0
Formaldehyde (ppm)	1	1	1	2	2	1	1
HCN (ppm)	8	32	50	24	4	0	0
MeOH (ppm)	-1	-3	-11	-4	-1	0	0
Methane (ppm)	391	1630	3213	1279	92	7	4
NH_3 (ppm)	68	233	544	272	82	32	11
NO_2 (ppm)	2	7	11	6	4	4	3
N_2O (ppm)	-1	-2	-2	-1	0	-1	-1
Phosgene (ppm)	0	0	1	1	1	1	0
Propane (ppm)	0	1	2	1	0	0	0
Propylene (ppm)	-1	-4	-6	-4	-2	-1	-1
Toluene (ppm)	-30	-68	-16	-64	-6	11	7

Table 38: PRB Coal – Axial Distance 243 cm.

Radial Dist. (cm)	10	20	30	40	50	60	70
The following eight gases were measured by the FTIR							
CO (ppm)	905	55	36	165	13	526	127
CO_2 (%)	18.11	16.93	14.30	16.34	16.74	16.47	17.11
H_2O (%)	12.21	11.77	10.49	12.18	12.18	12.18	11.63
H_2S (ppm)	-109	-84	-88	-211	-156	-78	-35
HCl (ppm)	0	0	0	0	1	1	0
NO (ppm)	196	213	241	190	227	230	229
SO_2 (ppm)	203	194	196	212	211	225	311
SO_3 (ppm)	10	8	7	8	7	8	11
The following four gases were measured by the Horiba PG-250							
NO (ppm)	216	215	163	193	231	233	219
CO (ppm)	290	60	45	120	11	46	144
CO_2 (%)	18.04	17.51	19.23	18.43	18.15	18.07	18.89
O_2 (%)	3.08	3.65	2.27	3.56	3.93	3.96	3.00
The following two gases were measured by the GC							
H_2 (%)	0.00	0.00	0.09	0.00	0.00	0.00	--
O_2 (%)	2.08	2.60	0.73	1.80	1.83	2.20	--
The following were additional species measured by the FTIR							
Acetylene (ppm)	9	6	-2	7	7	7	7
Aldehyde (ppm)	-3	-4	-4	-5	-7	-6	-4
Dodecane (ppm)	0	0	0	2	1	1	1
Ethanol (ppm)	-3	-2	-2	-3	-4	-9	-10
Ethylene (ppm)	0	0	0	0	0	0	0
Formaldehyde (ppm)	0	0	0	1	2	1	1
HCN (ppm)	0	0	0	0	0	0	0
MeOH (ppm)	0	0	0	-1	-1	-1	-1
Methane (ppm)	4	2	3	3	2	4	3
NH_3 (ppm)	12	9	8	19	12	11	12
NO_2 (ppm)	4	4	4	8	1	3	5
N_2O (ppm)	-1	-1	-1	-1	-1	-1	0
Phosgene (ppm)	0	0	0	0	0	0	0
Propane (ppm)	1	1	0	1	0	0	0
Propylene (ppm)	-1	-1	0	-1	-1	-1	-1
Toluene (ppm)	12	-2	8	-1	3	0	0

Table 39: PRB Coal – Axial Distance 243 cm.

Radial Dist. (cm)	10	20	30	40	50	60	70
The following eight gases were measured by the FTIR							
CO (ppm)	53	207	98	48	81	203	160
CO_2 (%)	15.45	17.81	17.56	14.78	17.45	17.62	17.14
H_2O (%)	11.77	12.01	11.77	9.90	11.67	11.92	11.64
H_2S (ppm)	44	-94	-34	-27	-5	51	-46
HCl (ppm)	1	0	1	0	0	1	1
NO (ppm)	234	207	204	232	205	184	178
SO_2 (ppm)	262	336	318	231	312	333	329
SO_3 (ppm)	7	10	10	6	9	7	10
The following four gases were measured by the Horiba PG-250							
NO (ppm)	174	160	74	47	68	184	175
CO (ppm)	340	217	74	47	59	222	128
CO_2 (%)	18.21	19.03	18.78	16.08	18.29	18.96	18.38
O_2 (%)	3.47	2.99	3.28	5.19	3.40	3.03	3.54
The following two gases were measured by the GC							
H_2 (%)	0.00	0.00	0.00	0.00	0.00	0.01	0.00
O_2 (%)	1.56	1.51	1.29	7.08	4.61	1.08	1.80
The following were additional species measured by the FTIR							
Acetylene (ppm)	5	7	7	2	7	8	7
Aldehyde (ppm)	4	7	2	6	3	8	5
Dodecane (ppm)	-1	-1	-2	-1	-1	-2	-2
Ethanol (ppm)	1	-2	-3	3	-7	1	1
Ethylene (ppm)	0	0	0	0	0	0	0
Formaldehyde (ppm)	0	0	0	0	0	0	0
HCN (ppm)	0	0	0	0	0	0	0
MeOH (ppm)	0	0	0	0	0	0	0
Methane (ppm)	2	3	3	3	3	3	3
NH_3 (ppm)	29	17	14	13	10	8	7
NO_2 (ppm)	0	-1	2	1	-3	0	-2
N_2O (ppm)	-1	-1	0	1	0	0	-1
Phosgene (ppm)	0	0	0	0	0	0	0
Propane (ppm)	2	1	1	2	2	1	2
Propylene (ppm)	-1	-1	-1	-1	-1	-1	-1
Toluene (ppm)	-1	2	-3	6	-3	1	-2

Table 40: PRB Coal – Axial Distance 90 cm.

Radial Dist. (cm)	10	20	30	40	50	60	70
The following eight gases were measured by the FTIR							
CO (ppm)	589	4205	8663	6061	12558	17384	251
CO_2 (%)	10.58	12.93	13.51	15.16	15.06	14.98	14.43
H_2O (%)	7.66	9.82	11.40	12.41	12.67	12.83	10.14
H_2S (ppm)	50	63	26	-70	26	81	-83
HCl (ppm)	0	1	1	0	1	0	0
NO (ppm)	362	359	369	315	265	253	448
SO_2 (ppm)	182	232	271	296	311	316	244
SO_3 (ppm)	2	8	8	9	7	8	7
The following four gases were measured by the Horiba PG-250							
NO (ppm)							
CO (ppm)							
CO_2 (%)							
O_2 (%)							
The following two gases were measured by the GC							
H_2 (%)							
O_2 (%)							
The following were additional species measured by the FTIR							
Acetylene (ppm)	-5	29	95	39	36	38	6
Aldehyde (ppm)	7	2	10	7	5	9	4
Dodecane (ppm)	0	-1	-1	0	-1	-1	-2
Ethanol (ppm)	-6	-3	3	2	-5	3	3
Ethylene (ppm)	0	5	21	3	1	1	0
Formaldehyde (ppm)	0	0	1	0	0	0	0
HCN (ppm)	0	2	5	2	3	4	0
MeOH (ppm)	0	0	0	0	0	0	0
Methane (ppm)	4	89	235	81	140	187	2
NH_3 (ppm)	6	8	12	17	21	34	26
NO_2 (ppm)	-1	3	0	2	2	1	-1
N_2O (ppm)	6	3	1	0	-1	-1	0
Phosgene (ppm)	0	0	0	0	0	0	0
Propane (ppm)	1	2	2	2	2	2	2
Propylene (ppm)	0	0	1	-1	-1	-1	-1
Toluene (ppm)	-3	-6	-36	-4	-3	-3	9

A.3 Beulah Zap

Table 41: Beulah Zap Coal – Axial Distance 77 cm.

Radial Dist. (cm)	10	20	30	40	50	60	70
The following eight gases were measured by the FTIR							
CO (ppm)	3009	6059	27633	32953	27659	15463	10278
CO_2 (%)	14	13	14	13	14	14	15
H_2O (%)	11	9	13	19	16	14	14
H_2S (ppm)	0	-18	254	444	309	69	137
HCl (ppm)	3	4	4	1	0	1	1
NO (ppm)	299	225	122	109	87	198	257
SO_2 (ppm)	490	263	125	82	6	315	377
SO_3 (ppm)	9	4	3	-6	-1	9	9
The following four gases were measured by the Horiba PG-250							
NO (ppm)	--	--	--	--	--	--	--
CO (ppm)	3700	> 5000	> 5000	> 5000	> 5000	> 5000	> 5000
CO_2 (%)	16.03	16.8	18.08	18.01	18.25	18.5	18.33
O_2 (%)	3.93	3.25	1.79	2.14	2.45	3.19	3.78
The following two gases were measured by the GC							
H_2 (%)	--	--	--	--	1.72	0.81	0.91
O_2 (%)	3.93	3.25	1.79	2.14	0.98	2.57	1.27
The following were additional species measured by the FTIR							
Acetylene (ppm)	4	30	354	607	366	128	63
Aldehyde (ppm)	3	7	31	50	40	9	5
Dodecane (ppm)	0	0	2	5	3	0	0
Ethanol (ppm)	7	4	25	59	32	7	8
Ethylene (ppm)	2	16	265	480	284	57	16
Formaldehyde (ppm)	1	1	1	1	1	1	1
HCN (ppm)	2	4	20	31	7	6	5
MeOH (ppm)	0	0	-1	-1	-5	0	0
Methane (ppm)	57	210	1389	1891	1480	585	282
NH_3 (ppm)	38	33	39	148	463	155	129
NO_2 (ppm)	0	-3	-6	-8	-3	-1	-1
N_2O (ppm)	0	1	-1	-2	-2	-1	-1
Phosgene (ppm)	0	0	1	1	1	0	0
Propane (ppm)	0	0	-1	2	0	0	0
Propylene (ppm)	0	1	17	46	8	0	-2
Toluene (ppm)	10	12	-38	-23	-30	-7	4

Table 42: Beulah Zap Coal – Axial Distance 77 cm.

Radial Dist. (cm)	10	20	30	40	50	60	70
The following eight gases were measured by the FTIR							
CO (ppm)	3392	10504	25426	35680	27675	15323	10278
CO_2 (%)	15	15	13	13	14	14	15
H_2O (%)	12	13	14	16	15	14	14
H_2S (ppm)	-7	93	240	391	264	172	137
HCl (ppm)	2	1	1	0	0	1	1
NO (ppm)	315	231	160	92	103	211	257
SO_2 (ppm)	434	326	56	7	14	365	377
SO_3 (ppm)	12	8	1	-1	-2	9	9
The following four gases were measured by the Horiba PG-250							
NO (ppm)	--	--	--	--	--	--	--
CO (ppm)	4100	> 5000	> 5000	> 5000	> 5000	> 5000	> 5000
CO_2 (%)	17.18	17.65	17.76	17.33	18.15	18.41	18.33
O_2 (%)	5.43	4.72	3.92	3.88	3.54	3.65	3.78
The following two gases were measured by the GC							
H_2 (%)	0.54	1.56	2.13	1.67	1.59	0.49	0.91
O_2 (%)	2.23	2.20	1.96	0.95	2.69	1.67	1.27
The following were additional species measured by the FTIR							
Acetylene (ppm)	3	135	553	842	409	0	0
Aldehyde (ppm)	2	10	35	63	37	545	282
Dodecane (ppm)	0	1	1	6	3	126	129
Ethanol (ppm)	12	7	16	62	30	-1	-1
Ethylene (ppm)	4	38	248	581	273	-1	-1
Formaldehyde (ppm)	1	1	1	1	1	0	0
HCN (ppm)	2	10	24	16	7	0	0
MeOH (ppm)	0	0	-2	-4	-3	0	-2
Methane (ppm)	85	430	1326	2163	1445	-5	4
NH_3 (ppm)	91	123	220	451	364	0	0
NO_2 (ppm)	-1	-2	-5	-7	-1	0	0
N_2O (ppm)	0	0	-2	-2	-2	0	0
Phosgene (ppm)	0	0	0	0	1	116	63
Propane (ppm)	0	0	0	2	1	118	66
Propylene (ppm)	-1	-1	9	41	11	6	22
Toluene (ppm)	6	2	-43	-18	-35	21	5

Table 43: Beulah Zap Coal – Axial Distance 243 cm.

Radial Dist. (cm)	10	20	30	40	50	60	70
The following eight gases were measured by the FTIR							
CO (ppm)	19	47	51	11	9	11	18
CO_2 (%)	13	14	14	14	13	13	14
H_2O (%)	10	11	11	11	12	12	12
H_2S (ppm)	157	189	201	225	117	103	108
HCl (ppm)	2	2	2	2	2	2	2
NO (ppm)	247	217	207	216	214	234	199
SO_2 (ppm)	274	391	400	463	447	495	523
SO_3 (ppm)	8	7	8	7	11	11	12
The following four gases were measured by the Horiba PG-250							
NO (ppm)	263	230	224	249	235	253	219
CO (ppm)	21	46	46	11	8	11	16
CO_2 (%)	14.39	15.69	16.01	14.79	14.85	15.52	15.60
O_2 (%)	5.71	5.08	4.98	6.30	6.40	5.96	6.02
The following two gases were measured by the GC							
H_2 (%)	0.30	--	0.04	0.00	0.00	0.00	0.00
O_2 (%)	2.02	5.08	9.79	5.71	4.75	7.92	4.61
The following were additional species measured by the FTIR							
Acetylene (ppm)	-15	-18	-17	-17	-17	-15	-17
Aldehyde (ppm)	-12	-11	-10	-10	-7	-12	-9
Dodecane (ppm)	0	-1	-1	-1	0	-1	-1
Ethanol (ppm)	8	5	11	7	9	4	10
Ethylene (ppm)	0	0	0	0	0	0	0
Formaldehyde (ppm)	2	1	2	1	1	1	1
HCN (ppm)	0	0	0	0	0	0	0
MeOH (ppm)	0	1	1	0	0	0	0
Methane (ppm)	5	5	4	4	3	3	3
NH_3 (ppm)	21	15	15	14	12	12	11
NO_2 (ppm)	-2	-1	0	0	0	-1	-1
N_2O (ppm)	1	1	0	0	0	0	0
Phosgene (ppm)	-1	-1	-1	-1	-1	-1	0
Propane (ppm)	1	2	2	2	2	1	1
Propylene (ppm)	1	1	1	1	1	1	1
Toluene (ppm)	7	5	4	4	4	4	2

Table 44: Beulah Zap Coal – Axial Distance 243 cm.

Radial Dist. (cm)	10	20	30	40	50	60	70
The following eight gases were measured by the FTIR							
CO (ppm)	9	22	20	16	15	23	40
CO_2 (%)	11	14	14	14	13	13	12
H_2O (%)	9	11	11	11	11	11	13
H_2S (ppm)	59	178	172	191	162	135	201
HCl (ppm)	2	2	2	2	2	1	1
NO (ppm)	304	264	269	264	261	253	250
SO_2 (ppm)	273	458	481	494	476	453	402
SO_3 (ppm)	2	9	11	12	10	7	7
The following four gases were measured by the Horiba PG-250							
NO (ppm)	212	287	296	288	280	268	273
CO (ppm)	26	21	18	13	61	28	35
CO_2 (%)	15.50	15.40	15.34	15.05	14.70	14.41	14.04
O_2 (%)	6.14	6.31	6.47	6.77	7.08	7.31	7.59
The following two gases were measured by the GC							
H_2 (%)	0.00	0.00	0.00	0.00	0.00	0.00	0.00
O_2 (%)	5.31	7.33	5.18	5.31	5.97	6.69	6.69
The following were additional species measured by the FTIR							
Acetylene (ppm)	-5	-18	-17	-17	-16	-15	-15
Aldehyde (ppm)	-12	-8	-12	-7	-9	-11	-10
Dodecane (ppm)	-1	-1	-1	-1	-1	-1	-1
Ethanol (ppm)	1	9	9	5	7	8	8
Ethylene (ppm)	0	0	0	0	0	0	0
Formaldehyde (ppm)	1	1	1	1	2	2	2
HCN (ppm)	0	0	0	0	0	0	0
MeOH (ppm)	0	0	0	0	0	1	1
Methane (ppm)	2	4	4	4	4	4	2
NH_3 (ppm)	9	9	8	8	8	7	8
NO_2 (ppm)	-4	0	-2	0	0	-1	1
N_2O (ppm)	1	0	0	0	0	0	0
Phosgene (ppm)	0	0	0	0	0	-1	-1
Propane (ppm)	0	1	1	1	1	1	2
Propylene (ppm)	1	1	1	1	1	1	1
Toluene (ppm)	-8	5	3	4	7	6	9

Table 45: Beulah Zap Coal – Axial Distance 243 cm.

Radial Dist. (cm)	10	20	30	40	50	60	70
The following eight gases were measured by the FTIR							
CO (ppm)	11	22	27	18	20	29	19
CO_2 (%)	13	14	14	14	14	14	13
H_2O (%)	11	11	11	12	12	11	11
H_2S (ppm)	180	228	184	243	183	194	111
HCl (ppm)	1	1	1	1	1	2	1
NO (ppm)	249	266	267	254	252	265	254
SO_2 (ppm)	457	490	500	602	596	520	485
SO_3 (ppm)	10	10	12	9	12	11	8
The following four gases were measured by the Horiba PG-250							
NO (ppm)	276	287	293	252	278	288	288
CO (ppm)	8	21	25	23	16	35	18
CO_2 (%)	15.30	15.45	15.21	17.05	16.09	15.33	14.96
O_2 (%)	6.62	6.62	6.84	5.56	6.32	6.89	7.12
The following two gases were measured by the GC							
H_2 (%)	0.00	0.00	0.00	0.00	0.00	0.10	0.00
O_2 (%)	5.25	5.37	5.19	5.72	3.96	4.76	5.22
The following were additional species measured by the FTIR							
Acetylene (ppm)	-17	-17	-17	-12	-18	-18	-15
Aldehyde (ppm)	-9	-11	-12	-8	-10	-11	-10
Dodecane (ppm)	-1	-1	-1	-1	-1	-1	-1
Ethanol (ppm)	4	10	9	7	9	6	7
Ethylene (ppm)	0	0	0	0	0	0	0
Formaldehyde (ppm)	1	1	1	1	1	2	2
HCN (ppm)	0	0	0	0	0	0	0
MeOH (ppm)	1	0	0	0	1	0	1
Methane (ppm)	4	4	4	3	3	4	4
NH_3 (ppm)	7	7	7	7	7	6	6
NO_2 (ppm)	-1	0	1	-1	-1	-2	-2
N_2O (ppm)	0	0	0	0	0	0	0
Phosgene (ppm)	-1	0	0	0	0	0	-1
Propane (ppm)	1	2	1	1	1	1	2
Propylene (ppm)	1	1	1	1	1	1	1
Toluene (ppm)	6	5	3	7	4	5	4

Table 46: Beulah Zap Coal – Axial Distance 77 cm.

Radial Dist. (cm)	10	20	30	40	50	60	70
The following eight gases were measured by the FTIR							
CO (ppm)	15064	38009	45991	47058	31676	5120	353
CO_2 (%)	18	19	18	18	18	19	19
H_2O (%)	18	18	21	22	19	16	15
H_2S (ppm)	69	67	358	442	250	3	41
HCl (ppm)	6	4	4	4	3	3	3
NO (ppm)	432	251	202	207	277	411	520
SO_2 (ppm)	791	817	325	317	608	681	655
SO_3 (ppm)	12	16	7	9	17	16	14
The following four gases were measured by the Horiba PG-250							
NO (ppm)	374	223	181	189	242	343	427
CO (ppm)	> 5000	> 5000	> 5000	> 5000	> 5000	3792	331
CO_2 (%)	17.77	17.99	18.25	18.09	18.62	17.52	15.91
O_2 (%)	2.20	1.87	3.04	3.58	4.46	6.01	7.36
The following two gases were measured by the GC							
H_2 (%)	0.39	1.22	2.09	2.13	1.00	0.14	0.01
O_2 (%)	2.62	0.85	0.80	0.81	1.41	3.02	4.79
The following were additional species measured by the FTIR							
Acetylene (ppm)	56	67	847	1193	350	35	8
Aldehyde (ppm)	4	4	45	62	21	3	2
Dodecane (ppm)	0	0	0	2	-1	0	0
Ethanol (ppm)	9	21	61	99	22	8	9
Ethylene (ppm)	3	15	174	449	97	3	0
Formaldehyde (ppm)	0	0	0	1	0	1	1
HCN (ppm)	1	2	37	44	18	5	1
MeOH (ppm)	0	-1	-5	-6	-4	-1	-1
Methane (ppm)	168	594	1723	2367	888	67	8
NH_3 (ppm)	7	158	327	429	312	153	90
NO_2 (ppm)	2	4	3	-3	2	3	1
N_2O (ppm)	0	-3	-3	-3	0	1	-1
Phosgene (ppm)	0	1	1	1	1	0	0
Propane (ppm)	1	1	2	4	1	0	-1
Propylene (ppm)	1	-3	-1	30	-2	-3	-2
Toluene (ppm)	-19	-29	-28	-36	-28	-18	-8

Table 47: Beulah Zap Coal – Axial Distance 77cm.

Radial Dist. (cm)	10	20	30	40	50	60	70
The following eight gases were measured by the FTIR							
CO (ppm)	11677	39437	48108	42543	28509	6234	1552
CO_2 (%)	18	19	17	18	18	18	18
H_2O (%)	17	19	20	21	19	17	15
H_2S (ppm)	72	192	569	442	117	-27	-31
HCl (ppm)	4	3	3	2	2	1	1
NO (ppm)	453	226	174	207	293	412	499
SO_2 (ppm)	783	630	299	408	665	716	683
SO_3 (ppm)	12	15	13	10	19	19	18
The following four gases were measured by the Horiba PG-250							
NO (ppm)	384	199	162	172	280	344	396
CO (ppm)	> 5000	> 5000	> 5000	> 5000	> 5000	> 5000	1692
CO_2 (%)	17.54	18.67	18.32	18.26	18.62	17.61	17.36
O_2 (%)	6.06	4.82	4.90	5.15	3.90	6.01	6.59
The following two gases were measured by the GC							
H_2 (%)	0.32	1.51	2.07	2.06	0.90	0.18	0.07
O_2 (%)	2.89	0.90	0.96	0.86	1.26	3.01	3.36
The following were additional species measured by the FTIR							
Acetylene (ppm)	50	226	838	924	316	44	13
Aldehyde (ppm)	6	14	42	50	21	-2	0
Dodecane (ppm)	-1	-1	0	1	1	0	1
Ethanol (ppm)	8	20	70	79	30	13	17
Ethylene (ppm)	2	39	208	366	70	3	0
Formaldehyde (ppm)	1	0	0	1	0	1	1
HCN (ppm)	3	14	35	34	15	3	1
MeOH (ppm)	0	-2	-8	-8	0	0	0
Methane (ppm)	132	879	1864	2021	752	89	16
NH_3 (ppm)	65	211	489	497	147	93	66
NO_2 (ppm)	3	3	4	-2	4	4	-1
N_2O (ppm)	0	-2	-3	-3	-1	0	0
Phosgene (ppm)	0	1	1	1	1	0	0
Propane (ppm)	0	1	3	4	1	-1	-1
Propylene (ppm)	-2	-4	-4	18	-1	-3	-2
Toluene (ppm)	-19	-45	-24	-27	-12	-3	-4

Table 48: Beulah Zap Coal – Axial Distance 243 cm.

Radial Dist. (cm)	10	20	30	40	50	60	70
The following eight gases were measured by the FTIR							
CO (ppm)	33	59	66	29	42	49	32
CO_2 (%)	18	18	18	18	19	18	18
H_2O (%)	14	15	15	15	15	15	15
H_2S (ppm)	-24	50	-47	-32	-7	20	-39
HCl (ppm)	2	2	2	2	1	2	1
NO (ppm)	361	349	351	353	344	351	356
SO_2 (ppm)	529	633	615	683	722	709	683
SO_3 (ppm)	14	15	16	14	15	16	15
The following four gases were measured by the Horiba PG-250							
NO (ppm)	292	287	286	292	287	289	292
CO (ppm)	26	39	32	24	34	33	16
CO_2 (%)	14.57	15.25	14.77	15.38	15.62	15.52	15.36
O_2 (%)	5.24	4.63	5.09	4.50	4.26	4.39	4.53
The following two gases were measured by the GC							
H_2 (%)	0.00	0.00	0.00	0.00	0.00	0.00	0.00
O_2 (%)	5.89	5.19	5.68	5.19	4.99	5.10	5.31
The following were additional species measured by the FTIR							
Acetylene (ppm)	8	8	8	7	7	7	0
Aldehyde (ppm)	-3	5	1	5	4	4	9
Dodecane (ppm)	1	1	0	1	0	1	9
Ethanol (ppm)	0	9	10	15	12	14	4
Ethylene (ppm)	0	0	0	0	0	0	-1
Formaldehyde (ppm)	1	1	1	2	1	1	0
HCN (ppm)	0	0	0	0	0	0	1
MeOH (ppm)	0	0	0	-1	0	0	-1
Methane (ppm)	3	9	6	9	9	9	-5
NH_3 (ppm)	17	13	12	12	10	9	0
NO_2 (ppm)	2	2	4	3	3	2	0
N_2O (ppm)	-1	0	0	-1	-1	-1	0
Phosgene (ppm)	0	0	0	0	0	0	0
Propane (ppm)	1	1	1	1	1	1	0
Propylene (ppm)	-1	-1	-1	0	0	-1	9
Toluene (ppm)	2	-3	0	-8	-7	-6	8

Table 49: Beulah Zap Coal – Axial Distance 243 cm.

Radial Dist. (cm)	10	20	30	40	50	60	70
The following eight gases were measured by the FTIR							
CO (ppm)	35	72	34	58	67	57	73
CO_2 (%)	18	18	18	18	18	18	19
H_2O (%)	15	15	15	15	15	15	15
H_2S (ppm)	-23	-36	-64	-46	-89	-74	-88
HCl (ppm)	2	1	2	1	1	1	1
NO (ppm)	341	342	356	335	339	338	341
SO_2 (ppm)	697	703	694	721	707	699	730
SO_3 (ppm)	15	15	16	14	17	13	16
The following four gases were measured by the Horiba PG-250							
NO (ppm)	282	278	288	277	282	272	279
CO (ppm)	29	51	26	44	44	53	68
CO_2 (%)	15.24	15.38	15.01	15.42	15.38	15.78	16.00
O_2 (%)	4.63	4.51	4.86	4.49	4.52	4.17	3.94
The following two gases were measured by the GC							
H_2 (%)	0.00	0.00	0.00	0.00	0.00	0.00	0.00
O_2 (%)	5.43	5.48	5.63	5.20	5.02	4.98	4.50
The following were additional species measured by the FTIR							
Acetylene (ppm)	7	7	7	7	7	7	8
Aldehyde (ppm)	2	2	5	6	4	4	6
Dodecane (ppm)	0	1	0	0	0	0	0
Ethanol (ppm)	13	11	15	13	11	11	13
Ethylene (ppm)	0	1	0	0	0	0	0
Formaldehyde (ppm)	1	1	1	1	1	1	1
HCN (ppm)	0	0	0	0	0	0	0
MeOH (ppm)	0	0	0	0	0	0	0
Methane (ppm)	9	10	9	9	9	9	9
NH_3 (ppm)	8	8	7	7	6	6	6
NO_2 (ppm)	2	3	4	2	4	2	4
N_2O (ppm)	-1	0	-1	-1	-1	-1	-1
Phosgene (ppm)	0	0	0	0	0	0	0
Propane (ppm)	1	0	0	0	1	1	1
Propylene (ppm)	-1	-1	-1	-1	-1	-1	-1
Toluene (ppm)	-5	-9	-10	-7	-13	-7	-7

A.4 Mahoning

Table 50: Mahoning Coal – Axial Distance 83 cm.

Radial Dist. (cm)	10	20	30	40	50	60	70
The following eight gases were measured by the FTIR							
CO (ppm)	2586	7803	20005	35225	17038	2297	485
CO_2 (%)	15	16	16	15	16	17	16
H_2O (%)	6	9	10	12	12	10	8
H_2S (ppm)	-73	9	-52	90	-51	-23	-33
HCl (ppm)	4	10	12	19	14	14	15
NO (ppm)	322	380	409	330	337	354	389
SO_2 (ppm)	1362	1747	1854	1712	1834	1635	1457
SO_3 (ppm)	35	35	41	30	34	34	33
The following four gases were measured by the Horiba PG-250							
NO (ppm)	288	317	344	287	287	292	314
CO (ppm)	2181	> 5000	> 5000	> 5000	> 5000	1891	380
CO_2 (%)	15.42	16.96	16.79	16.18	17.10	16.56	15.26
O_2 (%)	1.76	1.11	0.41	0.13	0.34	1.93	3.51
The following two gases were measured by the GC							
H_2 (%)	0.02	0.11	0.37	0.80	0.78	0.92	0.02
O_2 (%)	2.20	1.58	0.92	0.62	0.64	0.84	2.76
The following were additional species measured by the FTIR							
Acetylene (ppm)	15	79	308	697	247	21	6
Aldehyde (ppm)	0	3	15	34	12	-1	0
Dodecane (ppm)	1	0	0	-1	0	0	0
Ethanol (ppm)	-13	-11	-18	-9	-19	-13	-20
Ethylene (ppm)	1	5	25	42	23	1	0
Formaldehyde (ppm)	1	1	2	2	2	3	2
HCN (ppm)	6	13	38	98	37	8	3
MeOH (ppm)	-1	-1	0	-1	0	-1	-1
Methane (ppm)	18	106	448	1088	379	24	3
NH_3 (ppm)	1	0	0	0	0	0	0
NO_2 (ppm)	0	3	5	6	3	3	0
N_2O (ppm)	6	6	2	-1	2	7	7
Phosgene (ppm)	-1	0	1	1	1	0	0
Propane (ppm)	1	2	3	4	3	2	2
Propylene (ppm)	2	0	0	-1	0	0	0
Toluene (ppm)	-7	-20	-39	-59	-32	-10	-9

Table 51: Mahoning Coal – Axial Distance 243 cm.

Radial Dist. (cm)	10	20	30	40	50	60	70
The following eight gases were measured by the FTIR							
CO (ppm)	56	60	96	146	153	147	154
CO_2 (%)	16	17	18	17	17	17	17
H_2O (%)	8	8	8	8	8	8	8
H_2S (ppm)	-67	-79	-32	-123	-77	-82	-77
HCl (ppm)	16	24	39	54	66	79	82
NO (ppm)	268	263	258	268	272	276	283
SO_2 (ppm)	1428	1473	1599	1568	1553	1523	1471
SO_3 (ppm)	32	31	33	32	32	33	32
The following four gases were measured by the Horiba PG-250							
NO (ppm)	226	209	217	226	229	232	241
CO (ppm)	45	53	73	125	118	120	138
CO_2 (%)	15.08	16.04	16.33	16.09	15.97	15.76	15.38
O_2 (%)	3.82	2.88	2.55	2.78	2.88	3.08	3.49
The following two gases were measured by the GC							
H_2 (%)	0.00	0.00	0.00	0.00	0.00	0.00	0.00
O_2 (%)	4.20	2.98	2.89	3.12	3.25	3.34	3.64
The following were additional species measured by the FTIR							
Acetylene (ppm)	6	6	7	7	6	7	6
Aldehyde (ppm)	1	1	2	1	3	4	4
Dodecane (ppm)	2	2	2	1	1	1	1
Ethanol (ppm)	-18	-17	-19	-15	-17	-14	-16
Ethylene (ppm)	0	0	0	0	0	0	0
Formaldehyde (ppm)	1	1	1	2	2	2	2
HCN (ppm)	0	0	0	0	0	0	0
MeOH (ppm)	-1	-1	-1	-1	-1	-1	-1
Methane (ppm)	2	3	3	3	2	2	3
NH_3 (ppm)	0	0	0	0	0	0	0
NO_2 (ppm)	-2	-2	-1	-2	-2	-3	-3
N_2O (ppm)	1	2	2	1	1	2	3
Phosgene (ppm)	0	0	0	0	0	0	0
Propane (ppm)	3	2	3	3	4	4	4
Propylene (ppm)	-1	-1	-1	-1	-1	-1	-1
Toluene (ppm)	-15	-15	-14	-18	-17	-20	-17

Table 52: Mahoning Coal – Axial Distance 83 cm.

Radial Dist. (cm)	10	20	30	40	50	60	70
The following eight gases were measured by the FTIR							
CO (ppm)	8738	18748	32790	25560	9312	385	318
CO_2 (%)	18	16	15	15	17	12	16
H_2O (%)	10	12	12	12	11	7	8
H_2S (ppm)	-117	-29	-30	5	-42	-14	-44
HCl (ppm)	40	29	31	29	25	24	23
NO (ppm)	421	403	349	359	411	329	469
SO_2 (ppm)	1894	1800	1734	1875	1791	1078	1410
SO_3 (ppm)	43	37	39	38	38	26	30
The following four gases were measured by the Horiba PG-250							
NO (ppm)	346	337	302	296	353	360	389
CO (ppm)	> 5000	> 5000	> 5000	> 5000	4040	306	210
CO_2 (%)	17.09	16.95	16.25	16.69	16.89	14.91	14.85
O_2 (%)	0.95	0.39	0.16	0.26	1.44	4.10	4.05
The following two gases were measured by the GC							
H_2 (%)	0.16	0.38	0.77	0.47	0.08	0.00	0.00
O_2 (%)	1.27	0.81	0.62	0.80	1.82	4.50	4.47
The following were additional species measured by the FTIR							
Acetylene (ppm)	76	181	299	274	106	4	6
Aldehyde (ppm)	5	13	23	18	6	-1	1
Dodecane (ppm)	1	0	1	0	0	1	0
Ethanol (ppm)	-18	-18	-20	-19	-13	-16	-13
Ethylene (ppm)	1	8	15	15	5	0	0
Formaldehyde (ppm)	1	1	1	1	2	17	6
HCN (ppm)	10	16	61	52	22	4	0
MeOH (ppm)	0	-1	0	0	-1	0	-1
Methane (ppm)	109	282	725	584	160	3	3
NH_3 (ppm)	0	0	0	0	0	0	0
NO_2 (ppm)	1	3	5	4	3	1	0
N_2O (ppm)	2	0	-1	0	3	2	4
Phosgene (ppm)	0	0	1	0	0	0	0
Propane (ppm)	2	3	3	3	2	1	2
Propylene (ppm)	1	0	0	0	0	1	0
Toluene (ppm)	-2	-36	-59	-39	-19	-2	-5

Table 53: Mahoning Coal – Axial Distance 243 cm.

Radial Dist. (cm)	10	20	30	40	50	60	70
The following eight gases were measured by the FTIR							
CO (ppm)	324	193	321	83	82	220	149
CO_2 (%)	16	16	17	15	15	16	15
H_2O (%)	8	11	12	10	9	8	7
H_2S (ppm)	-56	-10	72	-50	-48	-31	-11
HCl (ppm)	7	9	10	12	11	13	14
NO (ppm)	234	229	230	251	254	266	282
SO_2 (ppm)	1546	1692	1668	1501	1434	1466	1374
SO_3 (ppm)	37	38	35	31	34	37	33
The following four gases were measured by the Horiba PG-250							
NO (ppm)	206	198	198	198	219	224	232
CO (ppm)	251	153	261	86	71	173	131
CO_2 (%)	16.70	16.60	16.53	15.23	15.47	15.30	14.52
O_2 (%)	2.15	2.27	2.33	3.68	3.41	3.59	4.42
The following two gases were measured by the GC							
H_2 (%)	0.00	0.00	0.00	0.00	0.00	0.00	0.00
O_2 (%)	2.54	2.70	2.86	4.55	3.89	4.05	4.89
The following were additional species measured by the FTIR							
Acetylene (ppm)	7	9	10	5	7	8	3
Aldehyde (ppm)	3	-2	-1	1	4	0	-1
Dodecane (ppm)	1	1	1	5	6	5	5
Ethanol (ppm)	-24	-25	-27	-25	-26	-21	-19
Ethylene (ppm)	0	0	0	0	0	0	0
Formaldehyde (ppm)	0	0	0	1	1	2	2
HCN (ppm)	0	0	0	0	0	1	0
MeOH (ppm)	-1	-1	-1	-1	-1	-1	-1
Methane (ppm)	2	4	4	4	4	2	2
NH_3 (ppm)	0	0	0	0	0	0	0
NO_2 (ppm)	1	3	2	2	0	-1	-1
N_2O (ppm)	1	1	2	1	1	3	2
Phosgene (ppm)	1	1	0	0	0	0	0
Propane (ppm)	2	2	3	9	7	5	4
Propylene (ppm)	-1	-1	-1	-1	-1	-1	-1
Toluene (ppm)	-46	-25	-14	-24	-31	-11	-11

Table 54: Mahoning Coal – Axial Distance 97 cm.

Radial Dist. (cm)	10	20	30	40	50	60	70
The following eight gases were measured by the FTIR							
CO (ppm)	4050	9578	20418	31398	21837	3313	674
CO_2 (%)	16	15	15	14	14	15	15
H_2O (%)	7	8	9	12	13	11	10
H_2S (ppm)	-54	-194	-17	-97	-84	-149	-88
HCl (ppm)	10	10	11	17	22	10	19
NO (ppm)	494	463	423	301	327	451	459
SO_2 (ppm)	1645	1701	1727	1562	1656	1518	1333
SO_3 (ppm)	37	30	33	26	31	29	28
The following four gases were measured by the Horiba PG-250							
NO (ppm)	406	389	343	245	332	390	386
CO (ppm)	2559	> 5000	> 5000	> 5000	> 5000	2344	531
CO_2 (%)	16.61	17.18	17.01	16.58	17.20	16.64	15.25
O_2 (%)	1.83	0.84	0.31	0.13	0.23	1.88	3.61
The following two gases were measured by the GC							
H_2 (%)	0.06	0.13	0.38	0.67	0.35	0.04	0.00
O_2 (%)	2.24	1.49	0.80	0.61	0.72	2.30	3.97
The following were additional species measured by the FTIR							
Acetylene (ppm)	22	54	127	195	131	21	7
Aldehyde (ppm)	4	7	13	16	14	5	6
Dodecane (ppm)	2	1	2	1	2	1	1
Ethanol (ppm)	-36	-38	-41	-54	-42	-43	-36
Ethylene (ppm)	0	3	6	10	7	1	0
Formaldehyde (ppm)	1	1	1	1	1	1	1
HCN (ppm)	2	6	15	31	23	5	2
MeOH (ppm)	0	-1	-1	-1	-1	-1	-1
Methane (ppm)	31	82	247	521	322	17	4
NH_3 (ppm)	0	0	0	0	0	0	0
NO_2 (ppm)	3	3	5	7	7	4	3
N_2O (ppm)	2	1	0	-1	-1	3	5
Phosgene (ppm)	0	0	0	0	0	0	0
Propane (ppm)	4	4	4	5	5	3	3
Propylene (ppm)	0	-1	-1	-1	-1	-1	-1
Toluene (ppm)	-12	-25	-29	-42	-33	-15	-20

Table 55: Mahoning Coal – Axial Distance 83 cm.

Radial Dist. (cm)	10	20	30	40	50	60	70
The following eight gases were measured by the FTIR							
CO (ppm)	3265	9393	22076	31968	10299	1133	602
CO_2 (%)	16	16	15	14	15	14	13
H_2O (%)	8	7	9	10	10	9	7
H_2S (ppm)	-73	-131	-41	-68	180	-59	-218
HCl (ppm)	24	27	16	17	16	16	48
NO (ppm)	522	467	520	450	490	473	447
SO_2 (ppm)	1580	1739	1775	1674	1678	1351	1192
SO_3 (ppm)	25	30	32	28	30	6	38
The following four gases were measured by the Horiba PG-250							
NO (ppm)	354	333	435	398	422	392	371
CO (ppm)	1912	> 5000	> 5000	> 5000	> 5000	905	476
CO_2 (%)	13.28	13.92	16.53	16.47	16.89	15.27	13.43
O_2 (%)	5.39	4.44	0.88	0.28	1.09	3.51	5.55
The following two gases were measured by the GC							
H_2 (%)	0.02	0.00	0.33	0.58	0.27	0.00	0.00
O_2 (%)	3.40	NA	1.48	0.77	1.26	3.20	5.96
The following were additional species measured by the FTIR							
Acetylene (ppm)	19	94	251	356	106	11	-17
Aldehyde (ppm)	11	12	19	22	11	14	18
Dodecane (ppm)	1	1	1	0	1	-1	4
Ethanol (ppm)	-31	-29	-29	-35	-46	-21	-36
Ethylene (ppm)	0	3	14	15	5	1	0
Formaldehyde (ppm)	2	2	2	2	2	1	2
HCN (ppm)	4	12	31	49	16	4	4
MeOH (ppm)	-1	0	-1	-1	-1	-1	-1
Methane (ppm)	22	121	359	579	135	7	2
NH_3 (ppm)	0	0	0	0	0	0	0
NO_2 (ppm)	4	2	6	7	7	1	6
N_2O (ppm)	6	6	1	0	5	6	6
Phosgene (ppm)	0	0	0	0	0	0	0
Propane (ppm)	3	3	4	5	3	1	4
Propylene (ppm)	-1	-1	-1	-1	-1	0	-1
Toluene (ppm)	-10	-32	-34	-40	-21	-9	-20

A.5 Indiana

Table 56: Indiana Coal – Axial Distance 250 cm.

Radial Dist. (cm)	10	20	30	40	50	60	70
The following eight gases were measured by the FTIR							
CO (ppm)	149	201	259	426	457	529	380
CO_2 (%)	13	12	12	12	13	13	13
H_2O (%)	7	7	7	7	7	7	7
H_2S (ppm)	8	-43	-45	-10	-6	-9	-61
HCl (ppm)	0	0	0	0	0	0	0
NO (ppm)	146	158	167	174	155	156	160
SO_2 (ppm)	800	793	783	763	846	831	793
SO_3 (ppm)	25	27	26	28	28	29	27
The following four gases were measured by the Horiba PG-250							
NO (ppm)	151	159	167	175	156	156	161
CO (ppm)	148	200	258	377	482	542	380
CO_2 (%)	15.28	15.00	14.73	14.51	16.14	15.75	15.24
O_2 (%)	3.75	4.04	4.30	4.52	2.96	3.43	3.98
The following two gases were measured by the GC							
H_2 (%)	0.00	0.00	0.00	0.00	0.00	0.00	0.00
O_2 (%)	3.73	4.21	4.45	4.77	3.14	3.51	4.03
The following were additional species measured by the FTIR							
Acetylene (ppm)	-21	-21	-21	-20	-22	-21	-21
Aldehyde (ppm)	6	6	4	5	6	5	6
Dodecane (ppm)	1	0	1	1	1	1	2
Ethanol (ppm)	-27	-24	-26	-26	-24	-22	-23
Ethylene (ppm)	0	0	0	0	0	0	0
Formaldehyde (ppm)	0	0	0	0	0	0	0
HCN (ppm)	1	1	1	1	1	1	1
MeOH (ppm)	0	0	0	0	0	0	0
Methane (ppm)	2	2	2	0	2	2	3
NH_3 (ppm)	0	0	0	0	0	0	0
NO_2 (ppm)	4	3	5	4	5	4	2
N_2O (ppm)	12	11	11	12	11	12	9
Phosgene (ppm)	0	0	0	0	0	0	0
Propane (ppm)	1	1	1	1	1	1	1
Propylene (ppm)	1	1	1	1	1	1	1
Toluene (ppm)	4	4	7	5	0	-1	3

Table 57: Indiana Coal – Axial Distance 70 cm.

Radial Dist. (cm)	10	20	30	40	50	60	70
The following eight gases were measured by the FTIR							
CO (ppm)	6038	33174	52866	48250	13256	5857	5599
CO_2 (%)	13	12	11	11	14	14	14
H_2O (%)	8	10	12	11	9	8	9
H_2S (ppm)	-25	21	-6	91	36	-97	-40
HCl (ppm)	1	3	12	39	12	7	10
NO (ppm)	344	122	80	108	278	314	347
SO_2 (ppm)	989	626	528	636	1312	1049	1032
SO_3 (ppm)	30	22	11	11	32	31	26
The following four gases were measured by the Horiba PG-250							
NO (ppm)	354	124	93	125	276	334	355
CO (ppm)	> 5000	> 5000	> 5000	> 5000	> 5000	> 5000	> 5000
CO_2 (%)	17.20	16.48	14.65	15.11	17.67	17.99	17.99
O_2 (%)	1.72	0.71	0.70	0.70	0.80	1.02	1.00
The following two gases were measured by the GC							
H_2 (%)	0.15	1.84	3.85	3.57	0.44	0.10	0.19
O_2 (%)	1.51	0.54	0.38	0.50	0.54	0.80	0.73
The following were additional species measured by the FTIR							
Acetylene (ppm)	-4	196	1103	1000	75	-7	18
Aldehyde (ppm)	6	19	67	64	12	5	6
Dodecane (ppm)	1	-1	8	8	1	0	1
Ethanol (ppm)	-27	-45	11	11	-27	-27	-29
Ethylene (ppm)	1	16	111	124	7	0	1
Formaldehyde (ppm)	1	0	1	1	1	1	1
HCN (ppm)	18	105	266	209	34	19	16
MeOH (ppm)	0	-2	-4	-5	-1	-1	-1
Methane (ppm)	42	1264	3459	3468	370	17	39
NH_3 (ppm)	0	0	0	1	1	0	0
NO_2 (ppm)	5	13	29	26	9	3	5
N_2O (ppm)	9	-2	-1	-1	1	11	5
Phosgene (ppm)	0	0	1	2	1	0	0
Propane (ppm)	1	3	7	8	2	1	2
Propylene (ppm)	1	0	1	2	1	0	0
Toluene (ppm)	-21	-70	-43	-27	-50	-11	-4

Table 58: Indiana Coal – Axial Distance 70 cm.

Radial Dist. (cm)	10	20	30	40	50	60	70
The following eight gases were measured by the FTIR							
CO (ppm)	4902	23211	43284	45719	37715	16096	10154
CO_2 (%)	14	13	11	11	11	12	12
H_2O (%)	8	10	11	12	11	9	8
H_2S (ppm)	26	-27	146	135	305	-27	-42
HCl (ppm)	12	19	46	41	34	16	13
NO (ppm)	355	226	116	130	162	280	348
SO_2 (ppm)	936	1015	674	743	797	1236	1128
SO_3 (ppm)	26	23	12	10	15	33	28
The following four gases were measured by the Horiba PG-250							
NO (ppm)	371	238	121	142	178	294	354
CO (ppm)	> 5000	> 5000	> 5000	> 5000	> 5000	> 5000	> 5000
CO_2 (%)	16.47	16.99	15.14	14.98	15.69	17.35	17.88
O_2 (%)	2.68	0.91	0.82	0.78	0.80	0.85	0.95
The following two gases were measured by the GC							
H_2 (%)	0.04	0.98	2.85	3.01	2.23	0.51	0.19
O_2 (%)	2.36	0.71	0.51	0.41	0.51	0.56	0.63
The following were additional species measured by the FTIR							
Acetylene (ppm)	-7	181	934	1245	798	86	5
Aldehyde (ppm)	8	17	61	79	48	12	5
Dodecane (ppm)	1	1	3	8	0	0	1
Ethanol (ppm)	-23	-30	-19	25	-20	-35	-29
Ethylene (ppm)	0	8	54	110	46	5	1
Formaldehyde (ppm)	2	1	2	1	2	1	1
HCN (ppm)	14	65	193	235	166	46	28
MeOH (ppm)	-1	-2	-3	-4	-3	-1	-1
Methane (ppm)	31	672	2545	3527	2181	377	55
NH_3 (ppm)	0	0	0	0	0	1	0
NO_2 (ppm)	5	10	22	24	19	6	4
N_2O (ppm)	12	0	-1	-1	-1	1	5
Phosgene (ppm)	0	0	1	2	1	1	0
Propane (ppm)	1	2	7	7	6	3	2
Propylene (ppm)	0	0	0	0	0	0	-1
Toluene (ppm)	-17	-67	-40	-26	-33	-35	-15

Table 59: Indiana Coal – Axial Distance 250 cm.

Radial Dist. (cm)	10	20	30	40	50	60	70
The following eight gases were measured by the FTIR							
CO (ppm)	607	465	701	769	750	118	389
CO_2 (%)	13	13	13	13	13	13	13
H_2O (%)	8	8	7	7	7	7	7
H_2S (ppm)	-4	-13	-5	-27	35	-47	-5
HCl (ppm)	7	9	16	19	24	23	26
NO (ppm)	110	143	154	148	152	153	147
SO_2 (ppm)	889	882	870	868	853	813	803
SO_3 (ppm)	29	26	28	25	25	25	24
The following four gases were measured by the Horiba PG-250							
NO (ppm)	108	128	152	148	153	152	142
CO (ppm)	532	464	566	746	761	144	356
CO_2 (%)	16.29	15.93	15.41	15.59	15.48	15.09	14.91
O_2 (%)	2.63	2.99	3.57	3.37	3.49	3.91	4.06
The following two gases were measured by the GC							
H_2 (%)	0.00	0.00	0.00	0.00	0.00	0.00	0.00
O_2 (%)	2.77	3.12	3.71	3.57	3.60	3.95	3.81
The following were additional species measured by the FTIR							
Acetylene (ppm)	-21	-21	-21	-21	-20	-20	-20
Aldehyde (ppm)	1	0	1	1	3	2	1
Dodecane (ppm)	1	1	1	1	0	1	1
Ethanol (ppm)	-26	-23	-19	-20	-22	-22	-20
Ethylene (ppm)	0	0	0	0	0	0	0
Formaldehyde (ppm)	0	0	1	1	1	1	1
HCN (ppm)	1	1	2	3	3	1	2
MeOH (ppm)	-1	-1	-1	-1	-1	-1	-1
Methane (ppm)	1	1	2	2	3	3	3
NH_3 (ppm)	0	0	0	0	0	0	0
NO_2 (ppm)	-2	0	-3	-1	0	-2	-2
N_2O (ppm)	12	8	6	6	6	6	9
Phosgene (ppm)	0	0	0	0	0	0	0
Propane (ppm)	1	1	0	1	1	1	1
Propylene (ppm)	0	0	0	0	0	0	0
Toluene (ppm)	-1	0	3	-2	1	2	1

Table 60: Indiana Coal – Axial Distance 250 cm.

Radial Dist. (cm)	10	20	30	40	50	60	70
The following eight gases were measured by the FTIR							
CO (ppm)	125	379	123	230	542	780	711
CO_2 (%)	12	12	14	14	13	13	12
H_2O (%)	7	7	7	7	7	7	7
H_2S (ppm)	7	-34	17	19	21	-58	-13
HCl (ppm)	29	37	37	41	44	46	51
NO (ppm)	163	157	162	163	173	168	161
SO_2 (ppm)	754	775	854	870	869	825	793
SO_3 (ppm)	26	25	25	25	29	24	26
The following four gases were measured by the Horiba PG-250							
NO (ppm)	166	155	161	163	176	169	164
CO (ppm)	97	394	127	224	517	746	673
CO_2 (%)	13.95	14.24	15.70	15.88	15.86	15.23	14.79
O_2 (%)	5.06	4.79	3.42	3.28	3.30	4.02	4.48
The following two gases were measured by the GC							
H_2 (%)	0.00	0.00	0.00	0.00	0.00	0.00	0.00
O_2 (%)	5.01	4.76	3.45	3.16	3.16	3.77	4.19
The following were additional species measured by the FTIR							
Acetylene (ppm)	-18	-20	-21	-21	-22	-20	-19
Aldehyde (ppm)	2	2	2	3	3	2	3
Dodecane (ppm)	1	1	1	1	1	0	1
Ethanol (ppm)	-21	-21	-22	-25	-20	-22	-25
Ethylene (ppm)	0	0	0	0	0	0	0
Formaldehyde (ppm)	1	1	1	1	1	1	1
HCN (ppm)	1	2	1	1	3	4	4
MeOH (ppm)	-1	-1	-1	-1	-2	-2	-2
Methane (ppm)	1	1	3	3	3	3	1
NH_3 (ppm)	0	0	0	0	0	0	0
NO_2 (ppm)	-2	-2	-2	-3	-3	-2	-1
N_2O (ppm)	6	5	4	4	6	6	6
Phosgene (ppm)	0	0	0	0	0	0	0
Propane (ppm)	1	1	1	1	1	2	2
Propylene (ppm)	0	0	0	0	0	0	0
Toluene (ppm)	7	4	1	-2	3	5	5

Table 61: Indiana Coal – Axial Distance 70 cm.

Radial Dist. (cm)	10	20	30	40	50	60	70
The following eight gases were measured by the FTIR							
CO (ppm)	652	17225	42635	39253	30262		
CO_2 (%)	12	12	11	11	11		
H_2O (%)	7	9	11	10	10		
H_2S (ppm)	-41	93	303	423	318		
HCl (ppm)	44	66	188	184	132		
NO (ppm)	375	212	76	66	80		
SO_2 (ppm)	800	910	522	436	432		
SO_3 (ppm)	29	23	8	7	14		
The following four gases were measured by the Horiba PG-250							
NO (ppm)	370	235	100	71	85		
CO (ppm)	835	> 5000	> 5000	> 5000	> 5000		
CO_2 (%)	14.30	16.87	15.29	15.17	15.97		
O_2 (%)	4.82	0.81	0.65	0.68	0.81		
The following two gases were measured by the GC							
H_2 (%)	0.00	0.87	2.56	3.18	2.19		
O_2 (%)	4.44	0.81	0.59	0.56	0.56		
The following were additional species measured by the FTIR							
Acetylene (ppm)	0.00	0.87	2.56	3.18	2.19		
Aldehyde (ppm)	4.44	0.81	0.59	0.56	0.56		
Dodecane (ppm)	0.00	0.87	2.56	3.18	2.19		
Ethanol (ppm)	4.44	0.81	0.59	0.56	0.56		
Ethylene (ppm)	0.00	0.87	2.56	3.18	2.19		
Formaldehyde (ppm)	4.44	0.81	0.59	0.56	0.56		
HCN (ppm)	0.00	0.87	2.56	3.18	2.19		
MeOH (ppm)	4.44	0.81	0.59	0.56	0.56		
Methane (ppm)	0.00	0.87	2.56	3.18	2.19		
NH_3 (ppm)	4.44	0.81	0.59	0.56	0.56		
NO_2 (ppm)	0.00	0.87	2.56	3.18	2.19		
N_2O (ppm)	4.44	0.81	0.59	0.56	0.56		
Phosgene (ppm)	0.00	0.87	2.56	3.18	2.19		
Propane (ppm)	4.44	0.81	0.59	0.56	0.56		
Propylene (ppm)	0.00	0.87	2.56	3.18	2.19		
Toluene (ppm)	4.44	0.81	0.59	0.56	0.56		

A.6 Illinois #6-2

Table 62: Illinois #6-2 Coal – Axial Distance 83 cm.

Radial Dist. (cm)	10	20	30	40	50	60	70
The following eight gases were measured by the FTIR							
CO (ppm)	810	23760	43424	33651	13403	10010	4807
CO_2 (%)	12	16	14	15	17	17	17
H_2O (%)	6	9	11	10	9	8	8
H_2S (ppm)	-110	90	757	930	79	-67	-47
HCl (ppm)	27	81	241	146	144	111	112
NO (ppm)	246	232	81	93	160	233	297
SO_2 (ppm)	1589	2356	1397	1651	3005	2519	2266
SO_3 (ppm)	38	50	19	27	54	54	52
The following four gases were measured by the Horiba PG-250							
NO (ppm)	246	299	83	96	140	241	300
CO (ppm)	870	4506	4506	4506	4506	4506	3595
CO_2 (%)	11.81	16.00	14.45	15.44	16.65	17.06	16.72
O_2 (%)	6.96	0.61	0.21	0.18	0.68	0.94	2.26
The following two gases were measured by the GC							
H_2 (%)	0.00	1.11	3.17	2.52	0.30	0.36	0.05
O_2 (%)	6.89	0.74	0.52	0.50	0.55	0.59	1.88
The following were additional species measured by the FTIR							
Acetylene (ppm)	0	362	1290	979	190	123	47
Aldehyde (ppm)	1	26	66	52	15	11	5
Dodecane (ppm)	1	3	-2	-1	0	0	1
Ethanol (ppm)	-13	-8	70	50	-28	-30	-20
Ethylene (ppm)	1	83	344	354	46	10	7
Formaldehyde (ppm)	1	5	3	3	4	4	3
HCN (ppm)	5	53	161	124	35	26	14
MeOH (ppm)	-1	-4	-9	-7	-3	-2	-1
Methane (ppm)	24	1739	3598	3548	1136	574	227
NH_3 (ppm)	0	1	2	1	1	0	0
NO_2 (ppm)	1	9	23	19	4	1	-1
N_2O (ppm)	13	-1	-4	-3	-1	0	6
Phosgene (ppm)	0	2	4	3	0	0	0
Propane (ppm)	1	5	12	10	6	6	5
Propylene (ppm)	0	1	4	6	-2	-2	-1
Toluene (ppm)	-7	-62	-14	-1	-40	-17	-9

Table 63: Illinois #6-2 Coal – Axial Distance 83 cm.

Radial Dist. (cm)	10	20	30	40	50	60	70
The following eight gases were measured by the FTIR							
CO (ppm)	4195	48264	51116	21587	3490	3375	2583
CO_2 (%)	12.22	10.68	10.40	12.02	13.56	14.28	13.57
H_2O (%)	7	10	10	9	8	8	7
H_2S (ppm)	-116	871	960	125	-53	-152	-30
HCl (ppm)	109	210	185	139	129	153	150
NO (ppm)	346	74	94	169	258	274	294
SO_2 (ppm)	2052	1016	1116	3135	2312	2278	2162
SO_3 (ppm)	49	17	21	53	54	52	44
The following four gases were measured by the Horiba PG-250							
NO (ppm)	348	72	101	166	253	282	304
CO (ppm)	4506	4506	4506	4506	3160	3038	2827
CO_2 (%)	14.99	14.33	14.23	15.69	15.72	17.19	17.23
O_2 (%)	3.14	0.32	0.59	1.23	2.95	1.67	1.72
The following two gases were measured by the GC							
H_2 (%)	0.13	3.43	0.03	0.01	0.07	0.05	--
O_2 (%)	3.46	0.31	0.59	1.23	2.81	1.38	1.72
The following were additional species measured by the FTIR							
Acetylene (ppm)	45	927	1077	294	39	14	-11
Aldehyde (ppm)	11	55	60	28	10	8	10
Dodecane (ppm)	1	-1	-1	2	0	1	1
Ethanol (ppm)	-16	35	39	-19	-16	-17	-21
Ethylene (ppm)	3	93	145	93	6	1	0
Formaldehyde (ppm)	2	3	3	3	2	1	1
HCN (ppm)	12	136	148	43	10	8	6
MeOH (ppm)	-1	-5	-5	-3	-1	-1	-1
Methane (ppm)	135	3288	3434	1433	150	48	24
NH_3 (ppm)	0	1	1	1	0	0	0
NO_2 (ppm)	1	17	18	6	-1	-1	1
N_2O (ppm)	8	-4	-4	-2	3	3	5
Phosgene (ppm)	0	3	3	2	0	0	0
Propane (ppm)	5	9	8	4	5	5	6
Propylene (ppm)	0	-1	0	1	0	0	0
Toluene (ppm)	-12	-26	-14	-48	-19	-4	-5

Table 64: Illinois #6-2 Coal – Axial Distance 257 cm.

Radial Dist. (cm)	10	20	30	40	50	60	70
The following eight gases were measured by the FTIR							
CO (ppm)	172	194	294	200	481	755	613
CO_2 (%)	13.47	13.26	12.97	13.30	13.21	12.14	11.23
H_2O (%)	5	6	7	6	6	6	6
H_2S (ppm)	35	-74	-63	-105	-43	-70	-82
HCl (ppm)	18	18	54	123	131	133	116
NO (ppm)	191	205	194	164	170	168	141
SO_2 (ppm)	2006	1943	1889	1927	1936	1822	1635
SO_3 (ppm)	55	51	45	49	46	48	43
The following four gases were measured by the Horiba PG-250							
NO (ppm)	173	206	196	177	171	144	88
CO (ppm)	182	187	292	119	457	542	624
CO_2 (%)	14.68	15.22	15.55	15.53	15.84	12.13	7.67
O_2 (%)	4.38	3.87	3.49	3.58	3.28	6.80	11.47
The following two gases were measured by the GC							
H_2 (%)	0.00	0.00	0.00	0.00	0.00	0.00	0.00
O_2 (%)	4.01	3.87	3.49	3.58	3.28	6.80	11.47
The following were additional species measured by the FTIR							
Acetylene (ppm)	-20	-20	-19	-20	-20	-18	-13
Aldehyde (ppm)	8	7	8	9	8	10	7
Dodecane (ppm)	1	1	0	1	0	1	1
Ethanol (ppm)	-16	-16	-18	-16	-20	-19	-18
Ethylene (ppm)	0	0	0	0	0	0	0
Formaldehyde (ppm)	0	0	1	1	1	1	1
HCN (ppm)	1	1	2	1	2	3	3
MeOH (ppm)	-1	-1	-1	-1	-1	-1	-1
Methane (ppm)	1	0	2	0	0	0	1
NH_3 (ppm)	0	0	0	0	0	0	0
NO_2 (ppm)	2	2	0	-1	1	0	2
N_2O (ppm)	2	2	3	4	5	6	6
Phosgene (ppm)	0	0	0	0	0	0	0
Propane (ppm)	2	2	3	5	5	5	4
Propylene (ppm)	0	0	0	0	0	1	1
Toluene (ppm)	1	5	4	3	5	7	3

Table 65: Illinois #6-2 Coal – Axial Distance 257 cm.

Radial Dist. (cm)	10	20	30	40	50	60	70
The following eight gases were measured by the FTIR							
CO (ppm)	493	95	152	237	608	464	1300
CO_2 (%)	14.01	13.86	13.67	13.55	13.22	14.80	15.13
H_2O (%)	7	6	6	6	7	7	7
H_2S (ppm)	7	-91	28	-11	-33	-15	14
HCl (ppm)	136	128	146	146	148	134	158
NO (ppm)	182	154	192	177	174	186	177
SO_2 (ppm)	2094	1989	1970	1962	1949	2208	2284
SO_3 (ppm)	54	49	46	54	54	46	54
The following four gases were measured by the Horiba PG-250							
NO (ppm)	170	156	185	165	173	185	175
CO (ppm)	502	233	129	179	606	592	1030
CO_2 (%)	16.45	14.91	15.44	15.30	15.57	16.78	17.49
O_2 (%)	2.63	4.21	3.65	3.84	3.56	2.34	1.70
The following two gases were measured by the GC							
H_2 (%)	0.00	0.00	0.00	0.00	0.00	0.00	0.00
O_2 (%)	2.63	3.55	3.62	3.53	3.31	1.88	1.39
The following were additional species measured by the FTIR							
Acetylene (ppm)	-14	-21	-21	-20	-20	4	5
Aldehyde (ppm)	8	10	11	10	10	10	10
Dodecane (ppm)	1	1	1	1	1	1	1
Ethanol (ppm)	-22	-19	-21	-17	-21	-22	-21
Ethylene (ppm)	0	0	0	0	0	0	0
Formaldehyde (ppm)	1	1	1	1	1	1	1
HCN (ppm)	2	1	1	1	2	2	5
MeOH (ppm)	-1	-2	-2	-2	-2	-2	-2
Methane (ppm)	0	0	0	0	0	2	2
NH_3 (ppm)	0	0	0	0	0	0	0
NO_2 (ppm)	-1	0	1	1	0	-1	-1
N_2O (ppm)	3	4	3	3	4	5	5
Phosgene (ppm)	0	0	0	0	0	0	0
Propane (ppm)	5	5	6	6	5	5	6
Propylene (ppm)	0	0	0	0	0	0	0
Toluene (ppm)	4	0	3	3	3	7	4

Table 66: Illinois #6-2 Coal – Axial Distance 83 cm.

Radial Dist. (cm)	10	20	30	40	50	60	70
The following eight gases were measured by the FTIR							
CO (ppm)	1295	28992	56054	29154	1896	732	522
CO_2 (%)	12.05	11.83	10.93	11.50	12.06	12.41	11.80
H_2O (%)	6	10	10	10	7	6	6
H_2S (ppm)	-99	111	710	380	-65	50	-8
HCl (ppm)	126	242	338	217	118	128	121
NO (ppm)	340	238	88	147	298	266	294
SO_2 (ppm)	1891	2136	989	2128	2221	2038	1887
SO_3 (ppm)	44	40	17	43	54	48	45
The following four gases were measured by the Horiba PG-250							
NO (ppm)	345	274	94	141	297	270	294
CO (ppm)	1178	4506	4506	4506	2552	724	584
CO_2 (%)	13.77	15.83	13.92	15.55	14.74	14.54	13.98
O_2 (%)	5.04	0.88	0.72	0.76	3.79	4.30	4.93
The following two gases were measured by the GC							
H_2 (%)	0.01	1.20	3.70	1.39	0.03	0.00	0.00
O_2 (%)	4.79	0.63	0.34	0.52	3.66	4.14	4.66
The following were additional species measured by the FTIR							
Acetylene (ppm)	-6	308	1080	424	4	-17	-18
Aldehyde (ppm)	8	29	60	38	8	11	9
Dodecane (ppm)	1	1	-1	4	1	1	1
Ethanol (ppm)	-13	-30	39	-8	-19	-25	-17
Ethylene (ppm)	0	26	137	112	2	0	0
Formaldehyde (ppm)	1	2	3	4	2	1	1
HCN (ppm)	3	50	145	52	6	3	2
MeOH (ppm)	-1	-3	-6	-4	-1	-1	-1
Methane (ppm)	22	1229	3546	1864	49	5	2
NH_3 (ppm)	0	0	1	1	0	0	0
NO_2 (ppm)	0	4	18	10	1	1	1
N_2O (ppm)	7	-2	-4	-3	4	4	4
Phosgene (ppm)	0	1	4	2	0	0	0
Propane (ppm)	4	7	11	7	5	5	5
Propylene (ppm)	0	-1	-1	0	0	0	0
Toluene (ppm)	3	-53	6	-43	5	6	6

Table 67: Illinois #6-2 Coal – Axial Distance 243 cm.

Radial Dist. (cm)	10	20	30	40	50	60	70
The following eight gases were measured by the FTIR							
CO (ppm)	302	1099	1355	303	346	428	488
CO_2 (%)	16.23	16.54	16.46	15.43	15.48	15.53	15.44
H_2O (%)	7	7	7	7	7	7	7
H_2S (ppm)	50	43	30	66	34	24	-37
HCl (ppm)	24	38	40	42	30	52	52
NO (ppm)	91	105	111	109	110	117	111
SO_2 (ppm)	2136	2145	2124	2030	2021	1967	1947
SO_3 (ppm)	50	48	48	47	55	44	45
The following four gases were measured by the Horiba PG-250							
NO (ppm)							
CO (ppm)							
CO_2 (%)							
O_2 (%)							
The following two gases were measured by the GC							
H_2 (%)	0.00	0.00	0.00	0.00	0.00	0.00	0.00
O_2 (%)	2.21	2.30	2.50	3.24	4.24	3.34	3.42
The following were additional species measured by the FTIR							
Acetylene (ppm)	3	3	2	2	2	2	2
Aldehyde (ppm)	3	3	3	2	7	3	3
Dodecane (ppm)	1	0	0	1	1	0	0
Ethanol (ppm)	-21	-18	-20	-21	-19	-16	-18
Ethylene (ppm)	0	0	0	0	0	0	0
Formaldehyde (ppm)	1	1	1	1	1	1	1
HCN (ppm)	2	4	4	2	2	2	2
MeOH (ppm)	-1	-1	-1	-1	-1	-1	-1
Methane (ppm)	3	3	4	1	1	3	3
NH_3 (ppm)	0	0	0	0	0	0	0
NO_2 (ppm)	0	0	1	0	1	1	-2
N_2O (ppm)	13	13	12	13	13	14	15
Phosgene (ppm)	0	0	0	0	0	0	0
Propane (ppm)	2	3	3	4	3	3	4
Propylene (ppm)	0	0	0	0	0	0	0
Toluene (ppm)	-11	-1	4	5	8	3	8

Table 68: Illinois #6-2 Coal – Axial Distance 97 cm.

Radial Dist. (cm)	10	20	30	40	50	60	70
The following eight gases were measured by the FTIR							
CO (ppm)	8259	24045	29357	26958	14617	6749	5469
CO_2 (%)	17	16	16	16	17	18	18
H_2O (%)	9	10	10	10	10	9	8
H_2S (ppm)	1	491	578	578	462	37	37
HCl (ppm)	30	262	255	243	184	99	74
NO (ppm)	213	49	36	41	79	168	228
SO_2 (ppm)	2402	1098	748	770	1925	3338	2840
SO_3 (ppm)	53	30	22	25	42	75	63
The following four gases were measured by the Horiba PG-250							
NO (ppm)							
CO (ppm)							
CO_2 (%)							
O_2 (%)							
The following two gases were measured by the GC							
H_2 (%)	1.10	1.04	1.16	1.32	0.61	0.23	0.07
O_2 (%)	0.53	0.50	0.53	0.52	0.52	0.54	0.74
The following were additional species measured by the FTIR							
Acetylene (ppm)	90	177	191	192	93	23	10
Aldehyde (ppm)	5	13	14	15	10	4	7
Dodecane (ppm)	0	0	1	1	0	1	0
Ethanol (ppm)	-30	-26	-29	-28	-21	-25	-24
Ethylene (ppm)	6	27	36	63	26	2	0
Formaldehyde (ppm)	2	2	2	2	2	1	1
HCN (ppm)	15	26	28	27	16	9	11
MeOH (ppm)	-1	-2	-2	-2	-1	-1	-1
Methane (ppm)	219	1091	1277	1300	567	74	19
NH_3 (ppm)	0	0	0	0	0	0	0
NO_2 (ppm)	2	3	6	7	1	-2	-1
N_2O (ppm)	0	-2	-2	-2	-2	0	5
Phosgene (ppm)	0	1	1	1	1	1	0
Propane (ppm)	3	8	7	8	6	5	4
Propylene (ppm)	0	-1	-1	-1	-2	-1	0
Toluene (ppm)	2	-39	-32	-30	5	1	-1

Table 69: Illinois #6-2 Coal – Axial Distance 77 cm.

Radial Dist. (cm)	10	20	30	40	50	60	70
The following eight gases were measured by the FTIR							
CO (ppm)	11830	21867	37972	37196	9971	4168	2384
CO_2 (%)	17.33	16.72	13.49	13.49	17.29	17.57	17.10
H_2O (%)	9	10	10	11	9	9	8
H_2S (ppm)	46	107	455	631	34	76	70
HCl (ppm)	49	85	142	158	85	74	77
NO (ppm)	166	168	68	68	276	211	226
SO_2 (ppm)	2316	2077	996	840	3637	2692	2296
SO_3 (ppm)	51	47	28	27	72	52	53
The following four gases were measured by the Horiba PG-250							
NO (ppm)							
CO (ppm)							
CO_2 (%)							
O_2 (%)							
The following two gases were measured by the GC							
H_2 (%)	0.33	0.49	1.25	1.73	0.54	0.19	0.02
O_2 (%)	2.15	0.58	0.55	0.13	0.21	0.42	1.27
The following were additional species measured by the FTIR							
Acetylene (ppm)	57	134	232	267	96	26	6
Aldehyde (ppm)	8	10	20	25	10	6	4
Dodecane (ppm)	1	1	4	4	0	1	0
Ethanol (ppm)	-31	-29	-28	-19	-30	-25	-26
Ethylene (ppm)	3	15	52	109	12	1	0
Formaldehyde (ppm)	1	1	2	2	2	2	2
HCN (ppm)	12	21	40	42	13	9	7
MeOH (ppm)	-1	-1	-2	-3	-1	-1	-1
Methane (ppm)	250	688	1774	1996	283	54	10
NH_3 (ppm)	0	0	0	0	0	0	0
NO_2 (ppm)	1	6	9	12	0	0	1
N_2O (ppm)	-1	-2	-2	-2	2	4	7
Phosgene (ppm)	1	1	1	1	1	0	0
Propane (ppm)	3	4	6	8	6	5	4
Propylene (ppm)	-1	-1	-1	-1	-1	0	0
Toluene (ppm)	12	-7	-50	-42	-1	-2	1

Table 70: Illinois #6-2 Coal – Axial Distance 230 cm.

Radial Dist. (cm)	10	20	30	40	50	60	70
The following eight gases were measured by the FTIR							
CO (ppm)	235	370	324	297	822	853	1122
CO_2 (%)	13.94	13.96	13.98	13.84	14.49	16.09	16.64
H_2O (%)	6	7	7	7	7	7	7
H_2S (ppm)	34	40	73	12	0	11	85
HCl (ppm)	29	43	47	47	81	75	75
NO (ppm)	115	123	127	128	135	131	124
SO_2 (ppm)	2080	2008	1985	1973	1939	2018	2151
SO_3 (ppm)	53	50	56	55	53	44	56
The following four gases were measured by the Horiba PG-250							
NO (ppm)							
CO (ppm)							
CO_2 (%)							
O_2 (%)							
The following two gases were measured by the GC							
H_2 (%)	0.00	0.00	0.00	0.00	0.00	0.00	0.00
O_2 (%)	2.06	3.24	3.47	3.51	3.50	3.22	2.62
The following were additional species measured by the FTIR							
Acetylene (ppm)	-27	-27	-27	-27	-27	2	2
Aldehyde (ppm)	5	4	8	4	6	3	5
Dodecane (ppm)	0	1	1	1	0	1	0
Ethanol (ppm)	-18	-19	-20	-19	-12	-19	-21
Ethylene (ppm)	0	0	0	0	0	0	0
Formaldehyde (ppm)	1	1	1	1	1	1	1
HCN (ppm)	2	2	1	1	3	3	4
MeOH (ppm)	0	-1	0	-1	-1	-1	-1
Methane (ppm)	3	2	2	2	2	2	4
NH_3 (ppm)	1	0	0	0	0	0	0
NO_2 (ppm)	-1	0	1	1	-1	-2	0
N_2O (ppm)	10	11	11	10	11	11	9
Phosgene (ppm)	0	0	0	0	0	0	0
Propane (ppm)	3	4	3	4	4	4	4
Propylene (ppm)	0	0	0	0	0	0	0
Toluene (ppm)	-10	-13	-9	-11	-12	7	3

Table 71: Illinois #6-2 Coal – Axial Distance 110 cm.

Radial Dist. (cm)	10	20	30	40	50	60	70
The following eight gases were measured by the FTIR							
CO (ppm)	8303	2825	1557	1822	3250	8256	2500
CO_2 (%)	17.63	17.14	16.58	16.74	17.39	18.01	17.45
H_2O (%)	8	8	8	8	8	8	8
H_2S (ppm)	40	25	115	88	46	22	59
HCl (ppm)	10	10	10	12	13	22	22
NO (ppm)	224	242	239	257	286	248	251
SO_2 (ppm)	2384	2368	2266	2298	2376	2386	2336
SO_3 (ppm)	51	59	52	46	60	51	51
The following four gases were measured by the Horiba PG-250							
NO (ppm)							
CO (ppm)							
CO_2 (%)							
O_2 (%)							
The following two gases were measured by the GC							
H_2 (%)	0.15	0.13	0.06	0.03	0.03	0.13	0.13
O_2 (%)	8.03	1.96	1.80	1.86	1.63	0.81	0.76
The following were additional species measured by the FTIR							
Acetylene (ppm)	47	24	16	17	27	13	6
Aldehyde (ppm)	4	5	1	3	3	5	3
Dodecane (ppm)	6	5	4	3	3	2	2
Ethanol (ppm)	-31	-28	-23	-20	-20	-16	-18
Ethylene (ppm)	3	2	1	1	2	1	0
Formaldehyde (ppm)	2	2	1	1	1	1	1
HCN (ppm)	9	4	3	3	5	10	4
MeOH (ppm)	0	0	1	1	1	1	1
Methane (ppm)	132	50	32	31	51	46	14
NH_3 (ppm)	0	0	0	0	0	0	0
NO_2 (ppm)	0	0	-3	1	2	0	1
N_2O (ppm)	0	3	6	6	6	0	4
Phosgene (ppm)	-1	-1	0	0	0	0	0
Propane (ppm)	9	8	7	6	5	3	4
Propylene (ppm)	0	0	0	0	0	0	0
Toluene (ppm)	2	0	5	4	3	0	4

Table 72: Illinois #6-2 Coal – Axial Distance 130 cm.

Radial Dist. (cm)	10	20	30	40	50	60	70
The following eight gases were measured by the FTIR							
CO (ppm)	2973	1562	1838	10871	21589	19433	7415
CO_2 (%)	13	17	17	17	17	17	18
H_2O (%)	6	7	7	7	8	9	9
H_2S (ppm)	71	-64	7	30	335	465	18
HCl (ppm)	62	42	44	58	143	137	98
NO (ppm)	188	225	218	100	25	63	124
SO_2 (ppm)	2811	2384	2363	2041	622	1024	2775
SO_3 (ppm)	71	54	50	54	24	31	60
The following four gases were measured by the Horiba PG-250							
NO (ppm)							
CO (ppm)							
CO_2 (%)							
O_2 (%)							
The following two gases were measured by the GC							
H_2 (%)	0.34	0.07	0.03	0.15	0.58	0.98	0.61
O_2 (%)	4.68	2.42	2.23	1.66	3.14	0.70	0.60
The following were additional species measured by the FTIR							
Acetylene (ppm)	-22	3	4	20	71	64	9
Aldehyde (ppm)	7	1	6	6	5	13	7
Dodecane (ppm)	1	1	1	0	1	1	1
Ethanol (ppm)	-19	-24	-23	-31	-33	-36	-26
Ethylene (ppm)	0	0	0	4	13	3	0
Formaldehyde (ppm)	1	1	1	1	1	1	1
HCN (ppm)	3	1	1	8	15	19	8
MeOH (ppm)	0	0	0	1	0	0	0
Methane (ppm)	6	4	5	176	668	354	26
NH_3 (ppm)	0	0	0	0	0	0	0
NO_2 (ppm)	-2	0	2	1	3	4	0
N_2O (ppm)	2	5	4	-2	-2	-2	-1
Phosgene (ppm)	0	0	0	1	1	1	1
Propane (ppm)	4	4	3	2	4	3	5
Propylene (ppm)	1	1	1	0	-1	-1	0
Toluene (ppm)	-8	7	6	8	8	7	-2

Table 73: Illinois #6-2 Coal – Axial Distance 150 cm.

Radial Dist. (cm)	10	20	30	40	50	60	70
The following eight gases were measured by the FTIR							
CO (ppm)	854	364	791	628	804	1934	2943
CO_2 (%)	13	13	14	17	16	15	17
H_2O (%)	6	5	7	7	8	7	7
H_2S (ppm)	-97	24	-4	-13	-129	-56	-103
HCl (ppm)	59	39	47	33	43	41	35
NO (ppm)	153	146	145	152	174	194	213
SO_2 (ppm)	2054	2001	2324	2346	2353	2295	2466
SO_3 (ppm)	57	58	57	57	55	63	58
The following four gases were measured by the Horiba PG-250							
NO (ppm)							
CO (ppm)							
CO_2 (%)							
O_2 (%)							
The following two gases were measured by the GC							
H_2 (%)	0.00	0.00	0.00	0.00	0.00	0.00	0.02
O_2 (%)	4.37	5.72	4.57	2.16	1.88	2.72	2.09
The following were additional species measured by the FTIR							
Acetylene (ppm)	-26	-26	-28	2	-1	-26	5
Aldehyde (ppm)	8	7	8	9	7	11	8
Dodecane (ppm)	1	1	1	2	1	1	2
Ethanol (ppm)	-17	-21	-21	-20	-25	-20	-23
Ethylene (ppm)	0	0	0	0	0	0	0
Formaldehyde (ppm)	1	1	1	1	1	1	1
HCN (ppm)	1	1	2	2	2	3	5
MeOH (ppm)	-1	0	0	-1	0	0	0
Methane (ppm)	4	2	4	5	5	8	11
NH_3 (ppm)	0	0	0	0	0	0	0
NO_2 (ppm)	2	2	4	3	5	2	0
N_2O (ppm)	6	5	8	5	7	6	6
Phosgene (ppm)	0	0	0	0	0	0	0
Propane (ppm)	3	2	2	2	2	2	2
Propylene (ppm)	1	1	1	0	1	1	1
Toluene (ppm)	-8	-8	-7	2	6	-8	9

Table 74: Illinois #6-2 Coal – Axial Distance 170 cm.

Radial Dist. (cm)	10	20	30	40	50	60	70
The following eight gases were measured by the FTIR							
CO (ppm)	1912	1573	1065	973	1035	1199	1216
CO_2 (%)	19	19	16	16	14	14	14
H_2O (%)	8	8	7	7	7	7	7
H_2S (ppm)	-98	-54	-38	-24	-29	-98	-111
HCl (ppm)	10	41	54	61	61	63	62
NO (ppm)	150	143	146	148	154	158	160
SO_2 (ppm)	2364	2273	2100	2032	1985	1936	1940
SO_3 (ppm)	44	40	33	33	39	37	40
The following four gases were measured by the Horiba PG-250							
NO (ppm)							
CO (ppm)							
CO_2 (%)							
O_2 (%)							
The following two gases were measured by the GC							
H_2 (%)	0.01	0.00	0.00	0.00	0.00	0.00	0.00
O_2 (%)	1.22	1.74	3.15	3.65	4.08	4.53	4.71
The following were additional species measured by the FTIR							
Acetylene (ppm)	1756	1461	973	879	926	1084	1094
Aldehyde (ppm)	111	89	53	41	50	83	81
Dodecane (ppm)	2	1	1	1	2	1	1
Ethanol (ppm)	-18	-14	-14	-17	-17	-13	-16
Ethylene (ppm)	0	0	0	0	0	0	0
Formaldehyde (ppm)	0	1	1	1	1	1	1
HCN (ppm)	3	5	4	4	4	4	4
MeOH (ppm)	0	-1	-1	0	0	0	0
Methane (ppm)	4	4	4	2	2	2	3
NH_3 (ppm)	0	0	0	0	0	0	0
NO_2 (ppm)	2	2	2	4	1	4	2
N_2O (ppm)	5	8	9	9	9	10	11
Phosgene (ppm)	0	0	0	0	0	0	0
Propane (ppm)	3	3	3	3	2	2	2
Propylene (ppm)	0	0	0	0	0	0	0
Toluene (ppm)	5	6	5	10	-9	-5	-8

Table 75: Illinois #6-2 Coal – Axial Distance 30 cm.

Radial Dist. (cm)	10	20	30	35	40	50	60	70
The following eight gases were measured by the FTIR								
CO (ppm)	168	235	1499	10742	66414	1876	618	633
CO_2 (%)	15	14	8	3	10	8	11	14
H_2O (%)	7	7	6	5	11	5	6	7
H_2S (ppm)	-61	-86	-163	-263	522	-89	-49	-104
HCl (ppm)	59	64	69	46	63	80	94	108
NO (ppm)	264	228	254	129	211	251	215	226
SO_2 (ppm)	1924	1766	1135	589	2020	1078	1640	2128
SO_3 (ppm)	36	32	16	2	17	16	28	51
The following four gases were measured by the Horiba PG-250								
NO (ppm)								
CO (ppm)								
CO_2 (%)								
O_2 (%)								
The following two gases were measured by the GC								
H_2 (%)	0.00	0.00	0.00	0.42	2.71	0.22	0.00	0.00
O_2 (%)	4.19	5.31	11.82	14.30	2.55	11.16	7.18	2.53
The following were additional species measured by the FTIR								
Acetylene (ppm)	173	235	1417	9586	85960	1838	624	625
Aldehyde (ppm)	3	6	107	5044	60119	148	18	23
Dodecane (ppm)	1	1	1	4	-12	2	2	2
Ethanol (ppm)	-13	-13	-13	11	276	-12	-16	-19
Ethylene (ppm)	0	0	7	243	828	4	1	0
Formaldehyde (ppm)	1	1	5	22	56	8	2	2
HCN (ppm)	1	1	4	31	157	9	4	3
MeOH (ppm)	-1	-1	0	2	-6	0	0	0
Methane (ppm)	4	4	21	792	4250	10	2	2
NH_3 (ppm)	0	0	0	0	2	1	0	0
NO_2 (ppm)	2	1	1	-6	7	3	3	2
N_2O (ppm)	5	6	7	2	-1	9	10	10
Phosgene (ppm)	0	0	0	-2	2	0	0	0
Propane (ppm)	2	3	3	20	36	4	4	4
Propylene (ppm)	0	0	2	54	178	2	0	0
Toluene (ppm)	2	4	-32	13	26	-12	-9	-7

Table 76: Illinois #6-2 Coal – Axial Distance 50 cm.

Radial Dist. (cm)	10	20	30	40	50	60	70
The following eight gases were measured by the FTIR							
CO (ppm)	278	484	13856	70952	1327	514	1271
CO_2 (%)	10	12	15	12	11	13	16
H_2O (%)	6	6	9	12	6	7	7
H_2S (ppm)	-59	-97	-262	533	-124	-19	-58
HCl (ppm)	85	128	143	133	113	119	122
NO (ppm)	289	246	537	241	243	226	230
SO_2 (ppm)	1288	1576	2269	2131	1472	1942	2041
SO_3 (ppm)	22	32	37	7	26	40	39
The following four gases were measured by the Horiba PG-250							
NO (ppm)							
CO (ppm)							
CO_2 (%)							
O_2 (%)							
The following two gases were measured by the GC							
H_2 (%)	0.00	0.00	0.38	3.88	0.01	0.00	0.00
O_2 (%)	9.35	7.58	3.67	0.67	8.33	4.47	3.26
The following were additional species measured by the FTIR							
Acetylene (ppm)	268	469	12704	102216	1291	513	1131
Aldehyde (ppm)	15	20	6721	71748	95	17	117
Dodecane (ppm)	1	2	1	-9	2	1	2
Ethanol (ppm)	-12	-14	-22	397	-9	-17	-14
Ethylene (ppm)	0	0	72	-1377	3	1	0
Formaldehyde (ppm)	1	1	9	49	4	2	2
HCN (ppm)	1	2	41	208	8	4	3
MeOH (ppm)	0	0	0	-13	-1	0	0
Methane (ppm)	3	3	615	5055	12	2	5
NH_3 (ppm)	0	0	0	3	1	0	0
NO_2 (ppm)	1	1	4	7	4	3	1
N_2O (ppm)	7	16	10	-2	13	10	7
Phosgene (ppm)	0	0	1	9	0	0	0
Propane (ppm)	3	4	7	35	3	4	4
Propylene (ppm)	1	0	2	213	2	1	1
Toluene (ppm)	-20	-7	-41	116	-6	-4	-11

Table 77: Illinois #6-2 Coal – Axial Distance 190 cm.

Radial Dist. (cm)	10	20	30	40	50	60	70
The following eight gases were measured by the FTIR							
CO (ppm)	552	701	854	860	964	1182	1203
CO_2 (%)	16	16	15	13	13	14	15
H_2O (%)	7	7	7	7	7	7	7
H_2S (ppm)	-56	-121	-35	-30	-70	-68	-180
HCl (ppm)	103	112	109	105	100	100	102
NO (ppm)	144	151	152	154	165	184	192
SO_2 (ppm)	2034	1976	1895	1825	1779	1931	2129
SO_3 (ppm)	41	36	41	41	36	37	47
The following four gases were measured by the Horiba PG-250							
NO (ppm)							
CO (ppm)							
CO_2 (%)							
O_2 (%)							
The following two gases were measured by the GC							
H_2 (%)	0.00	0.00	0.00	0.00	0.00	0.00	0.00
O_2 (%)	3.02	2.99	3.59	4.43	4.89	4.18	2.69
The following were additional species measured by the FTIR							
Acetylene (ppm)	523	654	778	781	870	1067	1091
Aldehyde (ppm)	14	22	45	46	55	82	100
Dodecane (ppm)	1	1	2	1	1	1	1
Ethanol (ppm)	-19	-21	-25	-17	-19	-19	-17
Ethylene (ppm)	0	0	0	0	0	0	0
Formaldehyde (ppm)	1	1	1	1	1	1	1
HCN (ppm)	2	2	3	3	3	3	3
MeOH (ppm)	0	0	0	0	0	0	0
Methane (ppm)	2	2	2	2	3	3	3
NH_3 (ppm)	0	0	0	0	0	0	0
NO_2 (ppm)	3	0	3	3	2	3	4
N_2O (ppm)	7	7	6	5	6	7	7
Phosgene (ppm)	0	0	0	0	0	0	0
Propane (ppm)	4	4	4	4	3	3	4
Propylene (ppm)	0	0	0	1	1	1	1
Toluene (ppm)	2	8	5	-6	-6	-10	-9

Table 78: Illinois #6-2 Coal – Axial Distance 210 cm.

Radial Dist. (cm)	10	20	30	40	50	60	70
The following eight gases were measured by the FTIR							
CO (ppm)	82	131	197	546	762	908	1055
CO_2 (%)	14	15	14	15	17	16	17
H_2O (%)	7	7	7	7	7	7	7
H_2S (ppm)	-108	-42	-96	-47	-55	-46	-185
HCl (ppm)	94	106	111	117	121	120	119
NO (ppm)	141	142	149	157	171	178	182
SO_2 (ppm)	2088	2121	2102	2058	2078	2083	2091
SO_3 (ppm)	45	41	46	43	38	40	42
The following four gases were measured by the Horiba PG-250							
NO (ppm)							
CO (ppm)							
CO_2 (%)							
O_2 (%)							
The following two gases were measured by the GC							
H_2 (%)	0.00	0.00	0.00	0.00	0.00	0.00	0.00
O_2 (%)	2.93	2.51	2.61	2.80	2.72	2.66	2.61
The following were additional species measured by the FTIR							
Acetylene (ppm)	84	135	197	514	702	826	958
Aldehyde (ppm)	2	3	5	18	34	42	64
Dodecane (ppm)	1	1	2	1	1	1	1
Ethanol (ppm)	-16	-18	-21	-18	-11	-15	-17
Ethylene (ppm)	0	0	0	0	0	0	0
Formaldehyde (ppm)	1	1	1	1	1	1	1
HCN (ppm)	0	1	1	2	3	3	3
MeOH (ppm)	0	0	0	0	0	0	-1
Methane (ppm)	3	3	4	3	3	2	3
NH_3 (ppm)	0	0	0	0	0	0	0
NO_2 (ppm)	1	1	1	1	1	1	0
N_2O (ppm)	3	3	3	5	6	6	7
Phosgene (ppm)	0	0	0	0	0	0	0
Propane (ppm)	3	4	4	4	3	4	4
Propylene (ppm)	0	0	0	0	0	0	0
Toluene (ppm)	-13	-13	-12	-13	6	6	7

A.7 Gatling

Table 79: Gatling Coal – Axial Distance 97 cm.

Radial Dist. (cm)	10	20	30	40	50	60	70
The following eight gases were measured by the FTIR							
CO (ppm)	18168	20853	27136	21515	13377	10594	6111
CO_2 (%)	17	17	15	17	17	17	18
H_2O (%)	10	10	10	10	10	10	9
H_2S (ppm)	353	404	760	680	307	305	-69
HCl (ppm)	15	53	15	10	5	4	3
NO (ppm)	164	115	92	107	125	127	190
SO_2 (ppm)	2861	2614	2154	2606	3112	3146	3643
SO_3 (ppm)	54	58	52	57	62	64	80
The following four gases were measured by the Horiba PG-250							
NO (ppm)							
CO (ppm)							
CO_2 (%)							
O_2 (%)							
The following two gases were measured by the GC							
H_2 (%)	0.62	0.81	1.21	0.74	0.47	0.31	0.12
O_2 (%)	0.01	0.02	0.01	0.04	0.05	0.04	0.13
The following were additional species measured by the FTIR							
Acetylene (ppm)	264	305	323	351	228	128	45
Aldehyde (ppm)	14	21	26	22	12	7	2
Dodecane (ppm)	1	1	2	1	1	1	0
Ethanol (ppm)	-26	-31	-31	-26	-28	-25	-27
Ethylene (ppm)	15	33	55	116	79	15	2
Formaldehyde (ppm)	1	2	1	1	2	2	1
HCN (ppm)	40	44	56	44	28	19	12
MeOH (ppm)	-1	-1	-1	-1	-1	0	0
Methane (ppm)	669	1025	1314	1264	860	417	116
NH_3 (ppm)	0	0	0	0	0	0	0
NO_2 (ppm)	7	6	8	8	8	4	2
N_2O (ppm)	-3	-4	-4	-4	-2	-2	0
Phosgene (ppm)	1	1	1	1	1	1	0
Propane (ppm)	-2	1	-1	-1	0	-1	0
Propylene (ppm)	-1	-1	0	4	2	-1	0
Toluene (ppm)	-33	-43	-74	-43	-27	-8	1

Table 80: Gatling Coal – Axial Distance 97 cm.

Radial Dist. (cm)	10	20	30	40	50	60	70
The following eight gases were measured by the FTIR							
CO (ppm)	16838	24856	29883	27280	13410	4236	3778
CO_2 (%)	17	16	15	16	17	17	17
H_2O (%)	5	5	11	11	10	10	9
H_2S (ppm)	134	249	693	801	280	70	45
HCl (ppm)	15	16	8	1	1	0	0
NO (ppm)	170	144	103	107	141	178	237
SO_2 (ppm)	2763	2405	2344	2342	3374	4250	3532
SO_3 (ppm)	64	61	48	54	58	81	70
The following four gases were measured by the Horiba PG-250							
NO (ppm)							
CO (ppm)							
CO_2 (%)							
O_2 (%)							
The following two gases were measured by the GC							
H_2 (%)	0.55	0.94	1.25	1.19	0.40	0.07	0.08
O_2 (%)	0.06	0.02`	0.01	0.00	0.05	0.29	0.63
The following were additional species measured by the FTIR							
Acetylene (ppm)	253	532	691	562	208	31	29
Aldehyde (ppm)	17	34	38	31	9	1	4
Dodecane (ppm)	1	2	3	2	0	1	1
Ethanol (ppm)	-31	-39	-25	-22	-22	-21	-25
Ethylene (ppm)	11	52	60	86	42	3	1
Formaldehyde (ppm)	6	1	1	1	1	1	1
HCN (ppm)	40	74	85	64	25	8	7
MeOH (ppm)	0	0	-2	-2	-1	-1	-1
Methane (ppm)	622	1331	1627	1372	606	77	54
NH_3 (ppm)	0	0	1	4	4	2	1
NO_2 (ppm)	2	5	10	8	6	2	0
N_2O (ppm)	-3	-4	-5	-5	-2	1	2
Phosgene (ppm)	1	1	1	1	1	0	0
Propane (ppm)	-2	-2	0	0	-1	0	0
Propylene (ppm)	-1	1	0	1	0	0	0
Toluene (ppm)	-38	-66	-32	-53	-31	1	-1

Table 81: Gatling Coal – Axial Distance 83 cm.

Radial Dist. (cm)	10	20	30	40	50	60	70
The following eight gases were measured by the FTIR							
CO (ppm)	25735	33539	37024	32014	11207	3866	7775
CO_2 (%)	16	14	14	14	17	17	18
H_2O (%)	10	11	11	10	9	9	10
H_2S (ppm)	417	527	833	661	6	-47	72
HCl (ppm)	1	0	1	0	0	0	19
NO (ppm)	174	139	103	134	212	225	185
SO_2 (ppm)	2873	2520	2132	2595	4403	4055	3483
SO_3 (ppm)	57	54	46	59	82	77	68
The following four gases were measured by the Horiba PG-250							
NO (ppm)							
CO (ppm)							
CO_2 (%)							
O_2 (%)							
The following two gases were measured by the GC							
H_2 (%)	0.80	1.48	1.59	1.24	0.25	0.02	0.25
O_2 (%)	0.04	0.02	0.01	0.04	0.12	1.12	0.12
The following were additional species measured by the FTIR							
Acetylene (ppm)	347	529	758	550	134	35	60
Aldehyde (ppm)	22	35	42	35	10	2	3
Dodecane (ppm)	1	2	3	2	1	1	1
Ethanol (ppm)	-37	-29	-25	-27	-33	-28	-17
Ethylene (ppm)	13	36	64	79	13	2	2
Formaldehyde (ppm)	2	2	2	2	1	1	1
HCN (ppm)	51	69	83	58	18	9	12
MeOH (ppm)	-2	-2	-3	-2	-1	0	-1
Methane (ppm)	1037	1463	1811	1531	331	71	170
NH_3 (ppm)	3	22	34	36	30	22	4
NO_2 (ppm)	6	10	11	9	2	1	3
N_2O (ppm)	-4	-5	-5	-4	-1	3	0
Phosgene (ppm)	1	1	1	1	1	0	1
Propane (ppm)	-2	-3	-2	-2	0	0	-1
Propylene (ppm)	0	-1	0	0	0	0	-1
Toluene (ppm)	-47	-57	-38	-61	-4	1	6

Table 82: Gatling Coal – Axial Distance 243 cm.

Radial Dist. (cm)	10	20	30	40	50	60	70
The following eight gases were measured by the FTIR							
CO (ppm)	366	229	185	152	141	108	73
CO_2 (%)	16	16	14	13	13	13	13
H_2O (%)	8	8	7	7	7	7	8
H_2S (ppm)	-61	65	52	43	49	-85	-98
HCl (ppm)	5	4	3	2	3	4	6
NO (ppm)	106	103	112	123	109	111	97
SO_2 (ppm)	3439	3228	2966	2794	2825	2794	2832
SO_3 (ppm)	71	74	69	67	67	67	63
The following four gases were measured by the Horiba PG-250							
NO (ppm)							
CO (ppm)							
CO_2 (%)							
O_2 (%)							
The following two gases were measured by the GC							
H_2 (%)	0.00	0.00	0.00	0.00	0.00	0.00	0.00
O_2 (%)	1.25	2.15	3.40	4.23	4.04	4.03	3.85
The following were additional species measured by the FTIR							
Acetylene (ppm)	3	2	-27	-26	-27	-27	-26
Aldehyde (ppm)	4	2	-1	0	3	1	1
Dodecane (ppm)	1	0	1	2	2	1	1
Ethanol (ppm)	-24	-19	-16	-20	-20	-17	-18
Ethylene (ppm)	0	0	0	0	0	0	0
Formaldehyde (ppm)	0	0	1	0	0	0	1
HCN (ppm)	1	1	1	1	0	0	0
MeOH (ppm)	-1	-1	-1	0	-1	-1	-1
Methane (ppm)	5	5	5	2	2	2	5
NH_3 (ppm)	7	4	2	1	1	1	0
NO_2 (ppm)	1	1	0	2	1	1	-1
N_2O (ppm)	8	10	11	11	14	15	10
Phosgene (ppm)	0	0	0	0	0	0	0
Propane (ppm)	0	0	0	0	0	0	0
Propylene (ppm)	0	0	0	0	0	0	1
Toluene (ppm)	6	10	-8	-8	-7	-9	-7

Table 83: Gatling Coal – Axial Distance 243 cm.

Radial Dist. (cm)	10	20	30	40	50	60	70
The following eight gases were measured by the FTIR							
CO (ppm)	74	74	106	74	73	93	71
CO_2 (%)	15	15	15	14	14	15	14
H_2O (%)	7	7	7	7	7	7	7
H_2S (ppm)	59	59	52	26	36	97	58
HCl (ppm)	-2	1	5	6	6	6	7
NO (ppm)	113	108	112	118	115	109	116
SO_2 (ppm)	2788	2823	2828	2650	2497	2711	2574
SO_3 (ppm)	54	60	56	53	46	50	52
The following four gases were measured by the Horiba PG-250							
NO (ppm)							
CO (ppm)							
CO_2 (%)							
O_2 (%)							
The following two gases were measured by the GC							
H_2 (%)	0.00	0.00	0.00	0.00	0.00	0.00	0.00
O_2 (%)	3.79	3.68	3.86	4.83	5.42	4.22	4.67
The following were additional species measured by the FTIR							
Acetylene (ppm)	2	2	2	2	1	2	1
Aldehyde (ppm)	2	7	4	5	4	5	2
Dodecane (ppm)	0	0	1	0	0	1	0
Ethanol (ppm)	-13	-16	-15	-16	-13	-15	-14
Ethylene (ppm)	0	0	0	0	0	0	0
Formaldehyde (ppm)	1	0	0	0	0	0	1
HCN (ppm)	0	0	0	0	0	0	0
MeOH (ppm)	-2	-1	-1	-1	-1	-1	-1
Methane (ppm)	3	4	4	4	4	4	4
NH_3 (ppm)	0	-2	-3	-3	-3	-3	-3
NO_2 (ppm)	3	3	2	3	2	3	3
N_2O (ppm)	12	12	9	10	11	13	12
Phosgene (ppm)	0	0	0	0	0	0	0
Propane (ppm)	1	0	1	1	1	0	1
Propylene (ppm)	-1	-1	0	0	0	-1	0
Toluene (ppm)	-6	-4	-3	5	7	0	4

Table 84: Gatling Coal – Axial Distance 63 cm.

Radial Dist. (cm)	10	20	30	40	50	60	70
The following eight gases were measured by the FTIR							
CO (ppm)	14087	13645	54466	51700	10791	3871	2647
CO_2 (%)	18	17	15	15	18	19	18
H_2O (%)	9	9	10	10	8	8	8
H_2S (ppm)	62	166	659	707	74	81	6
HCl (ppm)	11	8	17	5	0	-2	-3
NO (ppm)	276	361	163	163	269	209	235
SO_2 (ppm)	3229	3249	2443	2636	4610	3601	3365
SO_3 (ppm)	61	65	37	43	67	73	62
The following four gases were measured by the Horiba PG-250							
NO (ppm)							
CO (ppm)							
CO_2 (%)							
O_2 (%)							
The following two gases were measured by the GC							
H_2 (%)	0.30	0.40	2.24	2.32	0.23	0.07	0.03
O_2 (%)	0.77	1.62	0.02	0.02	0.34	0.92	1.59
The following were additional species measured by the FTIR							
Acetylene (ppm)	112	284	1191	1270	70	22	8
Aldehyde (ppm)	9	20	62	68	9	4	2
Dodecane (ppm)	0	0	0	-1	0	0	0
Ethanol (ppm)	-16	-17	8	32	-22	-17	-20
Ethylene (ppm)	2	12	150	345	7	1	1
Formaldehyde (ppm)	1	4	4	5	2	1	1
HCN (ppm)	19	32	108	103	16	7	4
MeOH (ppm)	-1	0	-3	-4	-1	-1	-1
Methane (ppm)	260	466	2569	3253	138	40	18
NH_3 (ppm)	-3	-3	-3	-2	-2	-3	-3
NO_2 (ppm)	6	8	19	23	4	3	2
N_2O (ppm)	1	5	-4	-4	4	4	4
Phosgene (ppm)	1	1	3	4	1	1	1
Propane (ppm)	1	2	5	6	1	1	1
Propylene (ppm)	-1	-1	-2	2	-1	-1	0
Toluene (ppm)	10	-46	-25	7	36	15	10

Table 85: Gatling Coal – Axial Distance 230 cm.

Radial Dist. (cm)	10	20	30	40	50	60	70
The following eight gases were measured by the FTIR							
CO (ppm)	1148	824	492	342	356	346	307
CO_2 (%)	17	16	15	13	13	13	13
H_2O (%)	7	7	7	6	6	6	6
H_2S (ppm)	92	122	24	72	100	20	97
HCl (ppm)	-4	-4	-4	-4	-4	-4	-3
NO (ppm)	116	117	115	125	115	116	125
SO_2 (ppm)	3293	3220	3031	2846	2770	2712	2583
SO_3 (ppm)	64	65	61	67	61	57	54
The following four gases were measured by the Horiba PG-250							
NO (ppm)							
CO (ppm)							
CO_2 (%)							
O_2 (%)							
The following two gases were measured by the GC							
H_2 (%)	0.00	0.00	0.00	0.00	0.00	0.00	0.00
O_2 (%)	2.32	2.15	2.94	3.94	4.18	4.42	4.57
The following were additional species measured by the FTIR							
Acetylene (ppm)	3	3	2	-26	-26	-26	-26
Aldehyde (ppm)	3	5	4	4	3	2	6
Dodecane (ppm)	1	0	0	0	0	1	0
Ethanol (ppm)	-14	-17	-14	-16	-14	-12	-16
Ethylene (ppm)	1	1	0	0	0	0	0
Formaldehyde (ppm)	1	0	0	0	0	0	0
HCN (ppm)	2	1	1	1	1	1	1
MeOH (ppm)	-1	0	0	0	0	0	0
Methane (ppm)	5	3	4	4	4	3	4
NH_3 (ppm)	-3	-3	-3	-3	-3	-3	-3
NO_2 (ppm)	4	5	3	4	2	3	5
N_2O (ppm)	8	7	8	9	12	12	12
Phosgene (ppm)	0	0	0	0	0	0	0
Propane (ppm)	1	1	0	1	0	1	1
Propylene (ppm)	4	3	2	2	2	2	2
Toluene (ppm)	6	9	12	-7	-8	-7	-5

Table 86: Gatling Coal – Axial Distance 83 cm.

Radial Dist. (cm)	10	20	30	40	50	60	70
The following eight gases were measured by the FTIR							
CO (ppm)	23141	34153	36695	24555	6994	5879	2265
CO_2 (%)	17	16	15	16	18	17	19
H_2O (%)	9	9	10	9	8	8	9
H_2S (ppm)	423	699	809	159	27	12	57
HCl (ppm)	6	0	-2	-4	-6	-6	-6
NO (ppm)	163	140	121	183	220	193	205
SO_2 (ppm)	2671	2354	2150	3062	3823	3423	3430
SO_3 (ppm)	49	43	38	52	66	75	71
The following four gases were measured by the Horiba PG-250							
NO (ppm)							
CO (ppm)							
CO_2 (%)							
O_2 (%)							
The following two gases were measured by the GC							
H_2 (%)	0.73	1.27	1.74	0.74	0.09	0.04	0.04
O_2 (%)	0.03	0.02	0.02	0.05	0.30	0.59	0.50
The following were additional species measured by the FTIR							
Acetylene (ppm)	133	356	750	315	39	11	6
Aldehyde (ppm)	11	25	47	22	4	2	4
Dodecane (ppm)	0	0	2	0	0	0	0
Ethanol (ppm)	-21	-32	-20	-36	-20	-15	-22
Ethylene (ppm)	4	17	49	35	5	3	1
Formaldehyde (ppm)	1	1	1	1	0	0	0
HCN (ppm)	25	48	81	36	11	7	4
MeOH (ppm)	0	0	-1	0	0	1	0
Methane (ppm)	449	1156	1784	904	79	104	10
NH_3 (ppm)	-3	-3	-3	-3	-2	-3	-3
NO_2 (ppm)	7	13	16	8	5	5	4
N_2O (ppm)	-3	-4	-5	-2	2	2	3
Phosgene (ppm)	1	2	2	1	1	2	0
Propane (ppm)	-3	-4	-3	-3	0	0	1
Propylene (ppm)	-2	-3	-4	-2	0	11	3
Toluene (ppm)	-30	-49	-42	-44	4	14	11

APPENDIX B: ORIGINAL ULTIMATE, PROXIMATE, AND ASH ANALYSES

The original coal analyses are all labeled except for the PRB-1 coal. This is the second coal analysis reported. For reference, the analyses appear in the following order:

1. Illinois #6-1 (2 pages)
2. PRB-1 (2 pages)
3. Beulah Zap (2 pages)
4. Mahoning (named Kensington on the analysis, 2 pages)
5. Indiana, Gibson (1 page)
6. Illinois #6-2 (1 page)
7. Gatling (2 pages)
8. Kentucky #11 (1 page)
9. Pittsburgh #8 (1 page)
10. PRB-2 (1 page)

Todd Reeder/Dr. Dale Tree
BYU Mechanical Engineering Dept.
435 CTB
Provo, UT 84602

Date: September 29, 2008
Request Number: 25929
Date Received: 9-19-08
Matrix: Coal

REPORT OF ANALYSIS

Lab Number	L5968		
Sample ID	**Illinois #6 Puverized**		
Proximate Analysis **Method: ASTM D-5142**	As Received wt%	Moisture Free wt%	MAF Basis wt%
Moisture	5.40	******	******
Ash	8.65	9.14	******
Volatile Matter	35.68	37.72	41.51
Fixed Carbon	50.27	53.14	58.49
Total	100.00	100.00	100.00

Ultimate Analysis **Method: ASTM D5142/5373**			
Moisture	5.40	******	******
Hydrogen	3.74	3.95	4.35
Carbon	70.16	74.16	81.62
Nitrogen	1.04	1.10	1.21
Sulfur	2.69	2.84	3.13
Oxygen	8.32	8.81	9.69
Ash	8.65	9.14	******
Total	100.00	100.00	100.00

Heating Value, Btu/lb **Method: ASTM D-5865**	12,575	13,293	14,630

Hydrogen and Oxygen values reported do not include hydrogen and oxygen in the free moisture associated with the sample.

Method: ASTM D-4326 Modified (XRF)

Chloride, wt% dry basis	0.3892

Monte L. Ellis
Laboratory Manager

MLE:tab

WYOMING ANALYTICAL LABORATORIES, INC.
1660 Harrison St. Wallaramie@wal-lab.com (307) 742-7995
Laramie, WY 82070 Fax: (307) 721-8956

Andrew Mackrory
BYU Mechanical Engineering Dept.
435 CTB
Provo, UT 84602

Date: September 29, 2008
Request Number: 25929
Date Received: 9-19-08
Matrix: Coal
Lab Number: 5968
Sample ID: Illinois #6
Puverized

COAL ASH ANALYSIS
wt% as Ignited Basis

Method: ASTM D-4326 (XRF)

Silicon Dioxide, % as SiO2	48.12
Aluminum Oxide, % as Al2O3	19.65
Iron Oxide, % as Fe2O3	17.64
Calcium Oxide, % as CaO	4.28
Magnesium Oxide, % as MgO	0.95
Sodium Oxide, % as Na2O	1.08
Potassium Oxide, % as K2O	2.59
Titanium Dioxide, % as TiO2	1.05
Manganese Dioxide, % as MnO2	0.07
Phosphorus Pentoxide, % as P2O5	0.08
Strontium Oxide, % as SrO	0.03
Barium Oxide, % as BaO	0.05
Sulfur Trioxide, % as SO3	4.41

Alkalies as Na20	2.79
Base to Acid Ratio	0.39
Silic Ratio	0.68
T250, ^{0}F	2429

MLE:tab

Monte L. Ellis
Laboratory Manager

WYOMING ANALYTICAL LABORATORIES, INC.
1660 Harrison St. Laramie, WY 82070
Wallaramie@wal-lab.com
(307) 742-7995
Fax: (307) 721-8956

Todd Reeder/Dr. Dale Tree
BYU Mechanical Engineering Dept.
435 CTB
Provo, UT 84602

Date: February 5, 2009
Request Number: 26346
Date Received: 1-27-09
Matrix: Coal

REPORT OF ANALYSIS

Lab Number	L7595		
Sample ID	**Puverized Coal**		
Proximate Analysis **Method: ASTM D-5142**	As Received wt%	Moisture Free wt%	MAF Basis wt%
Moisture	24.59	******	******
Ash	5.14	6.82	******
Volatile Matter	37.00	49.07	52.66
Fixed Carbon	33.27	44.11	47.34
Total	100.00	100.00	100.00

Ultimate Analysis **Method: ASTM D5142/5373**			
Moisture	24.59	******	******
Hydrogen	2.55	3.38	3.63
Carbon	54.75	72.60	77.91
Nitrogen	0.83	1.10	1.18
Sulfur	0.25	0.33	0.35
Oxygen	11.89	15.77	16.93
Ash	5.14	6.82	******
Total	100.00	100.00	100.00

Heating Value, Btu/lb **Method: ASTM D-5865**	9,156	12,142	13,031

Hydrogen and Oxygen values reported do not include hydrogen and oxygen in the free moisture associated with the sample.

Method: ASTM D-4326 Modified (XRF)

Chloride, wt% dry basis	0.0012

Monte L. Ellis
Laboratory Manager

MLE:tab

WYOMING ANALYTICAL LABORATORIES, INC.
1660 Harrison St. Wallaramie@wal-lab.com (307) 742-7995
Laramie, WY 82070 Fax: (307) 721-8956

Andrew Mackrory
BYU Mechanical Engineering Dept.
435 CTB
Provo, UT 84602

Date: February 5, 2009
Request Number: 26346
Date Received: 1-27-09
Matrix: Coal
Lab Number: L7595
Sample ID:Puverized Coal

COAL ASH ANALYSIS
wt% as Ignited Basis

Method: ASTM D-4326 (XRF)

Silicon Dioxide, % as SiO2	36.04
Aluminum Oxide, % as Al2O3	16.84
Iron Oxide, % as Fe2O3	5.86
Calcium Oxide, % as CaO	21.61
Magnesium Oxide, % as MgO	5.06
Sodium Oxide, % as Na2O	1.69
Potassium Oxide, % as K2O	0.50
Titanium Dioxide, % as TiO2	1.32
Manganese Dioxide, % as MnO2	0.02
Phosphorus Pentoxide, % as P2O5	1.00
Strontium Oxide, % as SrO	0.35
Barium Oxide, % as BaO	0.62
Sulfur Trioxide, % as SO3	9.09

Alkalies as Na20	2.02
Base to Acid Ratio	0.64
Silic Ratio	0.53
T250, ^{0}F	2228

Monte L. Ellis
Laboratory Manager

MLE:tab

WYOMING ANALYTICAL LABORATORIES, INC.
1660 Harrison St. Laramie, WY 82070
Wallaramie@wal-lab.com
(307) 742-7995
Fax: (307) 721-8956

Todd Reeder/Dr. Dale Tree
BYU Mechanical Engineering Dept.
435 CTB
Provo, UT 84602

Date: April 16, 2009
Request Number: 26560
Date Received: 4-2-09
Matrix: Coal

REPORT OF ANALYSIS

Lab Number	L8440		
Sample ID	**Bevlah Pulverized coal**		
Proximate Analysis Method: ASTM D-5142	As Received wt%	Moisture Free wt%	MAF Basis wt%
Moisture	27.33	******	******
Ash	8.66	11.92	******
Volatile Matter	33.77	46.47	52.76
Fixed Carbon	30.24	41.61	47.24
Total	100.00	100.00	100.00

Ultimate Analysis Method: ASTM D5142/5373			
Moisture	27.33	******	******
Hydrogen	2.03	2.79	3.17
Carbon	46.56	64.07	72.74
Nitrogen	0.86	1.18	1.34
Sulfur	0.67	0.92	1.04
Oxygen	13.89	19.12	21.71
Ash	8.66	11.92	******
Total	100.00	100.00	100.00

Heating Value, Btu/lb Method: ASTM D-5865	7,792	10,722	12,173

Hydrogen and Oxygen values reported do not include hydrogen and oxygen in the free moisture associated with the sample.

Chloride, wt% dry basis	0.001

Monte L. Ellis
Laboratory Manager

MLE:tab

WYOMING ANALYTICAL LABORATORIES, INC.
1660 Harrison St. Wallaramie@wal-lab.com (307) 742-7995
Laramie, WY 82070 Fax: (307) 721-8956

Todd Reeder/Dr. Dale Tree
BYU Mechanical Engineering Dept.
435 CTB
Provo, UT 84602

Date: April 16, 2009
Request Number: 26560
Date Received: 4-2-09
Matrix: Coal
Lab Number: L8440
Sample ID: Bevlah
Pulverized coal

COAL ASH ANALYSIS
wt% Ignited Basis

Method: ASTM D-4326 (XRF)

Silicon Dioxide, % as SiO2	32.25
Aluminum Oxide, % as Al2O3	12.23
Iron Oxide, % as Fe2O3	7.45
Calcium Oxide, % as CaO	19.91
Magnesium Oxide, % as MgO	6.47
Sodium Oxide, % as Na2O	3.29
Potassium Oxide, % as K2O	0.82
Titanium Dioxide, % as TiO2	0.65
Manganese Dioxide, % as MnO2	0.08
Phosphorus Pentoxide, % as P2O5	0.27
Strontium Oxide, % as SrO	0.64
Barium Oxide, % as BaO	0.73
Sulfur Trioxide, % as SO3	15.21

Alkalies as Na20	3.83
Base to Acid Ratio	0.84
Silic Ratio	0.49
T250, ^{0}F	2130

Monte L. Ellis
Laboratory Manager

MLE:tab

WYOMING ANALYTICAL LABORATORIES, INC.
1660 Harrison St. Wallaramie@wal-lab.com (307) 742-7995
Laramie, WY 82070 Fax: (307) 721-8956

Todd Reeder/Dr. Dale Tree
BYU Mechanical Engineering Dept.
435 CTB
Provo, UT 84602

Date: September 22, 2009
Request Number: 27145
Date Received: 9-8-09
Matrix: Coal

REPORT OF ANALYSIS

Lab Number	M0265		
Sample ID	**Kensington Coal**		
Proximate Analysis **Method: ASTM D-5142**	As Received wt%	Moisture Free wt%	MAF Basis wt%
Moisture	2.22	******	******
Ash	9.92	10.15	******
Volatile Matter	40.79	41.72	46.43
Fixed Carbon	47.07	48.13	53.57
Total	100.00	100.00	100.00

Ultimate Analysis **Method: ASTM D5142/5373**			
Moisture	2.22	******	******
Hydrogen	4.18	4.27	4.75
Carbon	74.67	76.37	85.00
Nitrogen	0.93	0.95	1.06
Sulfur	1.96	2.00	2.23
Oxygen	6.12	6.26	6.96
Ash	9.92	10.15	******
Total	100.00	100.00	100.00

Heating Value, Btu/lb **Method: ASTM D-5865**	13,404	13,708	15,257

Hydrogen and Oxygen values reported do not include hydrogen and oxygen in the free moisture associated with the sample.

Chloride, wt% dry basis	0.1989

Monte L. Ellis
Laboratory Manager

MLE:tab

WYOMING ANALYTICAL LABORATORIES, INC.
1660 Harrison St. Wallaramie@wal-lab.com (307) 742-7995
Laramie, WY 82070 Fax: (307) 721-8956

Todd Reeder/Dr. Dale Tree
BYU Mechanical Engineering Dept.
435 CTB
Provo, UT 84602

Date: September 22, 2009
Request Number: 27145
Date Received: 9-8-09
Matrix: Coal
Lab Number:M0265
Sample ID: Kensington Coal

COAL ASH ANALYSIS
wt% Ignited Basis

Method: ASTM D-4326 (XRF)

Silicon Dioxide, % as SiO2	42.65
Aluminum Oxide, % as Al2O3	29.07
Iron Oxide, % as Fe2O3	20.45
Calcium Oxide, % as CaO	1.76
Magnesium Oxide, % as MgO	0.52
Sodium Oxide, % as Na2O	0.34
Potassium Oxide, % as K2O	1.61
Titanium Dioxide, % as TiO2	1.41
Manganese Dioxide, % as MnO2	0.00
Phosphorus Pentoxide, % as P2O5	0.76
Strontium Oxide, % as SrO	0.12
Barium Oxide, % as BaO	0.07
Sulfur Trioxide, % as SO3	1.24

Alkalies as Na20	1.40
Base to Acid Ratio	0.34
Silic Ratio	0.65
T250, ^{0}F	2497

Monte L. Ellis
Laboratory Manager

MLE:tab

WYOMING ANALYTICAL LABORATORIES, INC.
1660 Harrison St. Wallaramie@wal-lab.com (307) 742-7995
Laramie, WY 82070 Fax: (307) 721-8956

Dr. Dale Tree
BYU Mechanical Engineering 0
435 CTB
Provo, UT 84602

Request : 27400

Analytical Report

Lab ID : M1017 Client Id Indiana #6 Gibson Coal Date: November 24, 2009

Proximate / Ultimate	As Rec.	Moisture Free	MAF
Total Moisture Wt%:	7.25		
Ash Wt%:	7.20	7.76	
Volatile Wt%:	30.87	33.28	36.08
Fixed	54.68	58.95	63.92
Sulfur Wt%:	1.14	1.23	1.33
Carbon Wt%:	69.48	74.91	81.22
Hydrogen	4.02	4.33	4.70
Nitrogen Wt%:	1.36	1.47	1.59
Oxygen Wt%:	9.55	10.30	11.16
Heating Value Btu/Lbs	12400	13369	14494

Hydrogen and Oxygen values DO NOT include free moisture from sample..

Coal Ash Analysis, wt.% Ignited

Silicon Dioxide, as SiO2 wt %	55.14	Chloride, mg/kg	2121
Aluminum Oxide, asAl2O3 wt %	21.10		
Iron Oxide, as Fe2O3 wt %	12.93		
Calcium Oxide, asCaO wt %	2.48		
Magnesium Oxide, asMgo wt %	0.86		
Sodium Oxide, asNa2O wt %	1.25		
Potassium Oxide, asK2O wt %	2.40		
Titanium Dioxide, as TiO2 wt %	1.30		
Manganese Dioxide, as MnO2 wt %	0.03		
Phosphorus Pentoxide, as P2O5	0.35		
Strontium Oxide, as SrO wt %	0.08		
Barium Oxide, as BaO wt %	0.06		
Sulfur Trioxide, as SO3 wt %	2.02		
Alkalies as Na2O	2.83		
Base/Acid	0.26		
Silica ratio	0.77		
T250 F	2624		

WYOMING ANALYTICAL LABORATORIES, INC.
1660 Harrison St. Wallaramie@wal-lab.com (307) 742-7995
Laramie, WY 82070 Fax: (307) 721-8956

Todd Reeder/Dr. Dale Tree
BYU Mechanical Engineering Dept.
435 CTB
Provo, UT 84602

Date: December 21, 2009
Request Number: 27539
Date Received: 12-11-09
Matrix: Coal

REPORT OF ANALYSIS

Lab Number: M1482
Sample ID: Illinois Galatia

Proximate Analysis:	As Received	Moisture Free	MAF Basis
Moisture, wt%	3.68	******	******
Ash, wt%	10.45	10.85	******
Volatile Matter, wt%	33.70	34.99	39.25
Fixed Carbon, wt%	52.17	54.16	60.75
Total	100.00	100.00	100.00

Ultimate Analysis:			
Moisture, wt%	3.68	******	******
Hydrogen, wt%	3.14	3.26	3.66
Carbon, wt%	67.66	70.25	78.80
Nitrogen, wt%	0.95	0.99	1.11
Sulfur, wt%	2.96	3.07	3.44
Oxygen, wt%	11.16	11.58	12.99
Ash, wt%	10.45	10.85	******
Total	100.00	100.00	100.00

Heating Value, Btu/lb	12,464	12,940	14,515

Coal Ash Analysis, wt% Ignited Basis	
Silicon Dioxide, % as SiO2	49.13
Aluminum Oxide, % as Al2O3	18.55
Iron Oxide, % as Fe2O3	16.38
Calcium Oxide, % as CaO	5.49
Magnesium Oxide, % as MgO	1.07
Sodium Oxide, % as Na2O	0.66
Potassium Oxide, % as K2O	2.34
Titanium Dioxide, % as TiO2	0.93
Manganese Dioxide, % as MnO2	0.04
Phosphorus Pentoxide, % as P2O5	0.09
Strontium Oxide, % as SrO	0.03
Barium Oxide, % as BaO	0.05
Sulfur Trioxide, % as SO3	5.24

Alkalies as Na20	2.20
Base to Acid Ratio	0.38
Silic Ratio	0.68
T250, ^{O}F	2439

Hydrogen and Oxygen values reported do not include hydrogen and oxygen in the free moisture associated with the sample.

Chloride, wt% dry basis	0.283

Monte L. Ellis
Laboratory Manager

WYOMING ANALYTICAL LABORATORIES, INC.
1660 Harrison St. Wallaramie@wal-lab.com (307) 742-7995
Laramie, WY 82070 Fax: (307) 721-8956

Todd Reeder/Dr. Dale Tree
BYU Mechanical Engineering Dept.
435 CTB
Provo, UT 84602

Date: September 22, 2009
Request Number: 27145
Date Received: 9-8-09
Matrix: Coal

REPORT OF ANALYSIS

Lab Number	M0264		
Sample ID	**Gatling Coal**		
Proximate Analysis **Method: ASTM D-5142**	As Received wt%	Moisture Free wt%	MAF Basis wt%
Moisture	3.77	******	******
Ash	11.34	11.78	******
Volatile Matter	40.73	42.33	47.98
Fixed Carbon	44.16	45.89	52.02
Total	100.00	100.00	100.00

Ultimate Analysis **Method: ASTM D5142/5373**			
Moisture	3.77	******	******
Hydrogen	4.07	4.23	4.79
Carbon	67.11	69.74	79.05
Nitrogen	0.94	0.98	1.11
Sulfur	4.31	4.48	5.08
Oxygen	8.46	8.79	9.97
Ash	11.34	11.78	******
Total	100.00	100.00	100.00

Heating Value, Btu/lb **Method: ASTM D-5865**	12,191	12,669	14,361

Hydrogen and Oxygen values reported do not include hydrogen and oxygen in the free moisture associated with the sample.

Chloride, wt% dry basis	0.0387

Monte L. Ellis
Laboratory Manager

MLE:tab

WYOMING ANALYTICAL LABORATORIES, INC.
1660 Harrison St. Wallaramie@wal-lab.com (307) 742-7995
Laramie, WY 82070 Fax: (307) 721-8956

Todd Reeder/Dr. Dale Tree
BYU Mechanical Engineering Dept.
435 CTB
Provo, UT 84602

Date: September 22, 2009
Request Number: 27145
Date Received: 9-8-09
Matrix: Coal
Lab Number:M0264
Sample ID: Gatling Coal

COAL ASH ANALYSIS
wt% Ignited Basis

Method: ASTM D-4326 (XRF)

Silicon Dioxide, % as SiO2	40.35
Aluminum Oxide, % as Al2O3	22.56
Iron Oxide, % as Fe2O3	28.33
Calcium Oxide, % as CaO	2.62
Magnesium Oxide, % as MgO	0.69
Sodium Oxide, % as Na2O	0.41
Potassium Oxide, % as K2O	1.28
Titanium Dioxide, % as TiO2	1.04
Manganese Dioxide, % as MnO2	0.05
Phosphorus Pentoxide, % as P2O5	0.22
Strontium Oxide, % as SrO	0.09
Barium Oxide, % as BaO	0.11
Sulfur Trioxide, % as SO3	2.25

Alkalies as Na20	1.25
Base to Acid Ratio	0.52
Silic Ratio	0.56
T250, ^{0}F	2295

Monte L. Ellis
Laboratory Manager

MLE:tab

WYOMING ANALYTICAL LABORATORIES, INC.
1660 Harrison St. Wallaramie@wal-lab.com (307) 742-7995
Laramie, WY 82070 Fax: (307) 721-8956

Dr. Dale Tree
BYU Mechanical Engineering
435 CTB
Provo, UT 84602

Request : 27400

Analytical Report

Lab ID : M1019 Client Id: Kentucky #11 Warrior Coal Date: November 24, 2009

Proximate / Ultimate	As Rec.	Moisture Free	MAF
Total Moisture Wt%:	3.39		
Ash Wt%:	8.46	8.76	
Volatile Wt%:	36.97	38.27	41.94
Fixed	51.18	52.98	58.06
Sulfur Wt%:	3.64	3.77	4.13
Carbon Wt%:	70.89	73.38	80.42
Hydrogen	4.34	4.49	4.92
Nitrogen Wt%:	1.23	1.27	1.40
Oxygen Wt%:	8.05	8.33	9.13
Heating Value Btu/Lbs	12905	13358	14640

Hydrogen and Oxygen values DO NOT include free moisture from sample.

Coal Ash Analysis, wt.% Ignited

Silicon Dioxide, as SiO2 wt %	41.70	Chloride, mg/kg	2057
Aluminum Oxide, asAl2O3 wt %	18.40		
Iron Oxide, as Fe2O3 wt %	26.09		
Calcium Oxide, asCaO wt %	4.80		
Magnesium Oxide, asMgo wt %	0.90		
Sodium Oxide, asNa2O wt %	0.53		
Potassium Oxide, asK2O wt %	2.43		
Titanium Dioxide, as TiO2 wt %	0.96		
Manganese Dioxide, as MnO2 wt %	0.03		
Phosphorus Pentoxide, as P2O5	0.31		
Strontium Oxide, as SrO wt %	0.05		
Barium Oxide, as BaO wt %	0.18		
Sulfur Trioxide, as SO3 wt %	3.62		
Alkalies as Na2O	2.13		
Base/Acid	0.57		
Silica ratio	0.57		
T250 F	2263		

Monte L. Ellis
Laboratory Manager

WYOMING ANALYTICAL LABORATORIES, INC.
1660 Harrison St. Wallaramie@wal-lab.com (307) 742-7995
Laramie, WY 82070 Fax: (307) 721-8956

Dr. Dale Tree
BYU Mechanical Engineering
435 CTB
Provo, UT 84602

Request : 27400

Analytical Report

Lab ID : M1018 Client Id: Pittsburg #8 Coal Date: November 24, 2009

Proximate / Ultimate	As Rec.	Moisture Free	MAF
Total Moisture Wt%:	1.05		
Ash Wt%:	10.45	10.56	
Volatile Wt%:	18.61	18.81	21.03
Fixed	69.89	70.63	78.97
Sulfur Wt%:	1.03	1.04	1.16
Carbon Wt%:	77.37	78.19	87.42
Hydrogen	3.86	3.90	4.36
Nitrogen Wt%:	1.44	1.46	1.63
Oxygen Wt%:	4.80	4.85	5.42
Heating Value Btu/Lbs	13715	13861	15497

Hydrogen and Oxygen values DO NOT include free moisture from sample.

Coal Ash Analysis, wt.% Ignited

Silicon Dioxide, as SiO2 wt %	56.77	Chloride, mg/kg	45
Aluminum Oxide, asAl2O3 wt %	29.28		
Iron Oxide, as Fe2O3 wt %	6.63		
Calcium Oxide, asCaO wt %	0.90		
Magnesium Oxide, asMgo wt %	0.56		
Sodium Oxide, asNa2O wt %	0.65		
Potassium Oxide, asK2O wt %	2.30		
Titanium Dioxide, as TiO2 wt %	1.53		
Manganese Dioxide, as MnO2 wt %	0.05		
Phosphorus Pentoxide, as P2O5	0.56		
Strontium Oxide, as SrO wt %	0.12		
Barium Oxide, as BaO wt %	0.12		
Sulfur Trioxide, as SO3 wt %	0.53		
Alkalies as Na2O	2.17		
Base/Acid	0.13		
Silica ratio	0.88		
T250 F	> 2900		

WYOMING ANALYTICAL LABORATORIES, INC.
1660 Harrison St. Wallaramie@wal-lab.com (307) 742-7995
Laramie, WY 82070 Fax: (307) 721-8956

Todd Reeder/Dr. Dale Tree
BYU Mechanical Engineering Dept.
435 CTB
Provo, UT 84602

Date: December 21, 2009
Request Number: 27539
Date Received: 12-11-09
Matrix: Coal

REPORT OF ANALYSIS

Lab Number: M1483
Sample ID: PBR Black Thunder

Proximate Analysis:	As Received	Moisture Free	MAF Basis
Moisture, wt%	21.23	******	******
Ash, wt%	5.53	7.02	******
Volatile Matter, wt%	33.76	42.86	46.10
Fixed Carbon, wt%	39.48	50.12	53.90
Total	100.00	100.00	100.00

Ultimate Analysis:			
Moisture, wt%	21.23	******	******
Hydrogen, wt%	2.06	2.62	2.82
Carbon, wt%	54.39	69.05	74.26
Nitrogen, wt%	0.86	1.09	1.17
Sulfur, wt%	0.26	0.33	0.35
Oxygen, wt%	15.67	19.89	21.40
Ash, wt%	5.53	7.02	******
Total	100.00	100.00	100.00

Heating Value, Btu/lb	9,479	12,034	12,943

Coal Ash Analysis, wt% Ignited Basis	
Silicon Dioxide, % as SiO2	37.42
Aluminum Oxide, % as Al2O3	17.18
Iron Oxide, % as Fe2O3	5.50
Calcium Oxide, % as CaO	17.41
Magnesium Oxide, % as MgO	3.94
Sodium Oxide, % as Na2O	1.08
Potassium Oxide, % as K2O	0.57
Titanium Dioxide, % as TiO2	1.20
Manganese Dioxide, % as MnO2	0.02
Phosphorus Pentoxide, % as P2O5	0.54
Strontium Oxide, % as SrO	0.25
Barium Oxide, % as BaO	0.43
Sulfur Trioxide, % as SO3	14.46

Alkalies as Na20	1.46
Base to Acid Ratio	0.51
Silic Ratio	0.58
T250, ^{O}F	2302

Hydrogen and Oxygen values reported do not include hydrogen and oxygen in the free moisture associated with the sample.

Chloride, wt% dry basis	0.001

Monte L. Ellis
Laboratory Manager

WYOMING ANALYTICAL LABORATORIES, INC.
1660 Harrison St. Wallaramie@wal-lab.com (307) 742-7995
Laramie, WY 82070 Fax: (307) 721-8956

APPENDIX C: DEPOSITION SLEEVE MANUFACTURING

C.1 Ordering Parts

The first step to making sleeves is to order the material. Previously I have ordered the stainless steel tubing from onlinemetals.com. I have ordered 3 different sizes of metal tubing depending on the temperature ranges I wanted. If I wanted the sleeves to be directly on the water cooled probe I ordered: 1" OD X 0.065" Wall X 0.87" ID stainless steel 304/304L seamless round tube. If I wanted the sleeves to rest on the 1.12" OD X 0.874" ID turned down spacers, than I ordered: 1.25" OD X 0.065" Wall X 1.12" ID stainless steel 304/304L seamless round tube. If I wanted the sleeves to rest on 1.25" OD X .874" ID spacers than I ordered: 1.375"OD X 0.065" wall 304/304L stainless steel seamless round tube. To order sleeve material for the air cooled probe, again I used onlinemetals.com and ordered: 0.625" OD X 0.065" Wall 304/304L stainless steel seamless round tube.

For all other equipment needed to assemble both probes I have been ordering from McMaster-Carr (www.mcmaster.com). I order two different size hose clamps (part #5011T241 and part #5011T171), one for the water cooled probe and one for the air cooled probe. I also order stainless steel wire part #9495K82.

To order thermocouples I have gone through omega.com. I order 3 different sizes for the 1/3, 1/2, and 2/3 positions on the probes. The part numbers are: KMQXL-040G-36, KMQXL-040G-40, and KMQXL-040G-44.

C.2 Manufacturing Sleeves

C.2.1 Slotting

For 3 of the 3 inch pieces a slot needs to be cut to provide a place for the thermocouple to sit level with the outside diameter. To do this first ask Ken for his slotting tool. Place it in the mill with a 3/4" collate. Use 2 V-blocks to insure the metal stays stationary on the mill. Use the low speed gear at 60 and insert the slotting tool into the metal 0.038". Than using conventional cutting techniques, cut the slot. After one pass has been made, repeat this same process but move the metal in the z direction a ¼ turn. This will guarantee that the thermocouple will fit in the slot (the thermocouple's outside diameter is thicker than the thickness of the slotting tool). After both passes are completed there will be a small burr at the end of the slot so just grind it off with a grinder. Next cut these 3, 3 inch pieces in half.

C.2.2 Chop Saw

I have been using Ken's shop to do all of the manufacturing. I start by using the chop saw and measure 3 inches, make a mark, and then line the blade up just past that mark and cut. Repeat this 6 times for each probe. Once you have the 3 inch sections cut, use the grinder to grind the edges to make the ends nice and clean. I do this by placing the end of a 3 inch piece up against the grinder and spin it around until the pieces start falling off. I then continue to grind until the inside of the end is soft enough to use a de-burring tool and clean out the inside.

C.2.3 Band Saw

Now that the 3 inch pieces are cleaned up I switch out the band saw blade (to cut stainless steel) to cut the 3 inch pieces into 3 inch halves. If you have never changed the band saw blade,

you MUST ask Ken for help. He is happy to give it and, after watching you do it a couple times, he will trust you enough that you can do it on your own. If you ruin his tools, however, he will NOT be happy. Going very slow I set the band saw to low gear and about 100 as the saw speed. Lining the guide up that is provided I cut the 3 inch pieces exactly in half. Using 2 pieces of wood (one to push through the saw and one to keep the metal tube butted up against the guide) I gently push the sleeves through the blade. This should take about 5-8 minutes per piece. **GO SLOW!** Make sure you cut the slotted sleeves such that the slot is in the middle of a sleeve half. In other words, cut 90 degrees off from the slot cut so that when the sleeve is sitting on the probe, the slot is centered on top.

C.2.4 Hand filing

I now have all of the 3 inch pieces cut in half and there are small burrs on the inside and outside edges of the half pieces. To remove these burrs, use a pair of vice grips and a hand file and hold onto the metal with the vice grips and file the burrs down. This takes time and may not be the fastest way but it will insure a smooth finish and it is important to have a smooth finish so the metal sits flush onto the probes (heat transfer problems).

C.2.5 Silver Soldering

Ken now assists in silver soldering the thermocouples into the slots. Using the three different size thermocouples (1/3, 1/2, 2/3) place one of each kind in a slot. After they are soldered I clean the flux off by running them under warm water and scrubbing them gentle. It would be helpful if you learned how to silver solder so we don't have to wait for Ken to get around to it.

C.3 Probe Assembly

Now that everything is manufactured and all parts have been shipped probe assembly can begin. It is important to place the sleeves in the correct position in the boiler. The boiler is 30 inches inside diameter. First slide all the hose clamps (you need 9 of them) onto the probe. Than measure the placement of the 2/3 sleeves, you should have 2 inches in-between each set of sleeves. Clamp the sleeves in place. Run the thermocouples along the side of each set of sleeves being mindful not to pinch the thermocouples. After all three sets of sleeves are placed and the thermocouples are run use the stainless steel wire to keep the thermocouples tight against the probe. Wrap the wire around the thermocouples, making sure they don't cross over each other, from the 1/3 set to the end where the door is attached. Now mount the door on the end of the probe based upon your measurements. The door should be placed at 41.25".

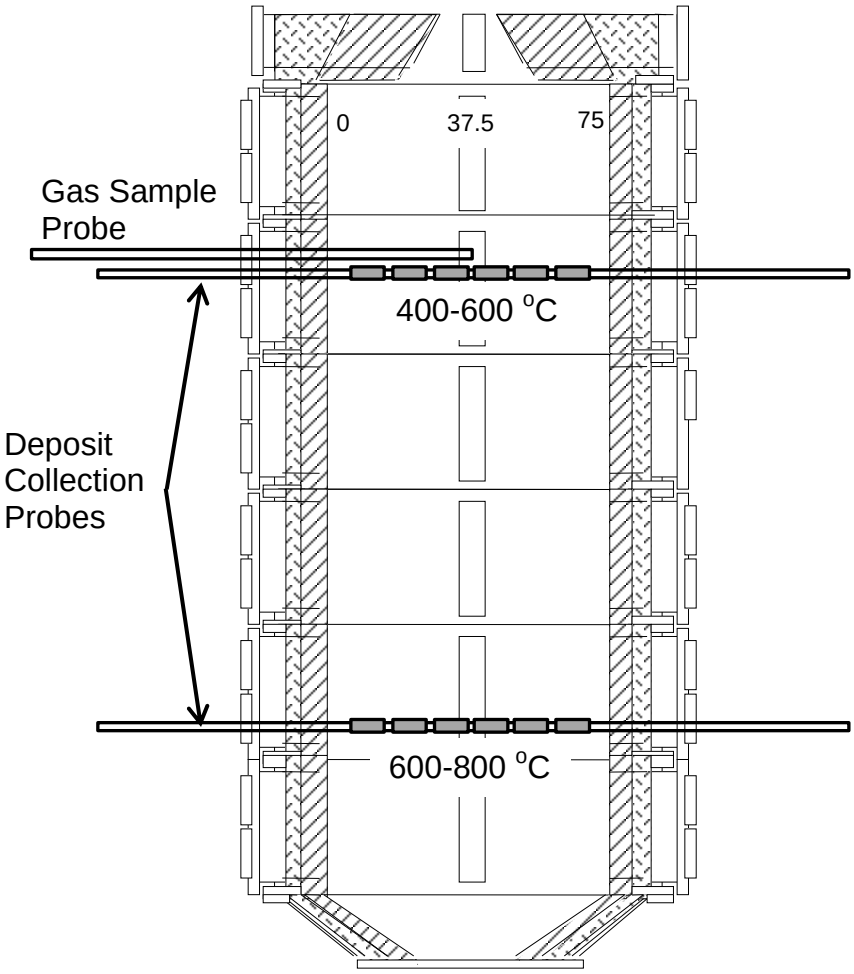

Figure 42: Location of Deposition Sleeves in the BFR.

APPENDIX D: LOCAL STOICHIOMETRIC RATIO DERIVATION

To calculate the local stoichiometric ratio at each sampling location, the stoichiometric ratio is first defined as

$$SR = \frac{\left(\frac{m_{air}}{m_f}\right)_{act}}{\left(\frac{m_{air}}{m_f}\right)_{stoich}} \tag{12}$$

where m is mass, f is fuel, act is the measured, or actual, mass flows, and stoich is the stoichiometric amounts of air and fuel. Rearranging the terms in Equation 12, we get

$$\left(\frac{m_{air}}{m_f}\right)_{act} = SR\left(\frac{m_{air}}{m_f}\right)_{stoich}. \tag{13}$$

Now we introduce the mixture fraction, *f*, defined as the mass of the fuel divided by the total mass. Expressed mathematically,

$$f = \frac{m_f}{m_f + m_{air}}. \tag{14}$$

Subbing Equation (13) into Equation (14),

$$f = \frac{1}{1 + SR\left(\frac{m_{air}}{m_f}\right)_{stoich}}. \tag{15}$$

Since f is defined as the mass of the fuel over the total mass, it can be rewritten as

$$f = \frac{m_f}{m_{tot}}. \tag{16}$$

We now introduce three more equations that will substitute together to rewrite Equation (16):

$$y_c = \frac{m_c}{m_f} \Rightarrow m_f = \frac{m_c}{y_c}, \tag{17}$$

$$MW_c = \frac{m_c}{N_c} \Rightarrow m_c = N_c MW_c, \tag{18}$$

and

$$N_c = \sum X_i C_i N_{tot} \tag{19}$$

where y is the mass fraction, subscript c is 'carbon,' N is number of moles, and MW is the molecular weight. X is the mole fraction, subscript i is for the i^{th} gas specie, C is the number of carbon atoms in the i^{th} specie, and subscript 'tot' stands for 'total.' Substituting (19) into (18), (18) into (17), and (17) into (16), Equation (16) can be rewritten as

$$f = \frac{N_{tot} MW_c \sum X_i C_i}{y_c m_{tot}} \tag{20}$$

but

$$\frac{N_{tot}}{m_{tot}} = \frac{1}{MW_{mix}} \tag{21}$$

and Equation (20) can be rewritten as

$$f = \frac{MW_c \sum X_i C_i}{Y_c MW_{mix}}. \tag{22}$$

Equating (22) with (15) and rearranging, we get our final result:

$$SR = \frac{\left[\frac{Y_c MW_{mix}}{MW_c \sum X_i C_i} - 1\right]}{\left(\frac{m_{air}}{m_f}\right)_{stoich}}. \tag{23}$$